

Design and Synthesis of Donor-Acceptor Truxenes

By
REKHA SHARMA



DISCIPLINE OF CHEMISTRY
INDIAN INSTITUTE OF TECHNOLOGY INDORE
FEBRUARY, 2018

Design and Synthesis of Donor-Acceptor Truxenes

A THESIS

*submitted in partial fulfillment of the
requirements for the award of the degree*

of

DOCTOR OF PHILOSOPHY

by

REKHA SHARMA



DISCIPLINE OF CHEMISTRY
INDIAN INSTITUTE OF TECHNOLOGY INDORE
FEBRUARY, 2018



INDIAN INSTITUTE OF TECHNOLOGY INDORE

CANDIDATE'S DECLARATION

I hereby certify that the work which is being presented in the thesis entitled **Design and Synthesis of Donor-Acceptor Truxenes** in the partial fulfillment of the requirements for the award of the degree of **DOCTOR OF PHILOSOPHY** and submitted in the **DISCIPLINE OF CHEMISTRY, Indian Institute of Technology Indore**, is an authentic record of my own work carried out during the time period from is an authentic record of my own work carried out during the time period from July 2013 to January 2018 under the supervision of Dr. Rajneesh Misra, Professor, Discipline of Chemistry, IIT Indore.

The matter presented in this thesis has not been submitted by me for the award of any other degree of this or any other institute.

Signature of the student with date
(**REKHA SHARMA**)

This is to certify that the above statement made by the candidate is correct to the best of my/our knowledge.

Signature of Thesis Supervisor with date
(**Dr. RAJNEESH MISRA**)

REKHA SHARMA has successfully given his/her Ph.D. Oral Examination held on.....

Signature of Chairperson (OEB)

Date:

Signature of External Examiner

Date:

Signature(s) of Thesis Supervisor(s)

Date:

Signature of PSPC Member #1

Date:

Signature of PSPC Member #2

Date:

Signature of Convener, DPGC

Date:

Signature of Head of Discipline

Date:

ACKNOWLEDGEMENTS

The work described in this thesis would not have been possible without my close association with numerous people who were always there when I required them the most. I take this opportunity to acknowledge them and extend my sincere gratitude for helping me make this Ph.D. thesis a possibility.

I would like to begin with the person who made the biggest difference in my life, my mentor and supervisor, Dr. Rajneesh Misra. He has been there, in front of my eyes throughout my Ph.D., motivating and inspiring every bit of me towards new possibilities in life. It's his vigor and hunger to perform in adverse situation, which has inspired me to thrive for excellence and nothing less. His excellent supervision, advice and guidance from the very early stage made the completion of this study possible. I am indebted to him for his support, motivation and better understanding.

I express my heart-felt gratitude to Dr. Shaikh M. Mobin for single crystal X-ray support and his valuable guidance. I would also like to extend my gratitude to my PSPC members Dr. Shaikh M. Mobin and Dr. Sarika Jalan for their valuable suggestions and guidance.

With great pleasure, I express my respect to Prof. Pradeep Mathur (Director, Indian Institute of Technology Indore) for his unending encouragement and providing all the facilities at Indian Institute of Technology Indore.

I am grateful to Dr. Satya S. Bulusu (Head, Discipline of Chemistry, Indian Institute of Technology Indore) for his suggestions and guidance in various aspects. I am also grateful to Dr. Suman Mukhopadhyay, Dr. Tridib K. Sarma, Dr. Anjan Chakraborty, Dr. Sampak Samanta, Dr. Biswarup Pathak, Dr. Sanjay Singh and Dr. Chelvam Venkatesh for their guidance and help during various activities.

I would like to acknowledge all the teachers I learnt from since my childhood, I would not have been here without their guidance, blessing and support.

I extend my profound thanks to my group members, Dr. Bhausahab, Dr. Prabhat Gautam, Dr. Thakshen, Dr. Ramesh, Dr. Ramana Reddi, Yuvraj, Madhurima, Yogajivan, Bijesh, Charu, Jeevan, Faizal, Depali, Aayushi, and Rahul for their generous co-operation and help to make my work successful.

My heart-felt thanks to my splendid juniors and seniors at IIT Indore for their generous co-operation and help.

I am also thankful to all my friends who helped me directly-indirectly during my Ph. D. I am thankful to Ms. Sarita Batra, Mr. Kinney Pandey, Mr. Ghanshyam Bhavsar, Mr. Manish Kushwaha and Ms. Vinita Kothari for their technical help and support.

I would like to express my thanks to IIT Indore for infrastructure and Council of Scientific and Industrial Research (CSIR), New Delhi for my Fellowship and all others who helped and supported me directly or indirectly.

I thank the Almighty for giving me the strength and patience to work through all these years.

Finally, I would like to acknowledge the people who mean world to me, my father Niranjan Lal Sharma, mother Veena Sharma, and my husband Rakesh Sharma, my son Priyansh Sharma. I don't imagine a life without their love, support and blessings.

REKHA SHARMA

DEDICATED TO

**MY TEACHERS, FAMILY AND
FRIENDS**

– REKHA SHARMA

SYNOPSIS

Truxene (10,15-dihydro-5*H*-diindeno[1,2-*a*;10,20-*c*]fluorene) is a planar polyaromatic hydrocarbon, which represents a fusion of three fluorene moieties in such a way, that it leads to a C_3 symmetric structure. Truxene scaffold appears to be a potential building block for the construction of larger molecular architectures, owing to its easy functionalization, rigid structure, high thermal and chemical stability. Literature reveals that the substitution at para position (2, 7 and 12 positions) of truxene core results in a variety of π -delocalized molecular systems. Truxene based donor-acceptor (D–A) systems are potential candidates for applications in two-photon absorption, organic light-emitting diodes (OLED), and organic fluorescent probes.

The electronic and photonic properties of the π -conjugated D–A molecular systems can be tuned by altering the HOMO-LUMO gap. The HOMO-LUMO gap in D– π –A molecular systems can be tuned either by altering the strength of D/A units or by varying the π -bridge. A variety of donors (triphenylamine, phenothiazene, ferrocene) and acceptors, tetracyanoethylene (TCNE) and 7,7,8,8-tetracyanoquinodimethane (TCNQ), naphthalimide have been explored in the design and synthesis of truxene based donor–acceptor systems.

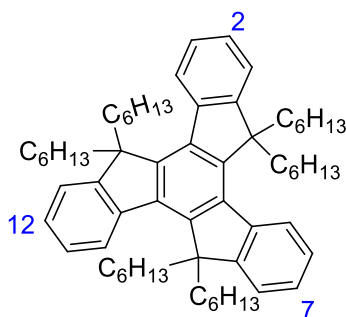


Figure 1. Structure of truxene.

The substitution of the donors and acceptors at 2, 7 and 12 position perturbs the photonic properties of truxene derivatives significantly. The effect of substitution

of various D/A systems on the photophysical and electrochemical properties were studied.

The main objectives of the present study are:

- To study the effect of substitution of different donor and acceptor units on truxene core and exploring the donor-acceptor interaction by tuning the HOMO-LUMO gap.
- To study the influence of various D/A units on photophysical, thermal and electrochemical properties.
- To improve the photonic properties of truxene derivatives by incorporating TCNE and TCNQ acceptors.
- To design and synthesize new donor-acceptor molecules for optoelectronic applications.

Chapter 1: Introduction

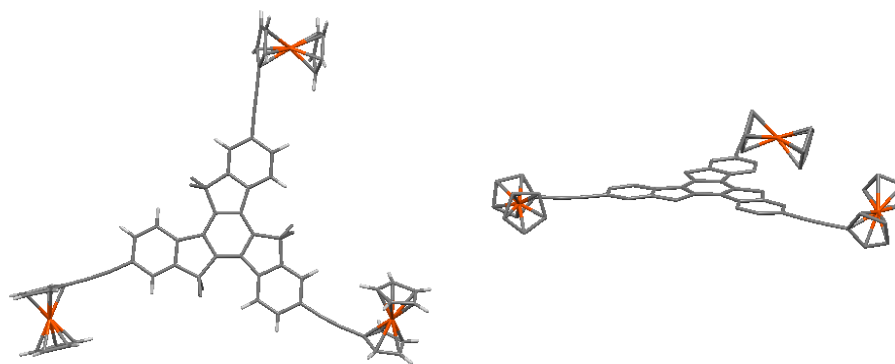
This chapter describes the synthesis and functionalization approaches of truxene derivatives, and their applications in different fields.

Chapter 2: Materials and Experimental Techniques

Chapter 2 summarizes the general experimental methods, characterization techniques and details of instruments used for characterization.

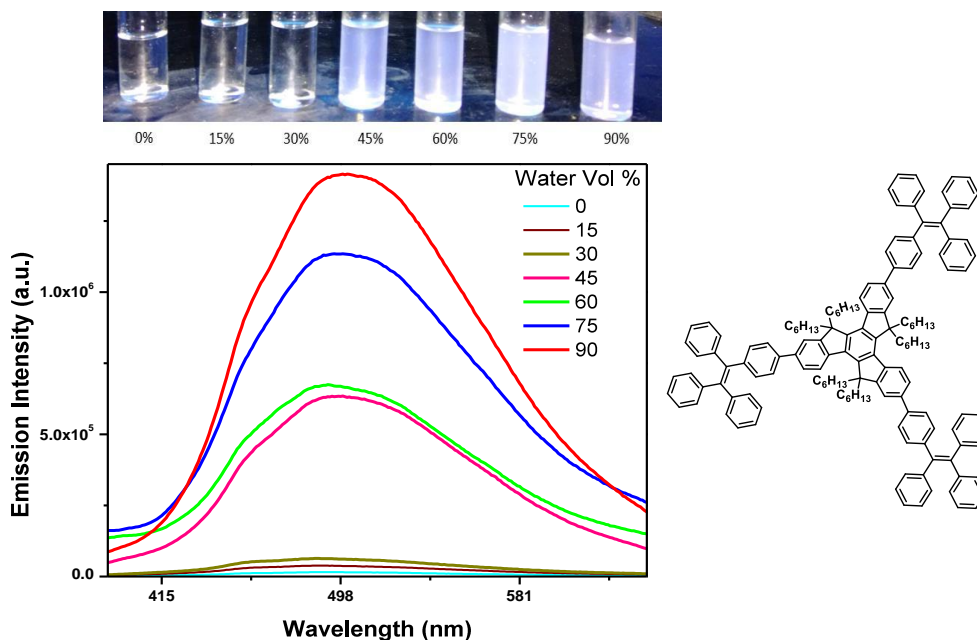
Chapter 3: Star Shaped Ferrocenyl Truxenes: Synthesis, Structure and Properties

Chapter 3 describes a series of donor–acceptor ferrocenyl substituted truxenes, synthesized by the Pd-catalyzed Sonogashira cross-coupling and Cycloaddition reactions. The electronic absorption and electrochemical studies of these truxenes show effective electronic interaction, which can be tuned by the introduction of different spacers.



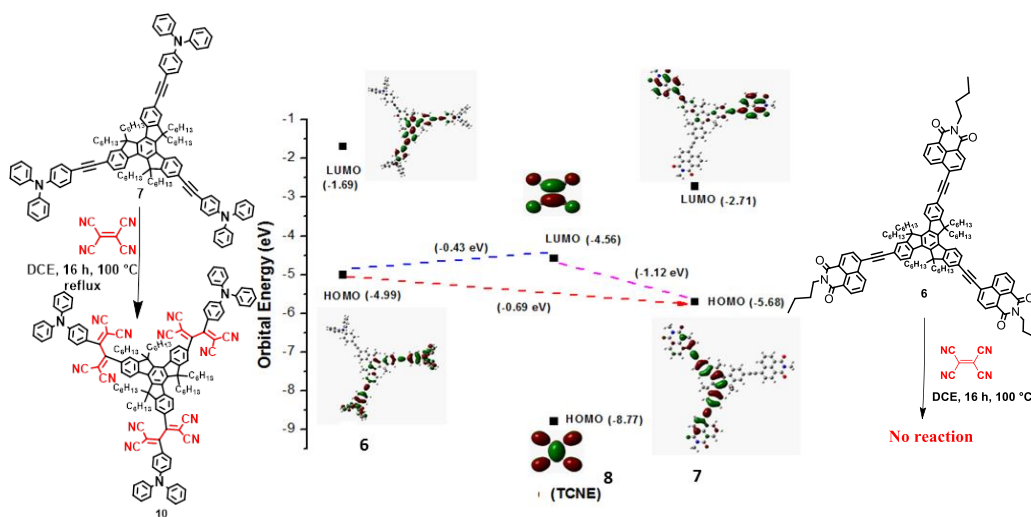
Chapter 4: Strategy Towards Tuning the Emission Behaviour of Star Shaped Tetraphenylethene Substituted Truxenes

Chapter 4 summarizes the synthesis of star shaped, C_3 -symmetric, tetraphenylethene (TPE) and 2,3,3-triphenyl acrylonitrile (TPAN) substituted truxenes by the Pd-catalyzed Suzuki and Sonogashira cross-coupling reactions. The TPE substituted truxenes show aggregation-induced emission (AIE) behavior, whereas TPAN substituted truxene shows aggregation-caused quenching (ACQ) effect in THF/water medium due to the π - π stacking. The computational calculation on truxenes was performed, which reveals that, electron density transfers from truxene to TPAN core.



Chapter 5: C₃-Symmetric Star Shaped Donor-Acceptor Truxenes: Synthesis, Photophysical, Electrochemical and Computational Studies

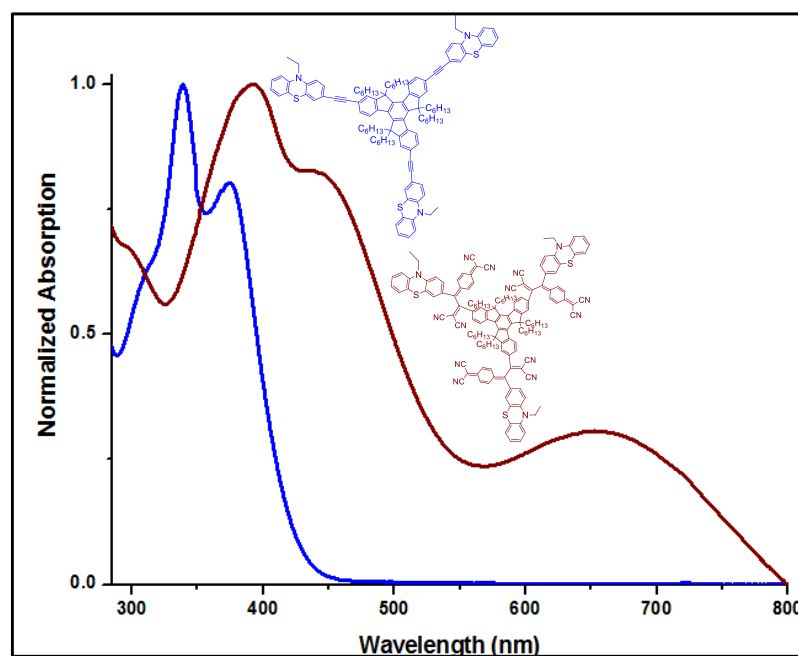
Chapter 5 reports the design and synthesis of donor and acceptor substituted truxenes using Pd-catalyzed Sonogashira cross-coupling and [2+2] Cycloaddition-retroelectrocyclization reactions. Their photophysical, electrochemical and computational studies were explored, which exhibits strong donor-acceptor interaction and effective tuning of the HOMO–LUMO gap. The computational studies reveal that the TCNE and TCNQ substituted truxenes exhibit lower HOMO–LUMO gap. The reaction pathway of [2+2] Cycloaddition-retroelectrocyclization was studied by computational calculations, which reveals that, the donor substituted truxene is favourable, whereas acceptor substituted truxene is not favourable for Cycloaddition-retroelectrocyclization reactions.



Chapter 6: Phenothiazene Based 1,1,4,4–Tetracyanobuta–1,3–Diene (TCBD) Substituted Donor-Acceptor Truxenes: Synthesis, Photophysical and Electrochemical Properties

Chapter 6 describes the synthesis of phenothiazene substituted truxenes, 1,1,4,4–tetracyanobuta–1,3–diene (TCBD) and cyclohexa–2,5–diene–1,4–ylidene–

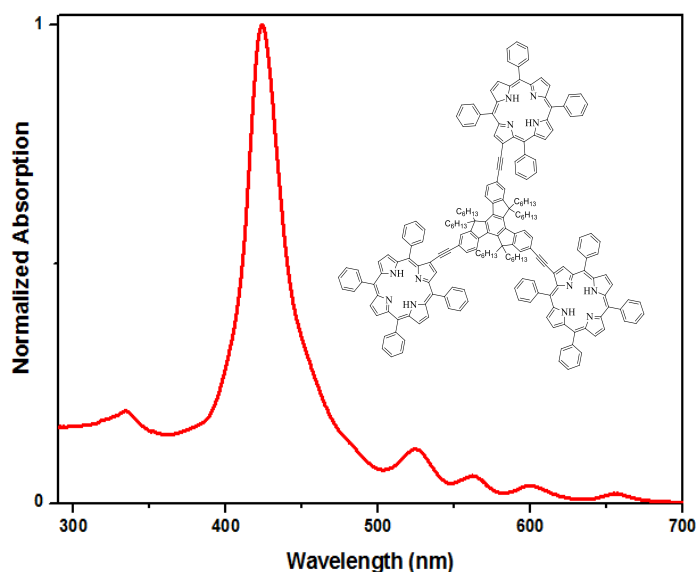
expanded TCBD functionalized donor-acceptor truxenes by using the Ullmann coupling, Pd-catalyzed Sonogashira cross-coupling and [2+2] Cycloaddition-retroelectrocyclization reactions. Their photophysical, electrochemical and thermal properties were studied. The effect of substitution through different positions of phenothiazine unit on truxene core was explored. The substitution through N-position (10-position) enhances the thermal stability of truxene compared to 3-position of phenothiazine. The incorporation of TCNE and TCNQ leads to red shifted absorption resulting in low HOMO–LUMO gap which was supported by DFT calculations.



Chapter 7: β -Substituted Truxene Porphyrins: Synthesis and Photophysical Properties

The Chapter 7 describes design and synthesis of the π -conjugated, β -Substituted truxene porphyrin and its metalated derivative by using the Pd-catalyzed Sonogashira cross-coupling and metalation reaction. Their photophysical properties were explored, which reveals that the substitution of porphyrin results in bathochromic shift of absorbance and fluorescence maxima. The results

indicate that there is considerable electronic communication between truxene core and porphyrin ring.



Chapter 8: Conclusions and Future Scope.

Chapter 8 summarizes the salient features of the work and its future prospects to develop the new materials for optoelectronic applications.

LIST OF PUBLICATIONS

1. Misra* R., **Sharma R.**, Mobin S. M., (2014), Star Shaped Ferrocenyl Truxenes: Synthesis, Structure and Properties, *Dalton Trans.*, 43, 6891-6896 (DOI: 10.1039/C4DT00210E).[†]
2. **Sharma R.**, Maragani R., Misra, R.,* (2018), C_3 -Symmetric Star Shaped Donor-Acceptor Truxenes: Synthesis, Photophysical, Electrochemical and Computational Studies, *New J. Chem.*, 42, 882–890, (DOI: 10.1039/C7NJ03934D).[†]

3. **Sharma R.**, Volyniuk D., Popli C., Bezvikonnyi O., Grazulevicius J. V., Misra R. (2018), Strategy Towards Tuning Emission of Star Shaped Tetraphenylethene Substituted Truxenes for Sky-Blue and Greenish-White OLEDs, *J. Phys. Chem. C*, 122, 15614–15624 (DOI: 10.1021/acs.jpcc.8b00777). †
4. **Sharma R.**, Gautam P., Misra R.,* Shukla S. K. (2015), β -Substituted triarylborane appended porphyrins: photophysical properties and anion sensing, *RSC Adv.*, 5, 27069-27074 (DOI: 10.1039/C5RA03931B).
5. **Sharma R.**, Gautam P., Mobin S. M., Misra R.* (2013), β -Substituted ferrocenyl porphyrins: synthesis, structure, and properties *Dalton Trans.*, 42, 5539-5545 (DOI: 10.1039/C3DT00003F).
6. **Sharma R.**, Maragani R, Mobin S. M., Misra R.* (2013), Ferrocenyl substituted calixarenes: synthesis, structure and properties, *RSC Adv.*, 3, 5785–5788 (DOI: 10.1039/C3RA00146F).
7. **Sharma R.**, Maragani, R., Misra R.* (2016), Ferrocenyl azadipyromethene and aza-BODIPY: Synthesis and properties, *J. Organomet. Chem.*, 825, (DOI: org/10.1016/j.jorganchem.2016.10.019).
8. Misra R.,* Gautam P., **Sharma R.**, Mobin S. M. (2013), Donor– π –acceptor– π –donor ferrocenyl benzothiadiazoles: synthesis, structure, and properties, *Tetrahedron Lett.*, 54, 381-383 (DOI: 10.1016/j.tetlet.2012.11.016).
9. Singh C. P., **Sharma R.**, Shukla V., Khundrakpam P., Misra R.,* Bindra K.S., Chari, R. (2014), Optical limiting and nonlinear optical studies of ferrocenyl substituted calixarenes, *Chem. Phys. Lett.*, 616, 189–195 (DOI: 10.1016/j.cplett.2014.10.030).
10. Maragani R., **Sharma R.**, Misra R.* (2017), Donor-Acceptor Triphenylvinyl and Tetraphenyl Conjugates: Synthesis, Aggregation and Computational Studies, *ChemistrySelect*, 2, 10033–10037 (DOI: 10.1002/slct.201701373).

11. Maragani R., Bijesh S., **Sharma R.**, Misra R.* (2017), *Cs*-Symmetric Donor–Acceptor Bis(thiazole)s: Synthesis and Photophysical, Electrochemical, and Computational Studies *Asian J. Org. Chem.*, 6, 1408-1414 (DOI: 10.1002/ajoc.201700274).
12. Misra R*., Jadhav T., Dhokale B., Gautham P., **Sharma R.**, Maragani R. (2014), Carbazole-BODIPY conjugates: design, synthesis, structure and properties, *Dalton Trans.*, 43, 13076 (DOI: 10.1039/c4dt00983e).

†Papers pertaining to the thesis.

TABLE OF CONTENTS

1. List of Figures	xxiv
2. List of Schemes	xxx
3. List of Tables	xxxii
4. Acronyms	xxxiv
5. Nomenclature	xxxv
Chapter 1: Introduction	
1.1. Background	1
1.2. Truxene	2
1.2.1. Different types of truxenes	4
1.2.2. Synthesis of truxene	4
1.3. Synthesis of other truxene derivatives:	5
1.3.1. Hexa-peri-hexabenzocoronene fused truxene derivative	
1.3.2. Fused truxene trimer	7
1.3.3. Cross-coupling of 5,10,15 hexahexylated 2,7,12 tri-iodo truxene	7
1.4. Applications of truxene derivatives	13
1.4.1. Nonlinear optics (NLO)	13
1.4.2. Dye sensitized solar cells (DSSCs)	15
1.4.3. Bulk heterojunction (BHJ) solar cells	16
1.4.7. Sensing	20
1.5. Organization of thesis	21
1.6. References	22
Chapter 2: Materials and experimental techniques	
2.1. Introduction	32
2.2. Chemicals for synthesis	32
2.3. Spectroscopic measurements	32
2.3.1. Mass spectrometry	32
2.3.2. NMR spectroscopy	32
2.3.3. UV-vis spectroscopy	33
2.3.4. Fluorescence spectroscopy	33

2.4	Electrochemical studies	33
2.5.	Single crystal X-ray diffraction studies	34
2.6	Powder X-ray diffraction (PXRD) studies	34
2.7	Computational calculations	34
2.8.	References	34
Chapter 3: Star Shaped Ferrocenyl Truxenes: Synthesis, Structure and Properties		
3.1.	Introduction	36
3.2.	Results and discussion	37
3.3.	Thermal properties	38
3.4.	Single crystal X-ray diffraction studies	39
3.5.	Photophysical properties	41
3.6.	Electrochemical propeties	43
3.7.	Experimental section	45
3.8.	Conclusions	48
3.10.	References	48
Chapter 4: Strategy Towards Tuning Emission of Star Shaped Tetraphenylethene Substituted Truxenes		
4.1.	Introduction	53
4.2.	Results and discussion	54
4.3.	Photophysical properties	56
4.4.	Aggregation study	57
4.5.	Computational calculations	59
4.6.	Experimental section	62
4.7.	Conclusions	64
4.8.	References	65

Chapter 5: C_3 -Symmetric Star Shaped Donor-Acceptor Truxenes: Synthesis, Photophysical, Electrochemical and Computational Studies

5.1.	Introduction	69
5.2.	Results and discussion	70
5.4.	Photophysical properties	74
5.5.	Electrochemical properties	75
5.6.	Theoretical calculations	77
5.7.	Experimental details	81
5.8.	Conclusions	84
5.9.	References	85
Chapter 6: Phenothiazene Based 1,1,4,4-Tetracyanobuta-1,3-Diene (TCBD) Substituted Donor-Acceptor Truxenes: Synthesis, Photophysical and Electrochemical Properties		
6.1.	Introduction	94
6.2.	Results and discussion	95
6.3.	Thermal stability	96
6.4.	Photophysical properties	97
6.5.	Electrochemical properties	99
6.6.	Theoretical calculations	100
6.7.	Experimental section	105
6.8.	Conclusions	107
6.9.	References	108
Chapter 7: β-Substituted Truxene Porphyrins: Synthesis and Photophysical Properties		
7.1.	Introduction	117
7.2.	Results and discussion	118
7.3.	Photophysical properties	120
7.4.	Theoretical calculations	122
7.5.	Experimental section	124
7.6.	Conclusions	125
7.7.	References	126
Chapter 8: Conclusions and future scope		

8.1.	Conclusions	131
8.2.	Future scope	132
8.3.	References	133

LIST OF FIGURES

Chapter 1. Introduction

Figure 1.1.	Different type of donors and acceptors.	1
Figure 1.2.	Effect of molecular orbital couplings of donor and acceptor systems on HOMO–LUMO gap.	2
Figure 1.3.	The molecular structure of truxene core.	2
Figure 1.4.	Single crystal X-ray structure of ferrocenyl substituted truxene	2
Figure 1.5.	Different types of truxene	4
Figure 1.6.	Molecular structure of triphenylamine-substituted truxene derivative.	13
Figure 1.7.	Molecular structures of two-photon absorbing truxene derivatives.	14
Figure 1.8.	Structures of triphenylamine substituted truxenes for DSSCs..	15
Figure 1.9.	Structures of truxene substituted triphenylamine for DSSCs.	16
Figure 1.10.	Structures of truxene based molecules for BHJ solar cell.	17
Figure 1.11.	Synthesis of truxene based molecules for OLEDs.	18
Figure 1.12.	Structures of thiophene substituted truxene for OFETs.	19
Figure 1.13.	Structures of truxene derivatives for self-assembly.	19
Figure 1.14.	Structures of truxene based molecule for explosive detection	20
Figure 1.15.	Structure of triarylborane substituted truxene for	

	F ⁻ ion detection	21
Chapter 3:	Star Shaped Ferrocenyl Truxenes: Synthesis, Structure and Properties	
Figure 3.1.	TGA plots of truxenes 4a–4c and 5a .	39
Figure 3.2.	Single crystal X-ray structure of compound 4a (a) Front view, and (b) Side view.	40
Figure 3.3.	The supramolecular structure of compound 4a along <i>b</i> axis. The secondary interactions are shown by dashed lines.	40
Figure 3.4.	Normalized electronic absorption spectra of truxenes 4a–4c and 5a .	41
Figure 3.5.	Cyclic voltammogram of 1.0×10^{-3} M solutions of compound 4a–4c and 5a in CH ₂ Cl ₂ containing 0.1M Bu ₄ NPF ₆ as supporting electrolyte, recorded at a scan speed of 100 mVs ⁻¹ .	43
Chapter 4:	Strategy Towards Tuning Emission of Star Shaped Tetraphenylethene Substituted Truxenes	
Figure 4.1.	TGA plots of truxene 7–9 .	56
Figure 4.2.	(a) Normalized electronic absorption and (b) fluorescence spectra of the solutions of truxenes 7 , 8 , and 9 in tetrahydrofuran at RT.	57
Figure 4.3.	Emission spectra of truxenes 7 (a), 8 (b), and 9 (c) (10^{-5} M) in THF/H ₂ O mixtures with different volume fractions of water. ($\lambda_{\text{ex}} = 283$ nm). Fluorescence color images of the truxenes in the presence of different THF/Water mixtures under UV light are presented above graphs.	58

- Figure 4.4.** The DFT optimized structures of the truxenes **7**, **8** and **9** with Gaussian 09 at the B3LYP/6-31G** level of theory. 60
- Figure 4.5.** The comparison of experimental and calculated (TD-DFT) at CAMB3LYP absorption spectrum the truxenes **7**, **8** and **9** in THF solution. 60
- Figure 4.6.** The energy level diagram of the frontier molecular orbitals of the TPE and TPAN substituted truxenes **7**, **8** and **9** using B3LYP/6-31G(d,p) level of DFT theory. 61
- Chapter 5: C_3 -Symmetric Star Shaped Donor-Acceptor Truxenes: Synthesis, Photophysical, Electrochemical and Computational Studies.**
- Figure 5.1.** The Gibbs free energy differences of the truxenes **6** and **7** by using 6-311+g(d,p)/B3LYP at 100 °C in 1,2-dichloroethane solvent. 72
- Figure 5.2.** The HOMO and LUMO molecular orbitals of truxene **7**, TCNE and truxene **6**. 73
- Figure 5.3.** TGA plots of truxenes **6**, **7**, **10** and **11**. 73
- Figure 5.4.** Normalized electronic absorption spectra of truxene **6**, **7**, **10** and **11** and fluorescence spectra of truxenes **6** and **7** (1.0×10^{-5} M concentration) in dichloromethane. 74
- Figure 5.5.** Truxenes **6**, **7**, **10** and **11** at 1×10^{-5} M concentration in dichloromethane in day light. 75
- Figure 5.6.** Cyclic voltammogram of 1.0×10^{-4} M solutions of truxenes **6**, **7**, **10** and **11** in CH_2Cl_2 containing 0.1M Bu_4NPF_6 as supporting electrolyte, recorded at a scan speed of 100 mV s^{-1} . 76
- Figure 5.7.** The comparison of experimental and calculated (TD-DFT at CAM-B3LYP level) absorption spectrum of truxene **6**, **7** in 1,2-dichloroethane solution. 78

Figure 5.8.	The major transitions in truxene 6 and 7	79
Figure 5.9.	The DFT optimized structures of the truxenes 6 , 7 , 10 and 11 with Gaussian 09 at the B3LYP/6-31G** level of theory.	79
Figure 5.10.	The energy level diagram of the frontier molecular orbitals of the truxenes 6 , 7 , 10 and 11 calculated using B3LYP/6-31G(d,p) level of DFT theory.	81
Chapter 6:	Phenothiazene Based 1,1,4,4-Tetracyanobuta-1,3-Diene (TCBD) Substituted Donor-Acceptor Truxenes: Synthesis, Photophysical and Electrochemical Properties	
Figure 6.1.	TGA plots of truxenes 4-7 .	97
Figure 6.2.	(a) Normalized electronic absorption spectra of truxene 4-7 and (b) fluorescence spectra of truxenes 4 and 5 (1.0×10^{-5} M concentration) in dichloromethane.	98
Figure 6.3.	Truxenes 4-7 at 1×10^{-5} M concentration in dichloromethane in day light.	98
Figure 6.4.	Cyclic voltammogram of 1.0×10^{-4} M solutions of truxene 4 in CH_2Cl_2 containing 0.1M Bu_4NPF_6 as supporting electrolyte, recorded at a scan speed of 100 mV s^{-1}	99
Figure 6.5.	The DFT optimized structures of the truxenes 4-7 with Gaussian 09 at the B3LYP/6-31G** level of theory.	101
Figure 6.6.	The comparison of experimental and calculated (TD-DFT at CAM-B3LYP level) absorption spectrum of truxene 4-7 in DCM solution.	102
Figure 6.7.	The major transitions in truxene 4 and 5	103

Figure 6.8. The energy level diagram of the frontier molecular orbitals of the truxenes **4–7** using B3LYP/6-31G(d,p) level of DFT theory. 104

Chapter 7: β -Substituted Truxene Porphyrins: Synthesis and Photophysical Properties

Figure 7.1. (a) Electronic absorption spectra of the **TPP**, **ZnTPP** and porphyrin substituted truxene **4** and **5** at 1.0×10^{-6} M concentration, recorded in dichloromethane. The inset shows enlarged view.

(b) Emission spectra of **TPP**, **ZnTPP** and porphyrin substituted truxene **4** and **5**. 121

Figure 7.2. The DFT optimized structure of porphyrin substituted truxene **4** and **5** using B3LYP level. The 6-31G** basis set for C, N, H and LANL2DZ for Zn. 123

LIST OF SCHEMES

Chapter 1. Introduction

- Scheme 1.1.** Synthetic scheme for the preparation of truxene and its iodo derivative. 5
- Scheme 1.2.** Synthesis of hexa-*peri*-hexabenzocoronene truxene derivative. 6
- Scheme 1.3.** Synthesis of star-shaped compounds with truxene core and cyclo-octatetraene core. *o*-DCB = ortho-dichlorobenzene. 7
- Scheme 1.4.** Synthesis of star shaped fluorene substituted truxene derivatives *via* Suzuki cross-coupling reaction 8
- Scheme 1.5.** Synthesis of truxene derivatives *via* Suzuki cross-coupling reaction of pinacol esters of truxene. 8
- Scheme 1.6.** Synthesis of truxene derivatives *via* Suzuki cross-coupling reaction using pinacol esters. 9
- Scheme 1.7.** Synthesis of truxene derivative *via* Sonogashira cross-coupling reaction. 9

Scheme 1.8. Synthesis of truxene derivatives <i>via</i> Sonogashira cross-coupling reaction.	10
Scheme 1.9. Synthesis of truxene derivative <i>via</i> Stille coupling reaction.	11
Scheme 1.10. Synthesis of star shaped truxene derivative <i>via</i> Heck coupling.	12
Scheme 1.11. Synthesis of truxene formylated derivative.	13
Chapter 3: Star Shaped Ferrocenyl Truxenes: Synthesis, Structure and Properties	
Scheme 3.1. Synthesis of ferrocenyl substituted truxenes 4a-4c .	37
Scheme 3.2. Synthesis of truxene 5a	38
Chapter 4: Strategy Towards Tuning Emission of Star Shaped Tetraphenylethene Substituted Truxenes	
Scheme 4.1. Synthesis of tri-iodotruxene 3 .	54
Scheme 4.2: Synthesis of TPE and TPAN substituted truxenes 7, 8 and 9	55
Chapter 5: C₃-Symmetric Star Shaped Donor-Acceptor Truxenes: Synthesis, Photophysical, Electrochemical and Computational Studies	
Scheme 5.1. Synthesis of tri-iodotruxene	71
Scheme 5.2: Synthesis of donor/acceptor substituted truxenes 6, 7, 10 and 11 .	72
Chapter 6: Phenothiazene Based 1,1,4,4-Tetracyanobuta-1,3-Diene (TCBD) Substituted Donor-Acceptor Truxenes: Synthesis, Photophysical and Electrochemical Properties	
Scheme 6.1. Synthesis of phenothiazine substituted truxenes 4-7 .	96
Chapter 7: β-Substituted Truxene Porphyrins: Synthesis and Photophysical Properties	
Scheme 7.1: Synthesis of ethynyl truxene 3 .	119

Scheme 7.2: Synthesis of porphyrin substituted truxene **4** and **5**. 120

LIST OF TABLES

Chapter 3: Star Shaped Ferrocenyl Truxenes: Synthesis, Structure and Properties

Table 3.1. Crystal data and structure refinement parameter for truxene **4a**. 42

Table 3.2. Photophysical and electrochemical data of ferrocenyl truxenes **4a–4c** and **5a**. 44

Chapter 4: Strategy Towards Tuning Emission of Star Shaped Tetraphenylethene Substituted Truxenes

Table 4.1. Photophysical and thermal properties of truxenes **7**, **8**, and **9**. 57

Table 4.2. Computed vertical transition energies and their Oscillator strengths (*f*) and major contributions for the truxene **7–9**. 62

Chapter 5: C₃-Symmetric Star Shaped Donor-Acceptor Truxenes: Synthesis, Photophysical, Electrochemical and Computational Studies

Table 5.1. Photophysical and electrochemical data of truxenes **6**, **7**, **10** and **11**. 75

Table 5.2. Computed vertical transition energies and their Oscillator strengths (*f*) and major contributions for the truxenes **6**, **7**, **10** and **11** 80

Chapter 6: Phenothiazene Based 1,1,4,4-Tetracyanobuta-1,3-Diene (TCBD) Substituted Donor-Acceptor Truxenes: Synthesis, Photophysical and Electrochemical Properties

Table 6.1. Photophysical and electrochemical data of truxenes **4–7** 101

Table 6.2. Computed vertical transition energies and their Oscillator strengths (*f*) and major contributions for the truxene **4–7** 103

**Chapter 7: β -Substituted Truxene Porphyrins: Synthesis and
Photophysical Properties**

Table 7.1. Absorption and emission data of porphyrin substituted truxene **4**
and **5** 122

ACRONYMS

D–A	Donor–acceptor
NLO	Nonlinear Optical
p ^H	The negative logarithm of hydronium ion concentration (- log ₁₀ [H ₃ O ⁺])
SCXRD	Single Crystal X-ray diffraction
PXRD	Powder X-ray diffraction
NMR	Nuclear Magnetic Resonance
PPh ₃	Triphenylphosphin
DMF	Dimethylformamide
DCM	Dichloromethane
TGA	Thermogravimetric Analysis
Ph	phenyl
IR	Infrared
UV-Vis	UV-Visible Spectroscopy
•••	Represents interaction
Calcd.	Calculated
CDCl ₃	Chloroform-d
ESI-MS	Electrospray Ionization- Mass Spectrometry
EtOH	Ethanol
MeOH	Methanol
THF	Tetrahydrofuran
TLC	Thin Layer Chromatography
TEA	Triethylamine

NOMENCLATURE

λ	Wavelength
ε	Extinction coefficient
α	Alfa
β	Beta
γ	Gamma
π	Pi
ϕ	Fluorescence quantum yield
σ	Sigma
\AA	Angstrom
Nm	Nanometer
Cm	Centimeter
$^{\circ}$	Degree
$^{\circ}\text{C}$	Degree Centigrade
mmol	Millimol
mL	Milliliter
μL	Microliter
a. u.	Arbitrary Unit

Chapter 1

Introduction

1.1. Background

The development of novel π -conjugated donor–acceptor (D–A) molecular systems have drawn immense attention of the scientific community due to their potential applications in multi-photon absorption, organic light emitting diodes (OLEDs) bioimaging and organic solar cells.^{1,2} The molecular systems with two and three dimensional structure exhibit better photophysical properties compared to the molecules with one dimensional structure.^{3,4} The photophysical properties of the π -conjugated D–A molecular systems can be tuned by altering its HOMO-LUMO gap.^{5,6}

In donor-acceptor systems the electron transfers from the donor to acceptor. In this process, the electrons are excited from HOMO to LUMO energy level which results in the formation of charge-transfer band. The tuning of charge transfer band in D–A systems is a significant factor for material science applications such as Organic photovoltaics (OPVs) and Organic field effect transistors (OFETs).^{7–16} The linkage of electron rich donor (D) and electron deficient acceptor (A) either directly or through a π -linker is the most common approach to tune the HOMO–LUMO gap.^{17,18}

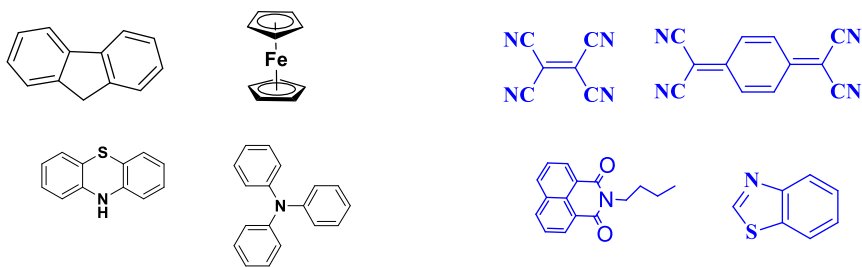


Figure 1.1. Different type of donors (black) and acceptors (blue)

The effect of orbital couplings of donor and acceptor on HOMO–LUMO gap is well-described by the molecular orbital (MO) theory (Figure 1.2). According to

the molecular orbital (MO) theory the donor groups have larger HOMO–LUMO gap as compared to the acceptor. However the donor-acceptor systems show smaller HOMO–LUMO gap as compared to the donor and acceptor units (Figure 1.2).¹⁹

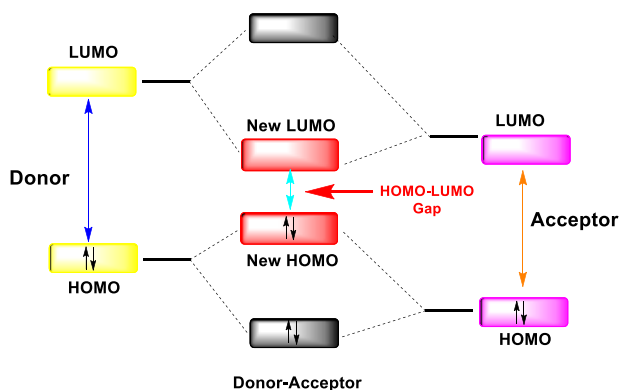
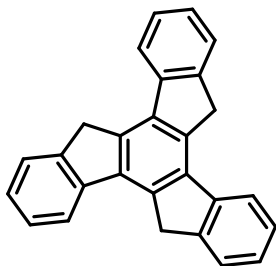


Figure 1.2. Effect of molecular orbital couplings of donor and acceptor systems on HOMO–LUMO gap.

1.2. Truxene

Among various polycyclic compounds, the heptacyclic polyarene truxene (10,15-dihydro-5*H*-diindeno[1,2-*a*;10,20-*c*]fluorene) has been recognized as an excellent starting material for the construction of larger polyarenes and bowlshaped fragments of fullerenes, liquid crystals, and C_3 -tripod materials in asymmetric catalysis and chiral recognition.^{20,21} Truxene is a planar polyaromatic hydrocarbon obtained by trimerization of indan-1-one, which represents a fusion of three fluorene moieties in such a way, that it leads to a C_3 -symmetric structure (Figure 1.3)²²



10,15-dihydro-5*H*-diindeno[1,2-*a*:1',2'-*c*]fluorene

Figure 1.3. The molecular structure of truxene core.

Truxene molecule have branched structure that consist of linear arms joined together by a central core. Similar to dendrimers, truxene molecule possesses well-defined molecular structures as well as superior chemical purity. In addition, they retain the solution-processability and precisely designable properties of polymers in device fabrication.²³ The C_3 -symmetric architecture with conjugated arms would bring new optical and morphological properties to the system. Truxene is a star shaped planar structure. The planar configuration was also confirmed in ferrocenyl truxene.²² The substitution at para position (2, 7, 12 positions) of truxene core results in a variety of π -delocalized molecular systems.

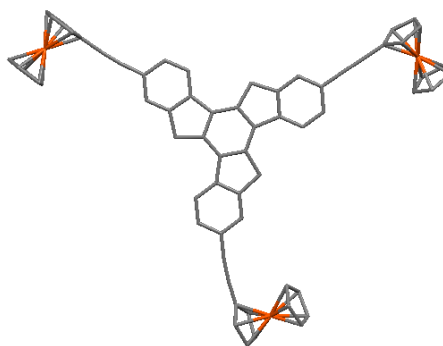


Figure 1.4. Single crystal X-ray structure of ferrocenyl substituted truxene (alkyl groups and hydrogens are removed for clarity)

Truxene scaffold appears to be a potential building block for the construction of larger molecular architectures owing to the following reasons:

1. Truxene has a large π -conjugated system and multi reactive sites which can further offer the extension of π -conjugation which leads to diverse derivatives.
2. Truxene has rigid planar structure and after alkylation it provides excellent solubility.
3. Truxene based donor-acceptor (D–A) systems exhibit excellent photochemical and thermal stability.

4. Due to the extended π -delocalized system truxene derivatives result in a significant red shift of the electronic absorption spectrum with high molar extinction coefficient.

1.2.1. Different types of truxenes:

Different types of symmetrical truxene and asymmetrical isotruxene and truxenone are reported in Literature based on the substitution pattern.²⁴ Truxene based donor-acceptor molecular systems are potential candidates for applications in two-photon absorption, organic light-emitting diodes (OLED), organic fluorescent probes and optoelectronic devices.²⁵⁻³⁰

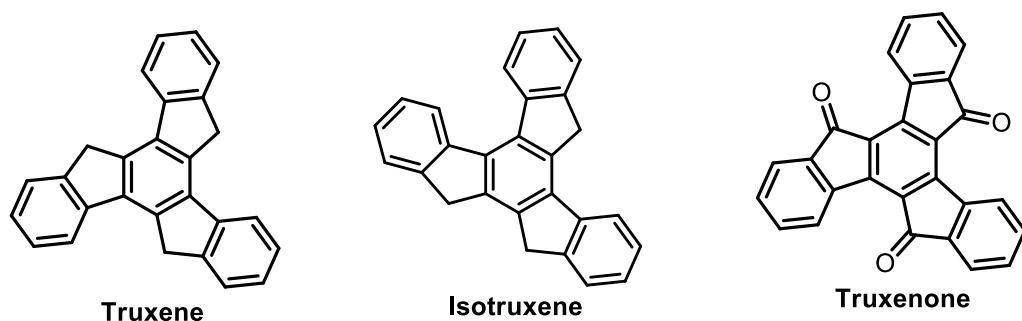
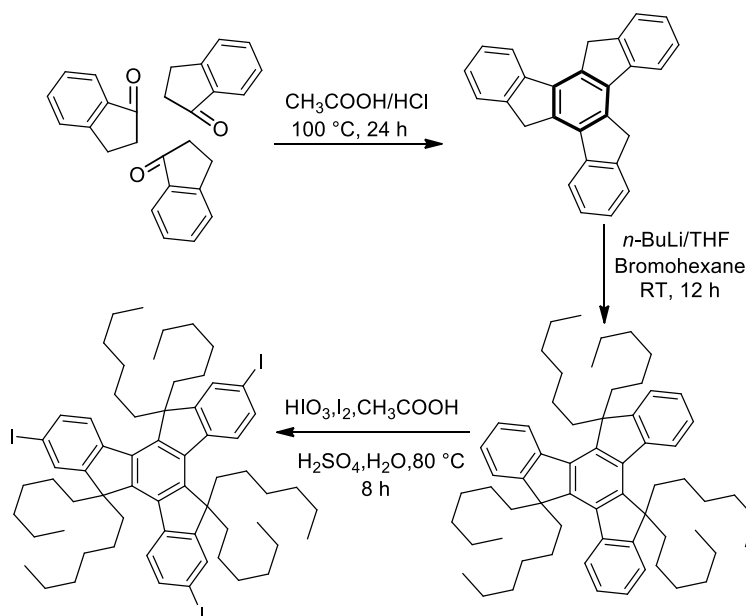


Figure 1.5. Different types of truxene

1.2.2. Synthesis of truxene:

The truxene core was synthesized by 1-indanone in the presence of acetic acid and hydrochloric acid.³¹ Truxene exhibits poor solubility due to its flat disc like conformation. Therefore, in order to improve the solubility six hexyl groups were attached at the C-5, C-10, and C-15 positions of the truxene moiety by alkylation reaction using bromo-hexane, which resulted readily soluble hexahexylated truxene.³¹ The iodination reaction of truxene in the presence of HIO_3 and I_2 resulted in tri-iodo truxene in 80% yield (Scheme 1.1).³²



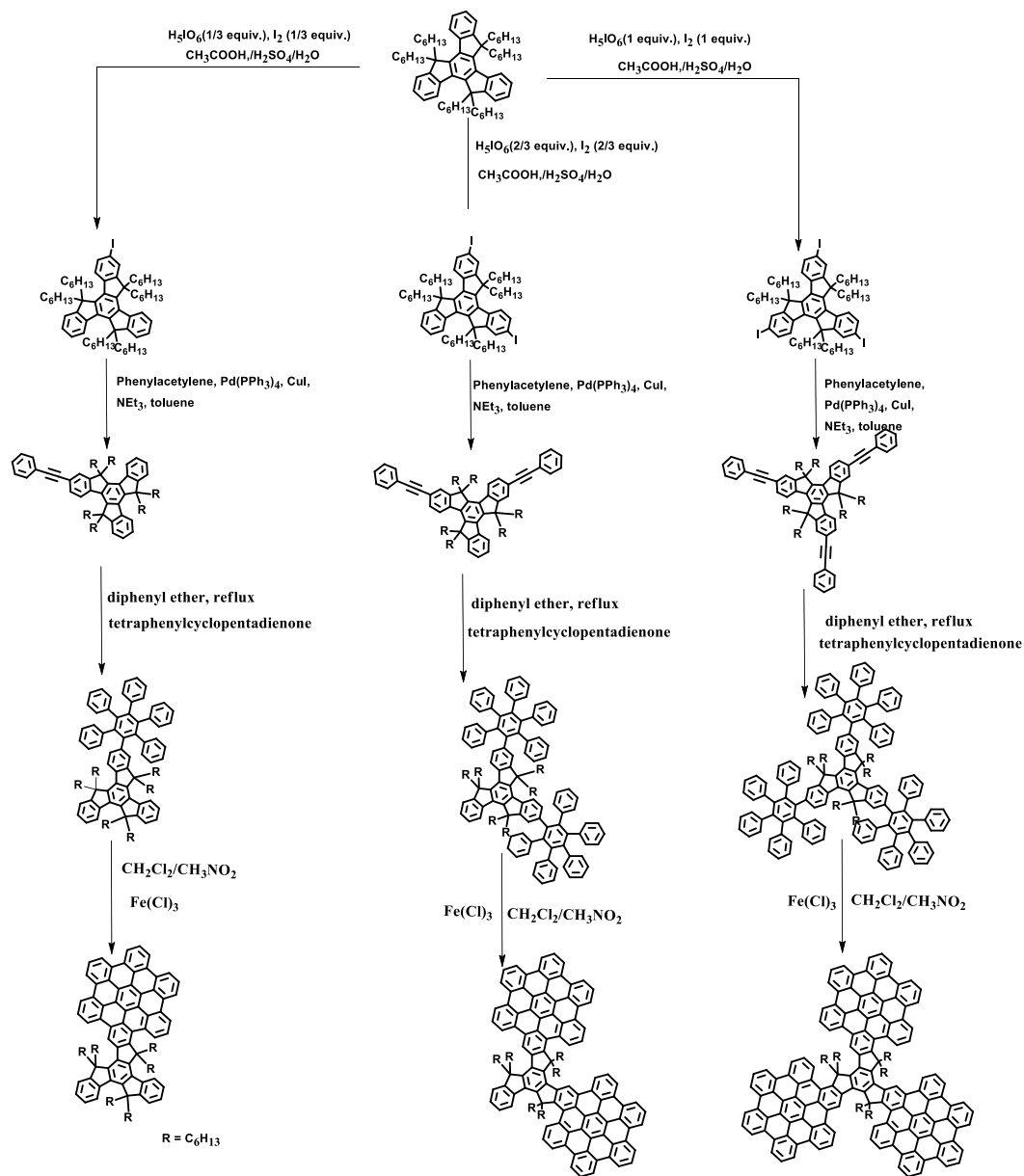
Scheme 1.1. Synthetic scheme for the preparation of truxene and its iodo derivative.

1.3. Synthesis of other truxene derivatives:

The synthetic methodology for the synthesis of different type of truxene based derivatives is summarized in the following sections.

1.3.1. Hexa-*peri*-hexabenzocoronene fused truxene derivative:

Truxene based polycyclic aromatics containing hexa-*peri*-hexabenzocoronene (HBC) was synthesized by employing oxidation by FeCl_3 (Scheme 1.2). Truxene core and HBCs were connected by sharing the same benzene rings. Three PAHs comprising respectively one, two and three hexa-*peri*-hexabenzocoronene units were synthesized starting from the highly soluble hexahexyltruxene (Scheme 1.2). In first step, truxene was iodinated using H_5IO_6 and I_2 under acidic conditions and the mono, bis and tris-iodinated truxene could be selectively prepared. Then, the Sonogashira cross-coupling reaction with phenylacetylene and finally, Diels-Alder reactions with tetraphenylcyclopentadiene followed by an oxidative cyclodehydrogenation with FeCl_3 , furnished the three targeted PAHs. This strategy greatly expands the π -conjugation, and at the same time, maintains the maximum rigidity of the molecule. As a result, the truxene cored HBC exhibits the highest degree of aggregation in solution compared with common HBC derivatives.³³

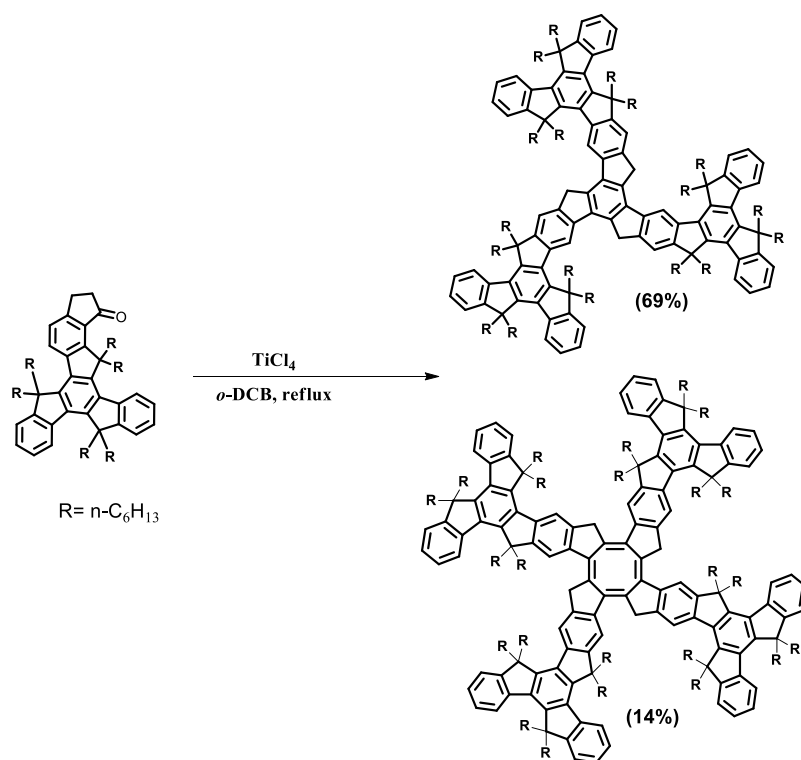


Scheme 1.2. Synthesis of hexa-*peri*-hexabenzocoronene truxene derivative.

1.3.2. Fused truxene trimer:

Truxenes can also be fused together through a smart synthetic strategy. The TiCl_4 -promoted cyclization reaction results the planar truxene core trimer efficiently through in situ generation of the benzene skeleton, as both branches and core are

connected by sharing benzene rings. The tubelike cyclo-octatetraene (COT) tetramer was also isolated unexpectedly (Scheme 1.3).³⁴



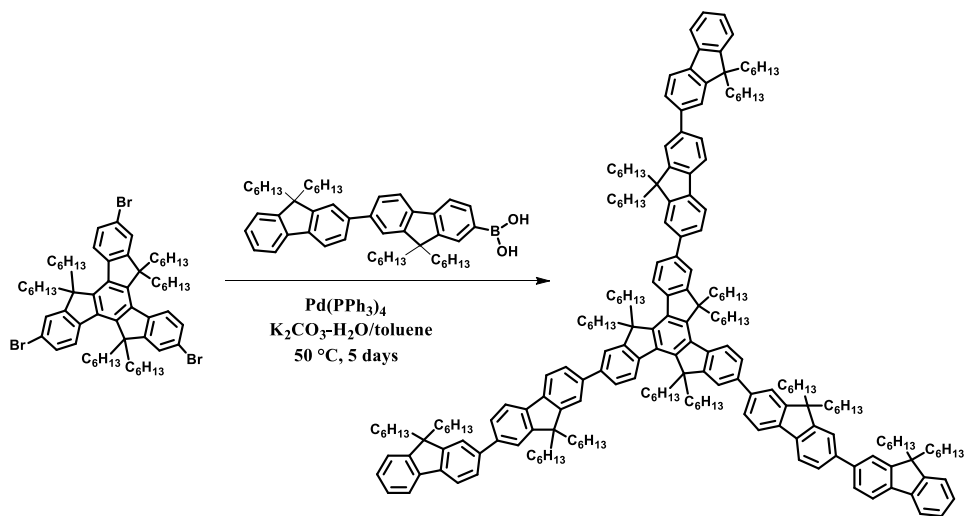
Scheme 1.3. Synthesis of star-shaped compounds with truxene core and cyclo-octatetraene core. *o*-DCB = ortho-dichlorobenzene.

1.3.3. Cross-coupling of 5,10,15 hexahexylated 2,7,12 tri-iodo truxene:

The synthesis of various truxene derivatives has been done by using Pd-catalyzed cross-coupling reaction of the 5,10,15 hexahexylated 2,7,12 tri-iodo truxene with the different type of aryl groups.

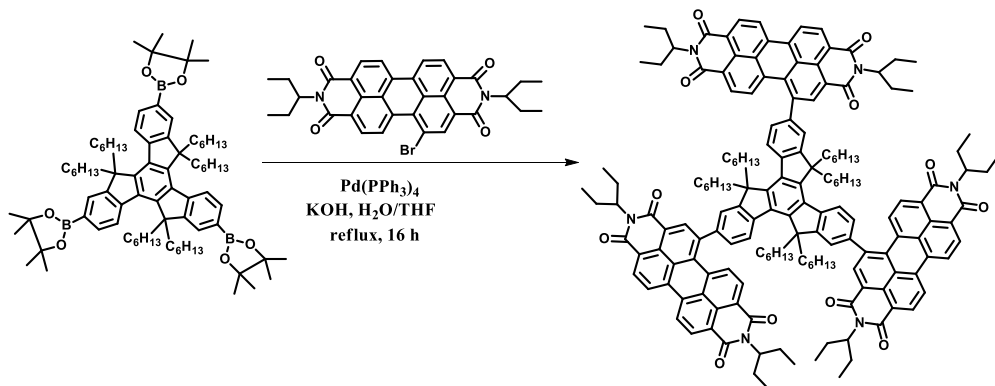
Suzuki Coupling: The design and synthesis of donor–acceptor truxene derivatives *via* the Pd-catalyzed Suzuki cross-coupling reaction is one of the most commonly used procedure. This procedure usually involves the reaction of 5,10,15 hexahexylated 2,7,12 tri-iodo truxene and arylboronic acids or esters in the presence of palladium catalysts-*tetrakis*(triphenylphosphine)palladium(0) [Pd(PPh₃)₄] and sodium or potassium carbonates as a base. Kanibolotsky *et al.* synthesized star-shaped oligofluorenes (from 1–4 fluorene units) with a central

truxene core and up to quaterfluorene arms by the reaction of tri-iodo truxene with fluorene boronic acids. In the case of four fluorene arms, the radius of the macromolecule is ca. 4 nm, which represents the largest known conjugated system (Scheme 1.4).³⁵



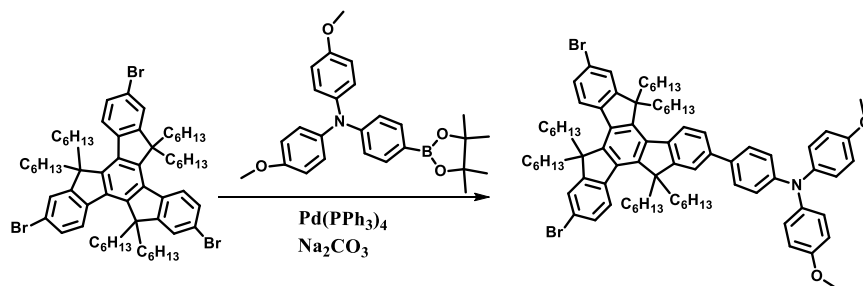
Scheme 1.4. Synthesis of star shaped fluorene substituted truxene derivatives *via* Suzuki cross-coupling reaction

Alternatively the Suzuki cross-coupling reaction has also been carried out with the pinacol esters of truxene in good yields (Scheme 1.5).³⁶



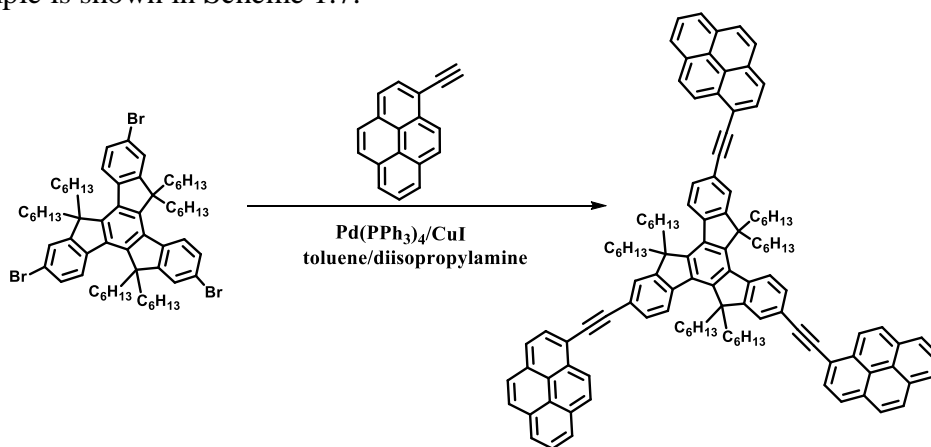
Scheme 1.5. Synthesis of truxene derivatives *via* Suzuki cross-coupling reaction of pinacol esters of truxene.

Yu *et al.* designed and synthesized various triphenyl amine substituted truxens using pinacol esters for dye sensitized solar cell applications.³⁷ One of the example is shown as follows-



Scheme 1.6. Synthesis of truxene derivatives *via* Suzuki cross-coupling reaction using pinacol esters.

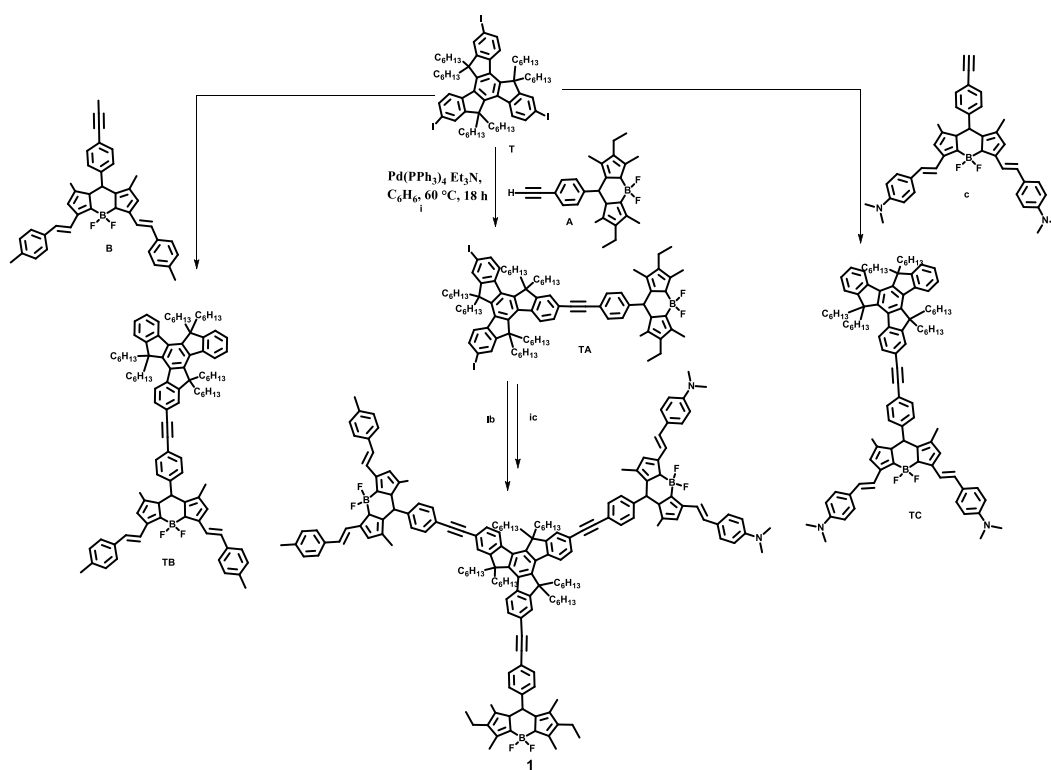
Sonogashira Coupling: The Pd-catalyzed Sonogashira cross-coupling is a significant procedure for the design and synthesis of donor–acceptor π -conjugated truxenes. The Sonogashira coupling involves the reaction of the tribromo truxene and the alkyne derivative with catalytic amounts of *tetrakis*(triphenylphosphine)palladium(0) [Pd(PPh₃)₄] and copper(I) iodide in the presence of an organic base (triethylamine or diisopropylamine). A common example is shown in Scheme 1.7.³⁸



Scheme 1.7. Synthesis of truxene derivative *via* Sonogashira cross-coupling reaction.

Raymond Ziessel *et al.* synthesized a novel star-shaped supramolecular system containing three different bodipy dyes logically arranged around a truxene core. Bodipy dyes and truxene species are compatible systems from a photochemical

point of view, since they absorb at different wavelengths (essentially UV region for truxene species, visible for the Bodipy dyes), so they can be addressed separately, to a large extent. By taking advantage of the structural and photophysical properties of truxene derivatives and Bodipy molecules, the target multichromophoric truxene **1** comprising separate Bodipys residues (abbreviated A, B, and C) was prepared in three steps from the preformed truxene platform **T** bearing three iodo functions (Scheme 1.8).

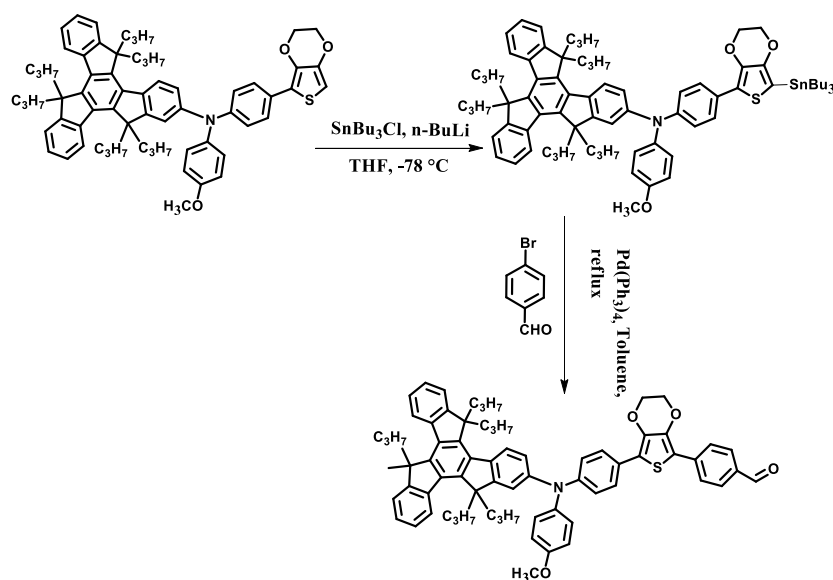


Scheme 1.8. Synthesis of truxene derivatives *via* Sonogashira cross-coupling reaction.

The key intermediate of the synthetic strategy is the step-by-step introduction of the ethynyl grafted dye **A**, dye **B**, and dye **C**. All reactions are promoted by Pd(0), and the first step provides **TA** in 40% yield. Under such conditions, di- and trisubstituted compounds are isolated as side products. The cross-coupling between **TA** and successively **B** and **C** provides dye **1** in 27% overall yield. Likewise crosscoupling between **T** and dye **B** or **C** provides the reference dye **TB**

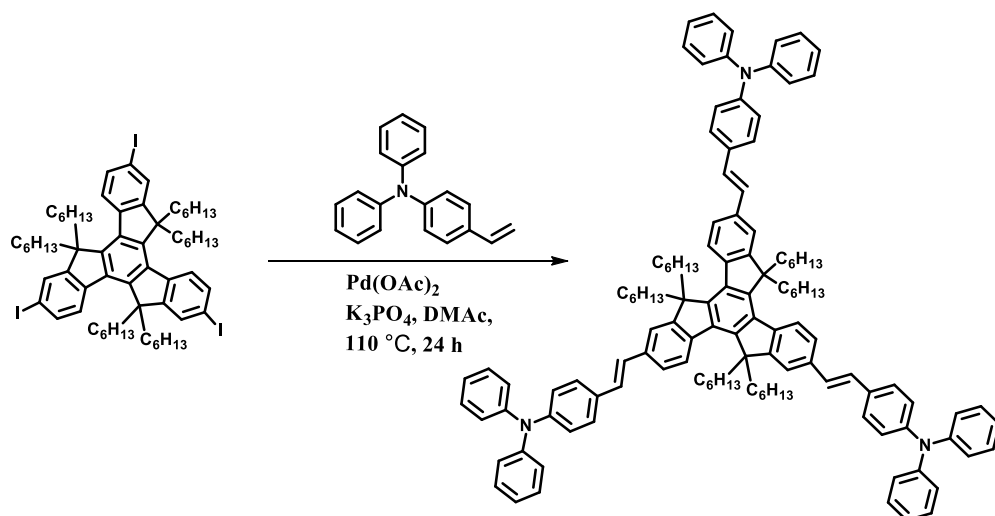
or TC in 22% and 19% yields, respectively. This is the first example of Bodipy and truxene chromophores are linked into the same molecule.^{38b}

Stille Coupling: The Pd-catalyzed Stille coupling reaction is alternative procedure for the synthesis of donor–acceptor truxenes. Zong *et al.* has introduced stannyl group at the truxene substituted derivative. Truxene stannyl compound was treated with bromo derivative in the presence of (triphenylphosphine)palladium(0) [Pd(PPh₃)₄].³⁹



Scheme 1.9. Synthesis of truxene derivative *via* Stille coupling reaction.

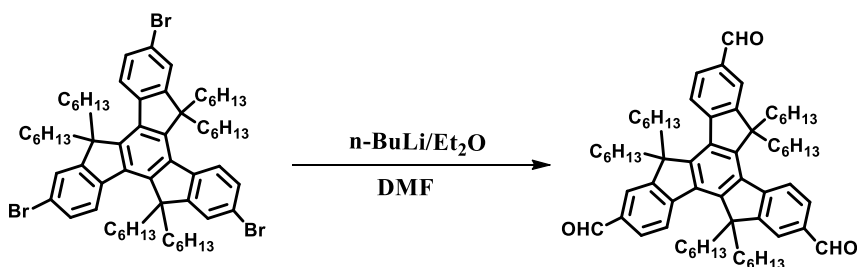
Heck Coupling: The Heck cross-coupling of 5,10,15 hexahexylated 2,7,12 tri-iodo truxene is a less commonly used procedure for the synthesis of truxene derivative as compared to the Suzuki and Sonogashira cross-coupling reactions. Nevertheless it is a significant procedure for incorporation of C=C bond for various optoelectronic applications. This procedure involves the reaction of 5,10,15 hexahexylated 2,7,12 tri-iodo truxene with alkenes catalyzed by palladium(II) acetate in the presence of a base as shown in Scheme 1.10.⁴⁰



Scheme 1.10. Synthesis of star shaped truxene derivative *via* Heck coupling.

Formylation reaction:

The formylation reaction is also an important procedure for the design and synthesis of donor–acceptor π -conjugated truxene derivatives. The normal conditions for formylation reaction involve the solution of tribromo truxene and *n*-BuLi in anhydrous ethyl ether at $-78\text{ }^\circ\text{C}$. After stirring for 0.5 h, mixture was allowed to warm to room temperature. Mixture was again cooled to $-78\text{ }^\circ\text{C}$, and DMF was added. The solution was stirred overnight while returning to room temperature. The final solution was acidified with 1M HCl solution and stirred for 2 h at room temperature. The aqueous phase was extracted with dichloromethane, and the organic layer was dried over magnesium sulfate. After evaporation of the solvent, the final crude product was purified by column chromatography on silica gel (PE/ $\text{CH}_2\text{Cl}_2=6:1$, *v/v*) to yield desired white solid (Scheme 1.11).⁴¹



Scheme 1.11. Synthesis of truxene formylated derivative.

1.4. Applications of truxene derivatives.

The star shaped donor–acceptor truxene based molecular systems have been explored for various applications. Some of the common applications are described below:

1.4.1. Nonlinear optics (NLO): There has been substantial attention in the improvement of organic nonlinear optical materials. The truxene core is a significant constructing block for NLO materials. Their octupolar character combined to their polyaromaticity and rigid planar skeleton is likely to result in more efficient NLO properties than the conventional dipolar molecules. Prasad *et al.* have designed a variety of donor-substituted truxene derivatives as a NLO material (Figure 1.6).⁴²

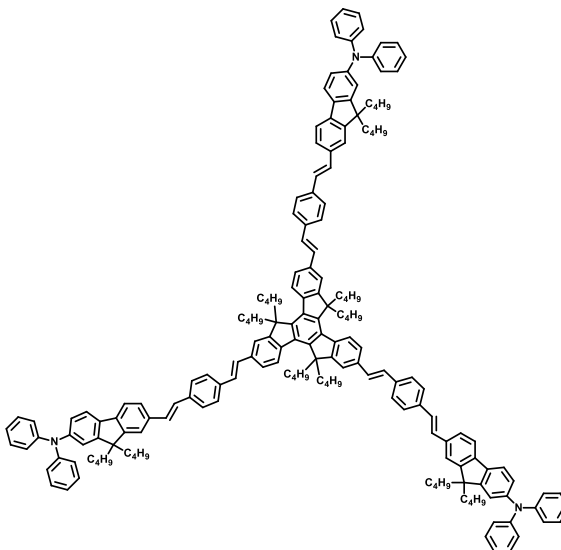


Figure 1.6. Molecular structure of triphenylamine-substituted truxene derivative.

The π -conjugated donor–acceptor organic materials with large two-photon absorption (TPA) cross-sections are prospective applicant for several applications such as optical limiting, two-photon laser scanning fluorescence imaging, three-dimensional optical data storage, and photodynamic therapy.⁴³⁻⁴⁸ The fluorophores with large TPA cross-sections are reported in the literature.⁴⁹⁻⁵² Prasad *et al.* and Wang *et al.* designed and synthesized different types of triphenylamine substituted truxene derivatives and explored their two-photon

absorption properties. The TPA cross-section was significantly high in C_3 -symmetric truxene derivatives as compared to other derivatives (Figure 1.7).⁵³

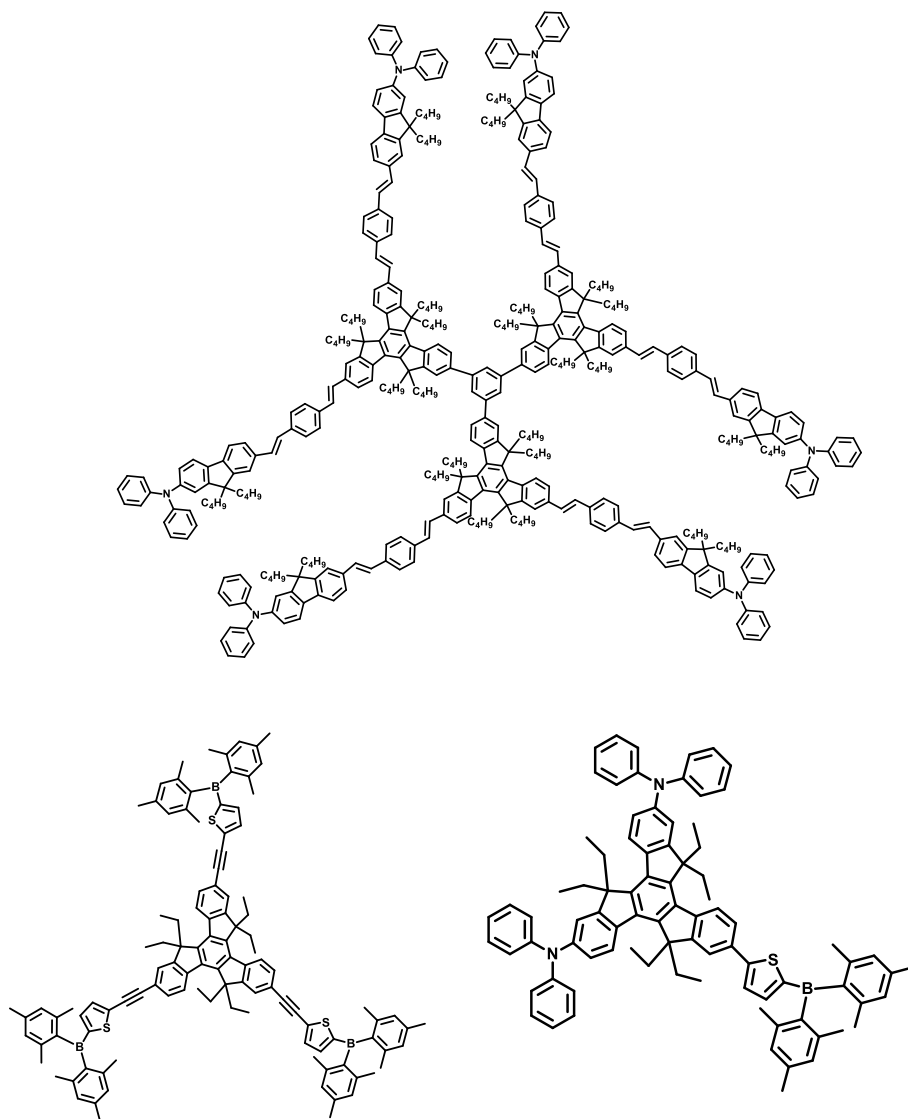


Figure 1.7. Molecular structures of two-photon absorbing truxene derivatives.

1.4.2. Dye sensitized solar cells (DSSCs):

O'Regan and Grätzel have reported polypyridyl ruthenium (II) complex adsorbed on a TiO_2 surface, which exhibited good efficiency in DSSC. In DSSC experiment the power conversion efficiency depends on the HOMO-LUMO gap

of donor-acceptor materials.⁵⁴⁻⁵⁹ Yu *et al.* reported a series of triphenylamine substituted truxene derivatives for DSSCs. The structure of triphenylamine substituted truxene derivatives are shown in the Figure 1.8.^{37,39}

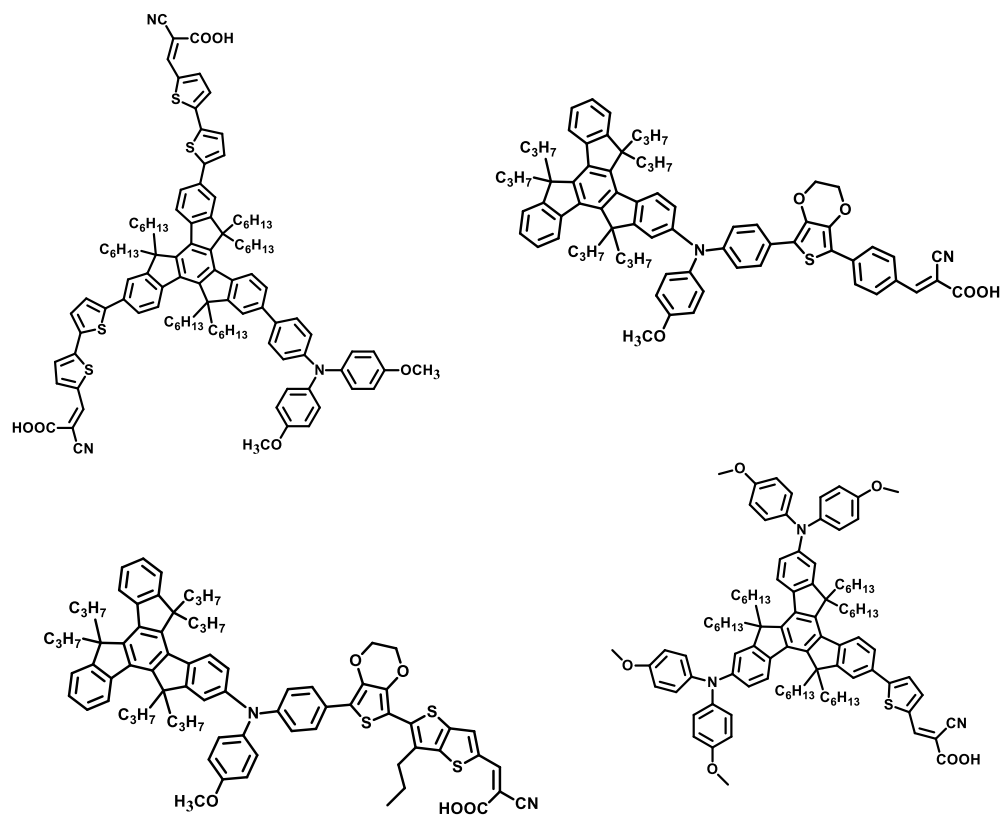
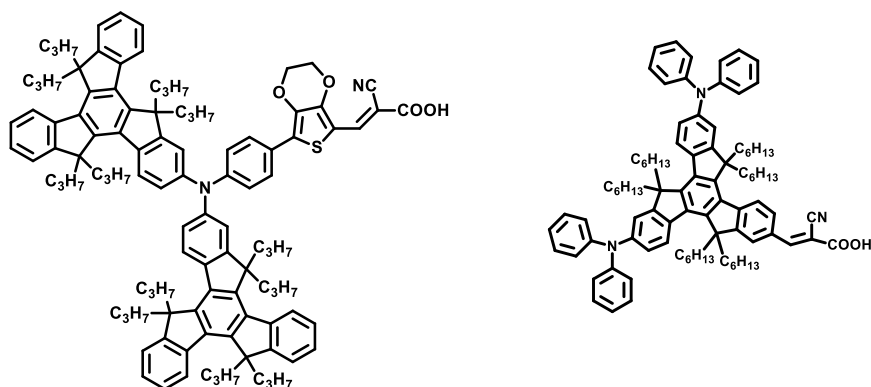


Figure 1.8. Structures of triphenylamine substituted truxenes for DSSCs. Similar type of truxene substituted triphenylamine compounds (Figure 1.9)⁶⁰ have been synthesized by Liang *et al.* and achieved power conversion efficiency over 6.13 % .



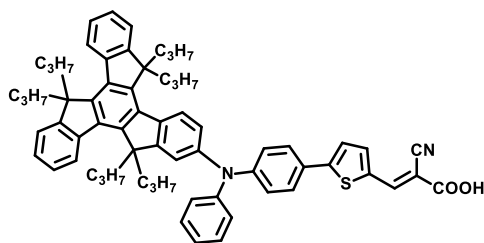


Figure 1.9. Structures of truxene substituted triphenylamine for DSSCs.

1.4.3. Bulk heterojunction (BHJ) solar cells:

The molecular systems having low HOMO-LUMO gap, strong charge transfer band are commonly used in bulk heterojunction (BHJ) solar cell devices.⁶¹ Compared with small molecules, the introduction of truxenes with hexyl substituents significantly decreases the aggregation of truxene derivatives and enhances the phase separation of D and A units in bulk heterojunction solar cells. Friend *et al.* and Heeger *et al.* first time reported bulk heterojunction (BHJ) solar cells in 1995.^{62,63}

A variety of low band gap truxene based donor-acceptor molecules have been designed and synthesized. Pie *et al.* synthesized a series of D- π -A molecules based on three chromophores- truxenes as nodes, TPA moieties as the donor units, and benzothiadiazole chromophores as the acceptor units. All D- π -A conjugated molecules show broad and strong absorption bands from 250 to 700 nm in thin films. By increasing the D-A ratio and changing the conjugated spacers between donor and acceptor, the PCE values continuously increased due to the increasing relative absorption intensity in the longer wavelength region. As a result, a PCE value up to 0.54% was obtained.⁶⁴

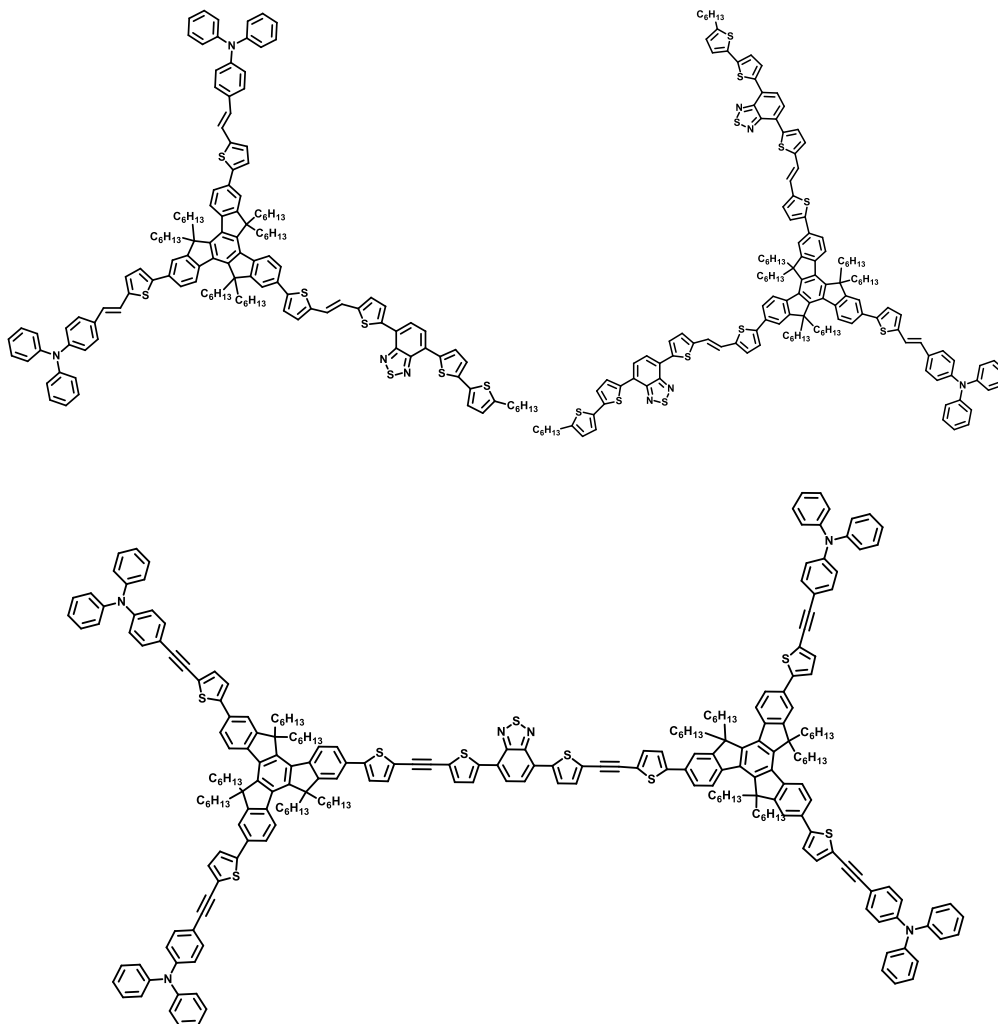


Figure 1.10. Structures of truxene based molecules for BHJ solar cell.

1.4.4. Organic light emitting diodes (OLEDs):

Organic Light Emitting Diodes (OLEDs) have become another major interest in the field of organic electronics. Since the pioneering works of Tang and Van Slyke on OLEDs, device elaboration has evolved towards multilayered devices with layers ensuring the different roles of charge injection and transport as well as emission.⁶⁵ The truxene derivatives exhibit the excellent blue-emitting property in OLED materials. Yao *et al.* synthesized a variety of truxene based derivatives and explored their OLED properties.⁶⁶

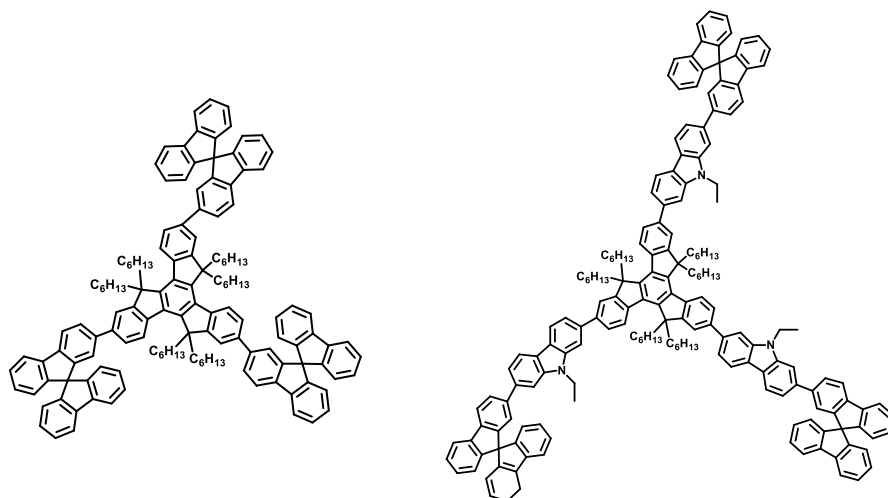


Figure 1.11. Synthesis of truxene based molecules for OLEDs.

1.4.5. Organic field-effect transistors (OFETs):

Organic field-effect transistors (OFETs) is considered one of the emerging field in optoelectronic applications.⁶⁷⁻⁷¹ The Koezuka group reported for the first time the use of organic materials in the Organic field-effect transistor (OFET) devices.⁷² Jian Pei *et al.* reported oligothiophene-functionalized truxene derivatives as good air-stable materials in p-channel OFETs. An increase in the oligothiophene length of the star-shaped molecules from 1 to 3 thiophenes leads to a dramatic decrease in hole mobility from 1.03×10^{-3} to $2.2 \times 10^{-4} \text{ cm}^2\text{V}^{-1}\text{s}^{-1}$.⁷³

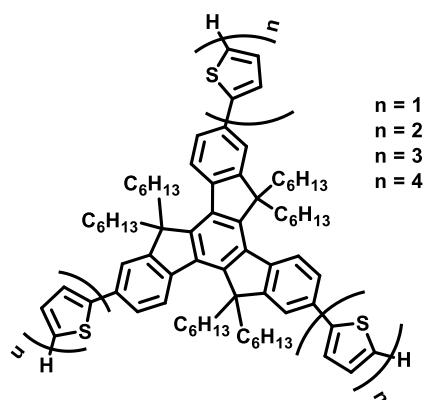


Figure 1.12. Structures of thiophene substituted truxene for OFETs.

1.4.6. Self-assembly and molecular wires:

Truxene was also used for two-dimensional monolayer structures on surface. These supramolecular networks were developed based on van-der Waals and hydrogen bonding interactions. As the first examples, supramolecular networks on highly oriented pyrolyted graphite resulting from the self-assembly. Modification of the molecular arrangement with the substitution of the elemental building-block was also demonstrated. Hence, higher density of molecules was observed for molecule shown Figure 1.13.

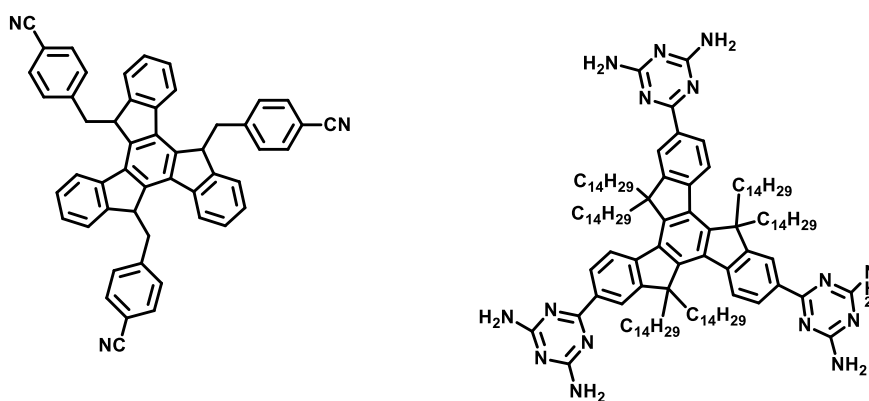


Figure 1.13. Structures of truxene derivatives for self-assembly.

These molecules have more tendency to stick together with the neighboring molecules by forming multi-hydrogen-bonds between tertriazine groups. If the former study mostly focused on the coverage density, the next one examined the diffusion behavior on surfaces. In this aim, a custom designed molecule (5,10,15-tris(4-cyanophenyl-methyl)truxene) was synthesized and a nanoscale structured KBr(001) surface was used.^{73b}

1.4.7. Sensing:

Recent literature reveals the use of truxene based derivatives used as a fluorescent sensor for explosive material.^{74,75} Sensing of nitro-group carrying arenes is an important task, as these species are not only degradation products of explosives contained in land mines, but also recognized as pollutants. Bunz *et al.*

reported truxene based molecules which could detect explosive analytes and successfully discriminate explosives as a fluorescent sensor for explosive materials.⁷⁶

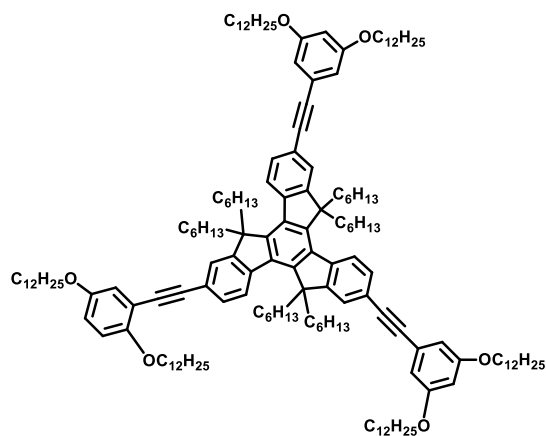


Figure 1.14. Structures of truxene based molecule for explosive detection

In another report, Yuan *et al.* have reported triarylborane substituted truxene derivative for fluoride ion detection.⁷⁷ Detection of fluoride ion is of interest because of their importance towards human health and impact on the environment.⁷⁸⁻⁸⁰ The importance of this anion in the treatment of osteoporosis and dental care leads to the continuous pursuit of the design and synthesis of new selective fluoride ion sensors. The truxene derivative shown in Figure 1.15 selectively sense fluoride anions.

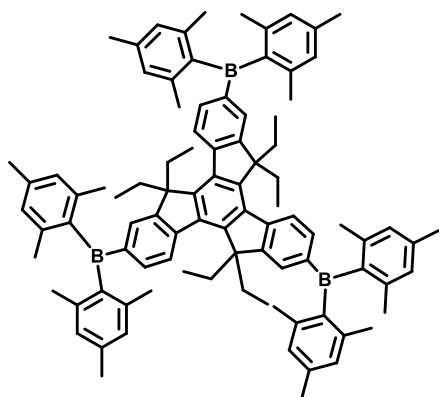


Figure 1.15. Structure of triarylborane substituted truxene for F⁻ ion detection

In this thesis truxene carrying different peripheral dye molecules (Ferrocene, Phenothiazene, Triphenyl amine and Porphyrin) have been synthesized for optoelectronic applications. The effect of substitution of different donor and acceptor units on photophysical, thermal and electrochemical properties was explored. The photonic properties of truxene derivatives were tuned by incorporating TCNE and TCNQ acceptors.

1.5. Organization of thesis

Chapter 1: This chapter gives an outline of the special features, importance and various synthetic strategies for the design of truxene derivatives and their applications in diverse fields.

Chapter 2: This chapter summarizes the instrumentation and general methods used for the present study.

Chapter 3: In this chapter, we describe a series of ferrocene-substituted truxenes and extended the conjugation length to tune the photonic properties.

Chapter 4: This chapter summarizes the synthesis of star shaped, C_3 -symmetric, tetraphenylethene (TPE) and 2,3,3-triphenyl acrylonitrile (TPAN) substituted truxenes. The aggregation-induced emission (AIE) behavior of truxene derivatives were investigated.

Chapter 5: Chapter 5 reports the design and synthesis of donor and acceptor substituted truxenes using Pd-catalyzed Sonogashira cross-coupling and [2+2] Cycloaddition-retroelectrocyclization reactions. The reaction pathway of [2+2] cycloaddition-retroelectrocyclization was studied by computational calculations.

Chapter 6: The Chapter 6 describes the synthesis of phenothiazene substituted truxenes, 1,1,4,4-tetracyanobuta-1,3-diene (TCBD) and cyclohexa-2,5-diene-1,4-ylidene-expanded TCBD functionalized donor-acceptor truxenes by using the Ullmann coupling, Pd-catalyzed Sonogashira cross-coupling and [2+2] Cycloaddition-retroelectrocyclization reactions. Their photophysical, electrochemical and thermal properties were studied. The effect of substitution through different positions of phenothiazine unit on truxene core was explored.

Chapter 7: The chapter 7 describes the design and synthesis of π -conjugated β -Substituted truxene porphyrin and its Zn-metalated derivative by using the Pd-

catalyzed Sonogashira cross-coupling and metalation reaction. Their photophysical properties were explored in this chapter.

Chapter 8: This chapter summarizes the noticeable features of the work and future prospects.

References

1. (a) Sonar P., Singh S. P., Li Y., Soh M. S., Dodabalapur A. (2010), A Low-Bandgap Diketopyrrolopyrrole Benzothiadiazole Based Copolymer for High-Mobility Ambipolar Organic Thin-Film Transistors, *Adv. Mater.*, 22, 5409–5413, (DOI: 10.1002/adma.201002973) (b) Kato S., Furuya T., Kobayashi A., Nitani M., Ie Y., Aso Y., Yoshihara T., Tobita S., Nakamura Y. (2012), Synthesis of Ladder-Type π -Conjugated Heteroacenes via Palladium-Catalyzed Double N-Arylation and Intramolecular O-Arylation, *J. Org. Chem.*, 77, 7595–7606, (DOI: 10.1021/jo070427p). (c) Omer K. M., Ku S. Y., Wong K. T., Bard A. J. (2009), Green Electrogenenerated Chemiluminescence of Highly Fluorescent Benzothiadiazole and Fluorene Derivatives, *J. Am. Chem. Soc.*, 131, 10733–10741, (DOI: 10.1021/ja904135y).
2. Kato S., Matsumoto T., Ishi-I T., Thiemann T., Shigeiwa M., Gorohmaru H., Maeda S., Yamashitad Y., Mataka S., (2004), Strongly red-fluorescent novel donor- π -bridge-acceptor- π -bridge-donor (D- π -A- π -D) type 2,1,3-benzothiadiazoles with enhanced two-photon absorption cross-sections, *Chem. Commun.*, 2342–2343, (DOI:10.1039/B410016F).
3. Jiang Y., Lu Y. X., Cui Y. X., Zhou Q. F., Ma Y., Pei J. (2007), Synthesis of Giant Rigid π -Conjugated Dendrimers, *Org. Lett.*, 4539–4542, (DOI: 10.1021/ol702063e).
4. Lo S. C., Burn P. L. (2007), Development of Dendrimers: Macromolecules for Use in Organic Light-Emitting Diodes and Solar Cells, *Chem. Rev.*, 107, 1097–1116, (DOI: 10.1021/cr050136l).
5. Zhang Q. T., Tour J. M. (1998), Alternating Donor/Acceptor Repeat Units in Polythiophenes. Intramolecular Charge Transfer for Reducing Band Gaps in Fully Substituted Conjugated Polymers, *J. Am. Chem. Soc.*, 120, 5355–5362, (DOI: 10.1021/ja972373e).
6. Gohier F., Frère P. R. (2013), 3-Fluoro-4-hexylthiophene as a Building Block for Tuning the Electronic Properties of Conjugated

- Polythiophenes, *J. Org. Chem.*, 78, 1497–1503, (DOI: 10.1021/jo302571u).
- Xu B., He J., Mu Y., Zhu Q., Wu S., Wang Y., Zhang Y., Jin C., Lo C., Chi Z., Lien A., Liua S., Xu J. (2015), Very bright mechano luminescence and remarkable mechanochromism using a tetraphenylethene derivative with aggregation-induced emission, *Chem. Sci.*, 6, 3236–3241 (DOI: 10.1039/C5SC00466G).
 - Lin Y., Cheng P., Liu Y., Shi Q., Hu W., Li Y., Zhan X. (2012), Small molecules based on bithiazole for solution-processed organic solar cells, *Organic Electronics* 13, 673-680 (DOI: 10.1016/j.orgel.2012.01.016).
 - Meyers F., Adant C., Bredas J. L. (1991), C₂-symmetric bis (phospholanes) and their use in highly enantioselective hydrogenation reactions, *J. Am. Chem. Soc.*, 113, 3709-3715 (DOI: 10.1021/ja00022a047).
 - Dehu C., Meyers F., Bred J. L. (1993), Donor-acceptor diphenylacetylenes: geometric structure, electronic structure, and second-order nonlinear optical properties, *J. Am. Chem. Soc.*, 115, 6187-6198 (DOI: 10.1021/ja00067a039).
 - Liu Y., Shi Q., Ma L., Dong H., Tan J., Hu W., Zhan X. (2014), Copolymers of benzo[1,2-*b*:4,5-*b'*]dithiophene and bithiazole for high-performance thin film phototransistors, *J. Mater. Chem. C.*, 2, 9505–9511 (DOI: 10.1039/C4TC01682C).
 - Cao J., Kamp J., Curtis M. D. (2003), Synthesis and Characterization of Bis (3,4-ethylene-dioxythiophene)-(4,4'-dialkyl-2,2'-bithiazole) Co-oligomers for Electronic Applications, *Chem. Mater.*, 15, 404-411 (DOI: 10.1021/cm020774+).
 - Li K. C., Huang K., Hsu Y. C., Huang P. J., Chu C. W., Lin J. T., Ho K. C., Wei K. H., Lin, H. C. (2009), Tunable Novel Cyclopentadithiophene-Based Copolymers Containing Various Numbers of Bithiazole and Thienyl Units for Organic Photovoltaic Cell Applications, *Macromolecules*, 42, 3681-3693 (DOI: 10.1021/ma900416d).
 - Wenjie Li., Katz H. E., Lovinger A. J., Laquindanum J. G. (1999), Field-Effect Transistors Based on Thiophene Hexamer Analogues with Diminished Electron Donor Strength, *Chem. Mater.*, 11, 458-465 (DOI: 10.1021/cm980672c).
 - Jadhav T., Dhokale B., Mobin S. M., Misra R. (2015), Mechanochromism and aggregation induced emission in benzothiazole substituted tetraphenylethylenes: a structure function

- correlation, *RSC Adv.*, 5, 29878-29884 (DOI: 10.1039/C5RA04881H).
16. Balan B., Vijayakumar C., Saeki A., Koizumi Y., Seki S. (2010), Anthradithio Phene-Containing Copolymers for Thin-Film Transistors and Photovoltaic Cells, *Macromolecules* 43, 6361–6367 (DOI: 10.1021/ma1001639).
 17. Štefko M., Tzirakis M. D., Ebert B. M. O., Dumele O., Schweizer W. B., Gisselbrecht J. P., Boudon C., Beels M. T., Biaggio I., Diederich, F. (2013), Donor–Acceptor (D–A)-Substituted Polyynes Chromophores: Modulation of Their Optoelectronic Properties by Varying the Length of the Acetylene Spacer, *Chem. –Eur. J.*, 19, 12693–12704, (DOI: 10.1002/chem.201301642).
 18. Gautam P., Misra R., Siddiqui S. A., Sharma G. D. (2015), Unsymmetrical Donor–Acceptor–Acceptor– π –Donor Type Benzothiadiazole-Based Small Molecule for a Solution Processed Bulk Heterojunction Organic Solar Cell, *ACS Appl. Mater. Interfaces*, 7, 10283–10292, (DOI: 10.1021/acsami.5b02250).
 19. Cheng C., Geng H., Yi Y., Shuai, Z. (2017), Super-exchange-induced high performance charge transport in donor–acceptor copolymers, *J. Mater. Chem. C*, 5, 3247-3253, (DOI: 10.1039/c6tc05534f).
 20. Perora T. S., Vij P. J. K. (1995), The influence of surface structure on the discotic liquid crystalline alignment. an infrared spectroscopy study, *Adv. Mater.*, 7, 919–922, (DOI: 10.1002/adma.19950071111).
 21. Boorum M. M., Vasil'ev Y. V., Drewello T., Scott L. T. (2001), Groundwork for a Rational Synthesis of C₆₀: Cyclodehydrogenation of a C₆₀H₃₀ Polyarene, *Science*, 294, 828–831, (DOI: 10.1126/science.1064250).
 22. Misra R., Sharma R., Mobin S. M. (2014), Star shaped ferrocenyl truxenes: synthesis, structure and properties. *Dalton Trans.*, 43, 689, (DOI:10.1039/C4DT00210E).
 23. Ke Shi, Jie-Yu Wang, Jian Pei, (2014), π -Conjugated Aromatics Based on Truxene: Synthesis, Self-Assembly, and Applications, *The Chemical record*, DOI: 10.1002/tcr.201402071.
 24. Goubard F., Dumur F. (2015), Truxene: a promising scaffold for future materials, *RSC Adv.*, 5, 3521–3551, (DOI:10.1039/C4RA11559G).
 25. Zong X., Liang M., Fan C., Tang K., Li G., Sun Z., Xue S. (2012), Design of Truxene-Based Organic Dyes for High-Efficiency Dye-Sensitized Solar Cells Employing Cobalt Redox Shuttle, *J. Phys. Chem. C*, 116, 11241–11250, (DOI: 10.1021/jp301406x). (b) Xie Y.,

- Zhang X., Xiao Y., Zhang Y., Zhou F., Qib J., Qu J. (2012), Fusing three perylenebisimide branches and a truxene core into a star-shaped chromophore with strong two-photon excited fluorescence and high photostability, *Chem. Commun.*, 48, 4338–4340, (DOI: 10.1039/C2CC31261A).
26. Yang Z., Xu B., He J., Xue L., Guo Q., Xia H., Tian W. (2009), Solution-processable and thermal-stable triphenylamine-based dendrimers with truxene cores as hole-transporting materials for organic light-emitting devices, *Org. Elec.*, 10, 954–959, (DOI: org/10.1016/j.orgel.2009.04.024).
27. Xua H. J., Dub B., Gros C. P., Richarda P., Barbea J. M., Pierre D. H. (2013), Shape-persistent poly-porphyrins assembled by a central truxene: synthesis, structure, and singlet energy transfer behaviors, *J. Porphyrins Phthalocyanines*, 17, 44–55, DOI: (10.1142/S1088424612501271).
28. (a) Kimura M., Kuwano S., Sawaki Y., Fujikawa H., Noda K., Taga Y., Takagi K. (2005), New 9-fluorene-type trispirocyclic compounds for thermally stable hole transport materials in OLEDs, *J. Mater. Chem.*, 15, 2393–2398, (DOI: 10.1039/B502268A). (b) Yuan M. S., Liu Z. Q., Fang Q. (2007), Donor-and-Acceptor Substituted Truxenes as Multifunctional Fluorescent Probes, *J. Org. Chem.*, 72, 7915–7922, (DOI: 10.1021/jo071064w).
29. Huang W., Smarsly E., Han J., Bender M., Seehafer K., Wacker I., Schröder R. R., Bunz U. H. F. (2017), Truxene-Based Hyperbranched Conjugated Polymers: Fluorescent Micelles Detect Explosives in Water, *ACS Appl. Mater. Interfaces*, 9, 3068–3074, (DOI: 10.1021/acsami.6b12419).
30. Ma L., Zhaoxin W., Guijiang Z., Fang Y., Yue Y., Chunliang Y., Shuya N., Xun H., Yu L., Shufeng, W., Qihuang G. (2015), The molecular picture of amplified spontaneous emission of star-shaped functionalized-truxene derivatives, *J. Mater. Chem. C*, 3, 7004–7013, (DOI: 10.1039/C5TC01040C).
31. Kanibolotsky A. L., Berridge R., Skabara P. J., Perepichka I. F., Bradley D. D. C., Koeberg M. (2004), Synthesis and properties of monodisperse oligofluorene-functionalized truxenes: highly fluorescent star-shaped architectures, *J. Am. Chem. Soc.*, 126, 13695, (DOI: 10.1021/ja039228n).
32. Cao X., Zi H., Zhang W., Lu H., Pei J. (2005), Star-Shaped and Linear Nanosized Molecules Functionalized with Hexa-peri-

- hexabenzocoronene: Synthesis and Optical Properties, *J. Org. Chem.*, 70, 3645-3653, (DOI: 10.1021/jo0480139).
33. Cao X., Zi H., Zhang W., Lu H., Pei J. (2005), Star-Shaped and Linear Nanosized Molecules Functionalized with Hexa-peri-hexabenzocoronene: Synthesis and Optical Properties, *J. Org. Chem.*, 70, 3645-3653, (DOI: 10.1021/jo0480139).
34. Zhang W., Cao X. Y., Zi H., Pei J. (2005), Single-molecule nanosized polycyclic aromatics with alternant five-and six-membered rings: synthesis and optical properties, *Org. Lett.*, 7, 959-962, (DOI: 10.1021/ol047625c).
35. Kanibolotsky A. L., Berridge R., Skabara P. J., Perepichka I. F., Bradley D. D. C., Koeberg M. (2004), Synthesis and properties of monodisperse oligofluorene-functionalized truxenes: highly fluorescent star-shaped architectures, *J. Am. Chem. Soc.*, 126, 13695, (DOI: 10.1021/ja039228n).
36. Xie Y., Zhang X., Xiao Y., Zhang Y., Zhou F., Qib J., Qu J. (2012), Fusing three perylenebisimide branches and a truxene core into a star-shaped chromophore with strong two-photon excited fluorescence and high photostability, *Chem. Commun.*, 48, 4338-4340, (DOI: 10.1039/C2CC31261A.)
37. Yu L., Xi J., Chan H., Su T., Antrobus L., Tong B., Dong Y., Kin Chan W., Phillips D. L. (2013), Novel Organic D- π -2A Sensitizer for Dye Sensitized Solar Cells and Its Electron Transfer Kinetics on TiO₂ Surface, *J. Phys. Chem. C*, 117, 2041-2052, (DOI: 10.1021/jp3113182).
38. (a) Tanga C., Liua X., Liua F., Wanga X., Xua H., Liua R., Ronga Z., Huanga W. (2013), π -Conjugated molecules based on truxene cores and pyrene substitution: synthesis and properties, *J. Chem. Research*. 242-247, (DOI:org/10.3184/174751913X13639408275103). (b) Diring S., Puntoriero F., Nastasi F., Campagna S., Ziessel R. (2009), Star-Shaped Multichromophoric Arrays from Bodipy Dyes Grafted on Truxene Core, *J. Am. Chem. Soc.*, 131, 6108-6110, (DOI: 10.1021/ja9015364).
39. Zong X., Liang M., Chen T., Jia J., Wang L., Sun Z., Xue S. (2012), Efficient iodine-free dye-sensitized solar cells employing truxene-based organic dyes, *Chem. Commun.*, 48, 6645-6647, (DOI:10.1039/C2CC32926C).
40. Yang Z., Xu B., He J., Xue L., Guo Q., Xia H., Tian W. (2009), Solution-processable and thermal-stable triphenylamine-based dendrimers with truxene cores as hole-transporting materials for

- organic light-emitting devices, *Organic Electronics*, 10 (2009) 954–959, (DOI:org/10.1016/j.orgel.2009.04.024).
41. Xua H., Dub B., Claude P., Richarda P., Barbea J., Harvey P. D. (2013), Shape-persistent poly-porphyrins assembled by a central truxene: synthesis, structure, and singlet energy transfer behaviors, *J. Porphyrins Phthalocyanines* 17 44–55, (DOI: 10.1142/S1088424612501271).
 42. Zheng Q., He G. S., Prasad P. N. (2005), Conjugated Dendritic Nanosized Chromophore with Enhanced Two-Photon Absorption, *Chem. Mater.* 17, 6004-6011, (DOI: 10.1021/cm051292b).
 43. Bhawalkar J. D., Kumar N. D., Zhao C. F., Prasad P. N. J. (1997), Two-photon photodynamic therapy, *Clin Laser Med Surg.*, 15, 201–202 (DOI: 10.1089/clm.1997.15.201).
 44. Brott L. L., Naik R. R., Pikas D. J. (2001), Ultrafast holographic nanopatterning of biocatalytically formed silica, *Nature*, 413, 291–296, (DOI :10.1038/35095031).
 45. Day D., Gu M., Smallridge A. (2001), Processing Additives for Improved Efficiency from Bulk Heterojunction Solar Cells, Rewritable 3D Bit Optical Data Storage in a PMMA-Based Photorefractive Polymer, *Adv Mater*, 13, 1005–1011, (DOI: 10.1002/1521-4095).
 46. Belfield K. D., Schafer K. J. (2002), Two-photon absorption and lasing properties of new fluorene derivatives *J. Chem Mater*, 14, 3656–3658 (DOI: 10.1039/B820950B).
 47. Belfield K. D., Liu Y., Negres R. A., Fan M., Pan G., Hagan D. J., Hernandez F. E. (2002), Linear and Two-Photon Photophysical Properties of a Series of Symmetrical Diphenylaminofluorenes, *Chem Mater*, 14, 3663–3665 (DOI: 10.1021/cm035253g).
 48. He G. S., Helgeson R., Lin T. C., Zheng Q., Wudl F., Prasad P. N. (2003), *IEEE J Quantum Electron.*, 39, 1003–1008 (DOI: 10.1109/JQE.2003.814372).
 49. He G. S., Lin T. C., Hsiao V. K. S., Cartwright A. N., Prasad P. N., Natarajan L. V., Tondiglia V. P., Jakubiak R., Vaia R. A., Bunning T. J. (2003), Synthesis, two-photon absorption, and optical power limiting of new linear and hyperbranched conjugated polyynes based on bithiazole and triphenylamine, *Appl Phys Lett.*, 83, 2733–2738 (DOI: 10.1002/pola.24608).
 50. Chandrasekhar V., Azhakar R., Murugesapandian B., Bag T. S. P., Pandey M. D., Maurya S. K., Goswami D. (2010), Synthesis, Structure, and Two-Photon Absorption Studies of

a Phosphorus-Based Tris Hydrazone Ligand (S)P[N(Me)N=CH-C₆H₃-2-OH-4 N(CH₂CH₃)₂]₃ and its Metal Complexes, *Inorg. Chem.*, 49, 4008–4016 (DOI: 10.1021/ic901531e)

51. Belfield K. D., Bondar M. V., Hernandez F. E., Przhonska O. V. (2008), Photophysical Characterization, Two-Photon Absorption and Optical Power Limiting of Two Fluorenylperylene Diimides, *J Phys Chem C.*, 112, 5618–5622 (DOI: 10.1021/jp711950z).
52. Qian Y., Meng K., Lu C. G., Lin B., Huang W., Cui Y. P. (2009), The synthesis, photophysical properties and two-photon absorption of triphenylamine multipolar chromophores, *Dyes Pigm.*, 80, 174–180. (DOI: org/10.1016/j.dyepig.2008.07.005).
53. Yuan M., Wang Q., Wang W., Wang D., Wang J., Wang J. (2014), Truxene-cored π -expanded triarylborane dyes as single and two-photon fluorescent probes for fluoride, *Analyst*, 139, 1541. DOI: 10.1039/c3an02179c.
54. O'Reagan B., Grätzel M. (1991), A low-cost, high-efficiency solar cell based on dye-sensitized colloidal TiO₂ films, *Nature*, 353, 737–740, (DOI: 10.1038/353737a0).
55. Mathew S., Yella A., Gao P., Humphry-Baker R., Curchod B. F., Ashari-Astani N., Tavernelli I., Rothlisberger U., Nazeeruddin M. K., Grätzel M. (2014), Dye-Sensitized Solar Cells with 13% Efficiency Achieved Through the Molecular Engineering of Porphyrin Sensitizers, *Nat. Chem.*, 6, 242–247, (DOI: 10.1038/nchem.1861).
56. Chen C. Y., Wang M., Li J. Y., Pootrakulchote N., Alibabaei L., Ngoc-le C. H., Decoppet J. D., Tsai J. H., Grätzel M., Wu S. M., Zakeeruddin C. G., Grätzel M. (2009), Highly Efficient Light-Harvesting Ruthenium Sensitizer for Thin-Film Dye-Sensitized Solar Cells, *ACS Nano.*, 3, 3103–3109 (DOI: /abs/10.1021/nn900756s).
57. Aghazada S. Gao P., Yella A., Marotta G., Moehl T., Teuscher J., Moser J. E., Angelis F. D., Grätzel M., Nazeeruddin M. K. (2016), Ligand Engineering for the Efficient Dye-Sensitized Solar Cells with Ruthenium Sensitizers and Cobalt Electrolytes, *Inorg. Chem.*, 55, 6653–6659, (DOI: 10.1021/acs.inorgchem.6b00204).
58. Yella A., Lee H. W., Tsao H. N., Yi C., Chandiran A. K., Nazeeruddin M. K., Diao E. W. G., Yeh C. Y., Zakeeruddin S. M., Grätzel M. (2011), Porphyrin-Sensitized Solar Cells with Cobalt(II/III)-Based Redox Electrolyte Exceed 12% Efficiency, *Science*, 334, 629–634, (DOI: 10.1126/science.1209688).

59. Mathew S., Yella A., Gao P., Baker, R. H., Curchod B. F. E., Astani C. A., Tavernelli L., Rothlisberger U., Nazeeruddin M. K., Grätzel M. (2014), Dye-Sensitized Solar Cells with 13% Efficiency Achieved Through the Molecular Engineering of Porphyrin Sensitizers, *Nat. Chem.*, 6, 242–247, (DOI: 10.1038/nchem.1861).
60. Liangwab M., Chen J. (2013), Arylamine organic dyes for dye-sensitized solar cells, *Chem. Soc. Rev.*, 42, 3453-3488, (DOI: 10.1039/c3cs35372a).
61. He J., Wu W., Hua, J., Jiang Y., Qu S., Li J., Long, Y., Tian H. (2011), Bithiazole-bridged dyes for dye-sensitized solar cells with high open circuit voltage performance, *J. Mater. Chem.*, 21, 6054 (DOI: 10.1039/c0jm03811c).
62. Marks R. N., Halls, J. J. M., Bradley D. D. C., Friend R. H., Holmes A. B. (1994), The photovoltaic response in poly(p-phenylene vinylene) thin-film devices, R. N. Marks, *J. Phys.: Condens Matter*, 6, 1379, (DOI: 10.1088/0953-8984/6/7/009).
63. Yu G., Gao J., Hummelen J. C., Wudl F., Heeger A. J. (1995), Polymer Photovoltaic Cells: Enhanced efficiencies via a network of internal donor-acceptor heterojunctions, *Science*, 270, 1789-1791 (DOI: 10.1126/science.270.5243.1789).
64. Wang J. L., He Z., Wu H., Cui H., Li Y., Gong Q., Cao Y., Pei J. (2010), Solution-Processed Bulk-Heterojunction Photovoltaic Cells Based on Dendritic and Star-Shaped D- π -A Organic Dyes, *Chem. Asian J.*, 5, 1455–1465, (DOI: 10.1002/asia.200900686).
65. Tang C. W., VanSlyke S. A. (1987), Energy Level Alignment and Interfacial Electronic Structures at Organic/Metal and Organic/Organic Interfaces, *Appl. Phys. Lett.*, 51, 913, DOI: 10.1002/(SICI)1521-4095(199906).
66. Yao C., Yu Y., Yang X., Zhang X., Huang Z., Xu X., Zhou G., Yue Ling, Wu Z. (2015), Effective blocking of the molecular aggregation of novel truxene-based emitters with spirobifluorene and electron-donating moieties for furnishing highly efficient non-doped blue-emitting OLEDs, *J. Mater. Chem. C*, 3, 5783–5794. DOI: 10.1039/c5tc01018g.
67. Shockley W., Sparks M., Teal G. K. (1951), p-n Junction Transistors, *Phys. Rev.*, 83, 151–153 (DOI: org/10.1103/PhysRev.83.151).
68. Narayan K. S., Kumar N. (2001), Sensitivity of the threshold voltage of organic thin-film transistors to light and water, *Appl. Phys. Lett.*, 79, 1891–1893 (DOI: org/10.1063/1.4919829).

69. Saragi T. P. I., Pudzich R., Fuhrmann T., Salbeck J. (2004), Stability Improvement of Organic Thin-Film Transistors Using Stacked Gate Dielectrics, *Appl. Phys. Lett.*, 84, 2334–2336 (DOI: dx.doi.org/2010.2067772).
70. Noh Y. Y., Kim D. Y., Yase K. (2005), Highly sensitive thin-film organic phototransistors: Effect of wavelength of light source on device performance, *J. Appl. Phys.*, 98, 074505–074507 (DOI: org/10.1063/1.2061892).
71. Baeg K. J., Binda M., Natali, D., Caironi M., Noh Y. Y. (2013), Organic Light Detectors: Photodiodes and Phototransistors, *Adv. Mater.*, 25, 4267–4295 (DOI: 10.1002/adma.201204979).
72. Koezuka H., Etoh S. (1983), Macromolecular electronic device: Field-effect transistor with a polythiophene thin film, *J. Appl. Phys.*, 54, 2511, (DOI: /abs/10.1063/1.97417).
73. (a) Sun Y., Xiao K., Liu Y., Wang J., Pei J., Yu G., Zhu D. (2005), Oligothiophene-Functionalized Truxene: Star-Shaped Compounds for Organic Field-Effect Transistors, *Adv. Funct. Mater.*, 15, 818, (DOI: 10.1002/adfm.200400380). (b) Mao X.-B., Ma Z., Yang Y. L., Lei S.-B., Wang C., Huang W. (2008), Self-assembly of truxene derivatives investigated by STM, *Front. Mater. Sci. China*, 2, 26, (DOI: org/10.1007/s11706-008-0005-9).
74. Zhang Y. Q., Wang G., Zhang J. P. (2014), Towards an automated MEMS-based characterization of benign and cancerous breast tissue using bio impedance measurements, *Sens. Actuators B.*, 200, 259–268 (DOI: /abs/10.1021/jo200065d).
75. Hu B., Fu S. J., Xu F., Tao T., Zhu H. Y., Cao K. S., Huang W., You X. Z. (2011), Linear heterocyclic aromatic fluorescence compounds having various donor–acceptor spacers prepared by the combination of carbon-carbon bond and carbon-nitrogen bond cross-coupling reactions, *J. Org. Chem.*, 76, 4444–4456 (DOI: 10.1021/jo200065d).
76. Huang W, Smarsly E., Han J., Bender M., Seehafer K., Wacker I., Schroeder R. R., Bunz U. H. F. (2017), Truxene-Based Hyperbranched Conjugated Polymers; Fluorescent Micelles Detect Explosives in Water, *ACS Appl. Mater. Interfaces*, 9, 3068–3074, (DOI: 10.1021/acsami.6b12419).
77. Yuan M., Fang Q., Liu Z., Guo J., Chen H., Yu W., Xue G., Liu D. S. (2006), Acceptor or Donor (Diaryl B or N) Substituted Octupolar Truxene: Synthesis, Structure, and Charge-Transfer-Enhanced Fluorescence, *J. Org. Chem.*, 71, 7858–7861, DOI: 10.1021/jo061210i.

78. Turan I. S., Cakmak F. P., Sozmen F. (2014), Highly selective fluoride sensing via chromogenic aggregation of a silyloxy-functionalized tetraphenylethylene (TPE) derivative, *Tetrahedron Lett.*, 55, 456–459, (DOI:org/10.1016/j.tetlet.2013.11.059).
79. Yang Z., Zhang K., Gong F., Li S., Chen J., Ma J. S., Sobenina L. N., Mikhaleva A. I., Yang G., Trofimov B., Beilstein A. (2011), A new fluorescent chemosensor for fluoride anion based on a pyrrole–isoxazole derivative, *J. Org. Chem.*, 7, 46–52, (DOI: 10.3762/bjoc.7.8).
80. Kubo Y., Yamamoto M., Ikeda M., Takeuchi M., Shinkai S., amaguchi S., Tamao K. (2003), A colorimetric and ratiometric fluorescent chemosensor with three emission changes: fluoride ion sensing by a triarylborane–porphyrin conjugate, *Angew. Chem., Int. Ed.*, 42, 2036–2040, (DOI: 10.1002/anie.200250788).

Chapter 2

Materials and experimental techniques

2.1. Introduction

This chapter describes the materials, general synthetic procedures, characterization techniques and the instrumentation employed in this thesis.

2.2. Chemicals for synthesis

The common solvents used for syntheses were purified according to established procedures.^[1] 1-indanone, n-BuLi, CuI, Pd(PPh₃)₄, Pd(dba)₂, ferrocene, tetrabutylammonium hexafluorophosphate (TBAF₆), phenothiazene, naphthalimide, ethynyl ferrocene, triphenylamine, and tetracyanoethylene, 7,7,8,8-tetracyanoquinodimethane, K₂CO₃, Zn(OAc)₂ were obtained from Aldrich chemicals USA. Silica gel (100–200 mesh and 230–400 mesh) were purchased from Rankem chemicals, India. TLC pre-coated silica gel plates (Kieselgel 60F254, Merck) were obtained from Merck, India. Dry solvents dichloromethane, 1,2-dichloroethane, chloroform, tetrahydrofuran (THF), triethylamine and methanol were obtained from spectrochem and S. D. Fine chem. Ltd. All the oxygen or moisture sensitive reactions were performed under nitrogen/argon atmosphere using standard Schlenk method. The solvents and reagents were used as received unless otherwise indicated. Photophysical and electrochemical studies were performed with spectroscopic grade solvents.

2.3. Spectroscopic measurements

2.3.1. Mass spectrometry

High resolution mass spectra (HRMS) were recorded on Bruker-Daltonics, micrOTOF-Q II mass spectrometer using positive and negative mode electrospray ionizations.

2.3.2. NMR spectroscopy

¹H NMR (400 MHz), and ¹³C NMR (100 MHz) spectra were recorded on the Bruker Avance (III) 400 MHz, using CDCl₃ as solvent. Chemical shifts in ¹H, and ¹³C NMR spectra were reported in parts per million (ppm). In ¹H NMR chemical shifts are reported relative to the residual solvent peak (CDCl₃, 7.26

ppm). Multiplicities are given as: s (singlet), d (doublet), t (triplet), q (quartet), m (multiplet), and the coupling constants J , are given in Hz. ^{13}C NMR chemical shifts are reported relative to the solvent residual peak (CDCl_3 , 77.36 ppm).

2.3.3. UV-Vis spectroscopy

UV-Vis absorption spectra were recorded using a Varian Cary100 Bio UV-Vis and Perkin Elmer LAMBDA 35 UV/Vis spectrophotometer.

2.3.4. Fluorescence spectroscopy

Fluorescence emission spectra were recorded upon specific excitation wavelength on a Horiba Scientific Fluoromax-4 spectrophotometer. The slit width for the excitation and emission was set at 2 nm.

The fluorescence quantum yields (ϕ_F)

The fluorescence quantum yields (ϕ_F) of compounds were calculated by the steady-state comparative method using following equation,

$$\phi_F = \phi_{st} \times S_u/S_{st} \times A_{st}/A_u \times n_2 D_u/n_2 D_{st} \dots\dots\dots \text{(Eq. 1)}$$

Where ϕ_F is the emission quantum yield of the sample, ϕ_{st} is the emission quantum yield of the standard, A_{st} and A_u represent the absorbance of the standard and sample at the excitation wavelength, respectively, while S_{st} and S_u are the integrated emission band areas of the standard and sample, respectively, and nD_{st} and nD_u the solvent refractive index of the standard and sample, u and st refer to the unknown and standard, respectively.

2.4. Electrochemical studies

Cyclic voltamograms (CVs) were recorded on CHI620D electrochemical analyzer using Glassy carbon as working electrode, Pt wire as the counter electrode, and Saturated Calomel Electrode (SCE) as the reference electrode. The scan rate was 100 mVs^{-1} . A solution of tetrabutylammonium hexafluorophosphate (TBAPF₆) in CH_2Cl_2 (0.1 M) was employed as the supporting electrolyte.

2.5. Single crystal X-ray diffraction studies.

Single crystal X-ray diffraction studies were performed on SUPER NOVA diffractometer. The strategy for the Data collection was evaluated by using the CrysAlisPro CCD software. The data were collected by the standard 'phi-omega scan techniques, and were scaled and reduced using CrysAlisPro RED software. The structures were solved by direct methods using SHELXS-97, and refined by full matrix least-squares with SHELXL-97, refining on F^2 .¹ The positions of all the atoms were obtained by direct methods. All non-hydrogen atoms were refined anisotropically. The remaining hydrogen atoms were placed in geometrically constrained positions, and refined with isotropic temperature factors, generally $1.2U_{eq}$ of their parent atoms. The CCDC numbers contain the respective supplementary crystallographic data. These data can be obtained free of charge via www.ccdc.cam.ac.uk/conts/retrieving.html (or from the Cambridge Crystallographic 42 Data Centre, 12 union Road, Cambridge CB21 EZ, UK; Fax: (+44) 1223-336-033; or deposit@ccdc.cam.ac.uk).

2.6. Computational calculations

The density functional theory (DFT) calculation were carried out at the B3LYP/6-31G** level for C, N, S, H, and Lan12DZ level for Zn in the Gaussian 09 program.^[2]

References

- (a) Vogel A. I., Tatchell A. R., Furnis B. S., Hannaford A. J., & Smith, P. W. G. (1996), *Vogel's Textbook of Practical Organic Chemistry (5th Edition)* (5th ed.). (b) Wei Ssberger A. Proskraner E. S. Riddick J. A., Toppos Jr. E. F. (1970). *Organic Solvents in Techniques of Organic Chemistry*, Vol. IV, 3rd Edition, Inc. New York.
- (a) Lee C., Yang W., & Parr R. G. (1988). Development of the Colle-Salvetti correlation-energy formula into a functional of the electron density. *Physical Review B*, 37(2), 785–789 (DOI: 10.1103/PhysRevB.37.785). (b) A. D. Becke (1993), A new mixing of Hartree-Fock and local densityfunctional theories, *J. Chem. Phys.* 98 (2),

1372–377 (DOI: 10.1063/1.464304). (c) Frisch M. J., Trucks G. W., Schlegel H. B., Scuseria G. E., Robb M. A., Cheeseman J. R., Scalmani G., Barone V., Mennucci B., Petersson G. A., Nakatsuji H., Caricato M., Li X., Hratchian H. P., Izmaylov A. F., Bloino J., Zheng G., Sonnenberg J. L., Hada M., Ehara M., Toyota K., Fukuda R., Hasegawa J., Ishida M., Nakajima T., Honda Y., Kitao O., Nakai H., Vreven T., Montgomery J. A. Jr., Peralta J. E., Ogliaro F., Bearpark M., Heyd J. J., Brothers E., Kudin K. N., Staroverov V. N., Kobayashi R., Normand J., Raghavachari K., Rendell A., Burant J. C., Iyengar S. S., Tomasi J., Cossi M., Rega N., Millam N. J., Klene M., Knox J. E., Cross J. B., Bakken V., Adamo C., Jaramillo J., Gomperts R., Stratmann R. E., Yazyev O., Austin A. J., Cammi R., Pomelli C.; Ochterski J. W., Martin R. L., Morokuma K., Zakrzewski V. G., Voth G. A., Salvador P., Dannenberg J. J., Dapprich S., Daniels A. D., Farkas O., Foresman J. B., Ortiz J. V., Cioslowski J., Fox D. J. (2009), *Gaussian 09, revision A.02*; *Gaussian, Inc.*: Wallingford, CT.

Chapter 3

Star Shaped Ferrocenyl Truxenes: Synthesis, Structure and Properties

3.1. Introduction

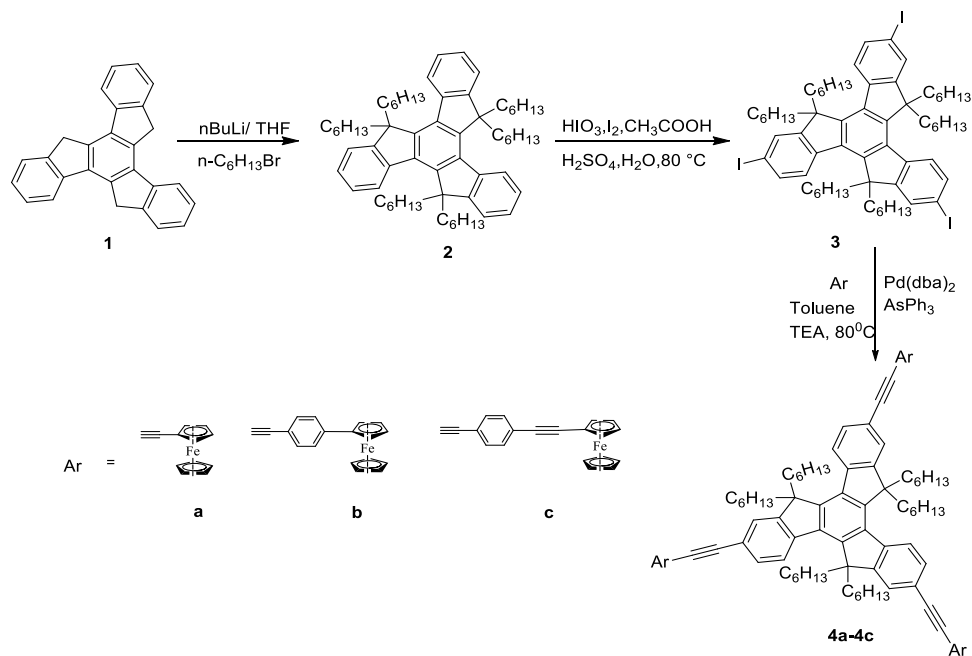
Organic π -conjugated molecules have shown remarkable properties in the field of non-linear optics and electroluminescent devices.¹⁻³ The molecular systems with two and three dimensional structure exhibit better photophysical properties compared to the molecules with one dimensional structure.⁴⁻⁵ Truxene (10,15-dihydro-5*H*-diindeno[1,2-*a*;10,20-*c*]fluorene) is a planar polyaromatic hydrocarbon, which represents a fusion of three fluorene moieties in such a way, that it leads to a C_3 -symmetric structure.⁶ Truxene scaffold appear to be a potential building block for the construction of larger molecular architectures, owing to its easy functionalization, rigid structures, high thermal and chemical stability.⁷⁻⁸ Literature reveals that the substitution at para position (2,7,12, positions) of truxene core results in a variety of π -delocalized molecular systems.⁹ Jian Pei *et al.* have reported star shaped π -conjugated molecules based on the truxene core, which exhibited interesting optoelectronic properties.¹⁰ Recent reports on truxene based donor-acceptor systems reveal that these molecular systems are potential candidates for applications in two-photon absorption, organic light-emitting diodes (OLED), and organic fluorescent probes.¹²⁻¹³

Our group has explored ferrocene as a strong donor, and attached it with various acceptor molecules.¹⁴⁻¹⁵ In this contribution, we wish to report the design and synthesis of the ferrocenyl substituted truxenes and the effect of ferrocenyl substituents with different spacer length on the structural, thermal, and photophysical properties. The tetracyanoethylene (TCNE) group was incorporated into ferrocenyl substituted truxene by [2 + 2] cycloaddition reaction, followed by ring-opening, which resulted in donor-accepter truxene **5a**.¹⁶

3.2. Results and discussion

The synthesis of ferrocenyl substituted truxenes **4a–4c** and **5a** are shown in Scheme 1 and Scheme 2. Truxenes **4a–4c** were synthesized by the Pd-catalyzed Sonogashira cross-coupling reaction of tri-iodotruxene **3** with the corresponding ethynyl ferrocenes **a–c** (Scheme 3.1).

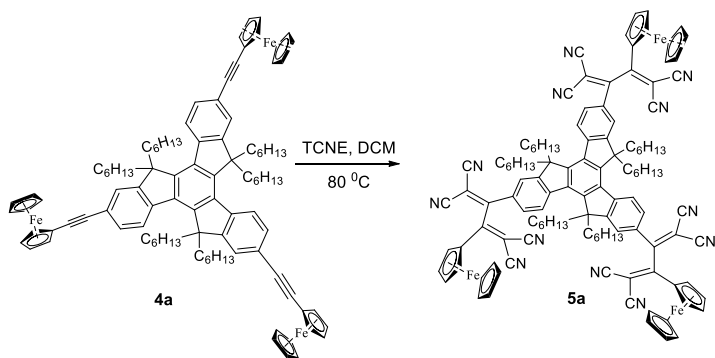
The truxene core **1** was synthesized by 1-indanone in the presence of acetic acid and hydrochloric acid.^{9b} The alkylation reaction of the truxene **1** with bromohexane resulted in readily soluble hexahexylated truxene **2**.^{9b} The iodination reaction of truxene **2** in the presence of HIO₃ and I₂ resulted in hexahexylated tri-iodo truxene **3** in 80% yield.¹⁷ The reaction of tri-iodo truxene **3** with ethynylferrocene (**a**), 4-ferrocenylphenylacetylene (**b**), and 4-(ferrocenylethynyl)phenylacetylene (**c**), under the catalytic system Pd(dba)₂/AsPh₃ resulted truxenes **4a**, **4b**, and **4c** in 75%, 70% and 72% yields respectively.



Scheme 3.1: Synthesis of ferrocenyl substituted truxenes **4a–4c**

The [2+2] cycloaddition reaction of tetracyanoethylene (TCNE) with truxene **4a** followed by ring-opening, resulted truxene **5a** as a dark green solid in 60% yield (Scheme 3.2)¹⁸⁻¹⁹. The reaction of TCNE with truxenes **4b** and **4c** resulted in the formation of multiple products, which were difficult to purify. The truxenes **4a-4c** and **5a** are readily soluble in common organic solvents. The truxenes, **4a-4c**, and **5a** were well characterized by ¹H NMR, ¹³C NMR, and HRMS techniques. The truxene **4a** was also characterized by single crystal X-ray diffraction.

The ¹H NMR spectrum of the truxene **4a-4c** show characteristic doublet at 8.30 ppm, and multiplet between 7.52 to 7.68 ppm corresponding to the truxene core. The unsubstituted cyclopentadienyl ring of the ferrocene exhibited a multiplet in the region of 4.20-4.36 ppm for truxene **4a-4c** and at 4.33-4.48 ppm for truxene **5a**. The monosubstituted cyclopentadienyl ring of ferrocene exhibits a triplet at 4.54 ppm for truxene **4a, 4b** and at 4.39 and 4.72 ppm for truxene **4c**. The truxene **5a** shows two singlets at 4.8 and 5.0 ppm and two multiplets in the region of 5.27-5.41 ppm and 4.63-4.75 ppm corresponding to the monosubstituted cyclopentadienyl ring.



Scheme 3.2: Synthesis of truxene **5a**

3.3. Thermal properties

The thermal properties of the ferrocenyl substituted truxenes **4a-4c** and **5a** were explored using thermogravimetric analysis (TGA) at a heating rate of 10 °C min⁻¹

under nitrogen atmosphere (Fig. 3.1). The decomposition temperatures for 10% weight loss in the ferrocenyl truxenes **4a-4c** was above 390 °C, whereas the truxene **5a** shows 10% weight loss at 230 °C. The thermal stability of the ferrocenyl truxenes follow the order **4a > 4c > 4b > 5a**.

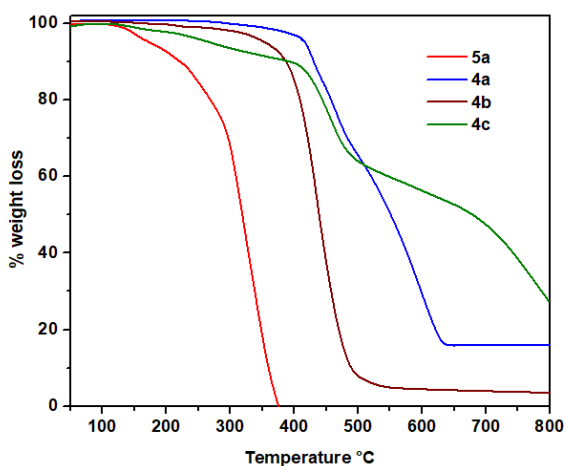


Figure 3.1. TGA plots of truxenes **4a-4c** and **5a**.

3.4. Single crystal X-ray diffraction studies

The single crystal of the ferrocenyl truxene **4a** was obtained via slow diffusion of methanol into dichloromethane solution at room temperature. The truxene **4a** crystallizes in $P 2_1/n$ space group. The crystal structure of **4a** is shown in Figure 3.2, and the important crystallographic parameters are listed in Table 3.1. The truxene core shows planar structure. The interplanar angle between the plane of phenyl rings of truxene core, and the plane of cyclopentadienyl ring of different ferrocenyl subunits are 89.76°, 63.87° and 77.61° respectively. The cyclopentadienyl rings of the ferrocene (Fe1) show staggered conformation, whereas ferrocene (Fe2 and Fe3) shows eclipsed conformation.

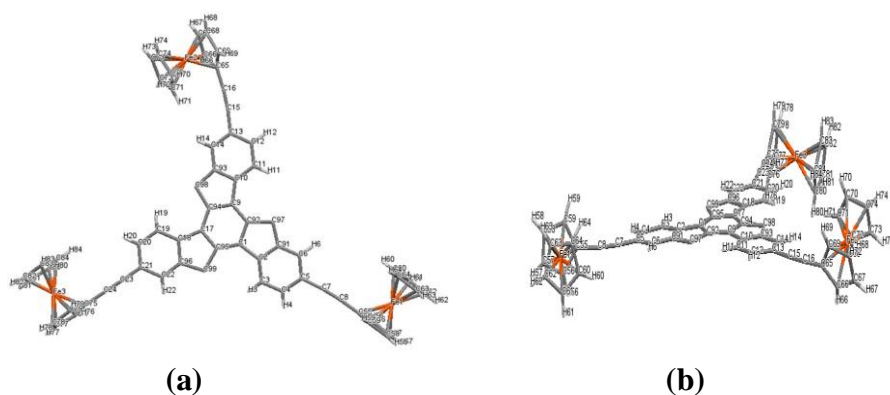


Figure 3.2: Single crystal X-ray structure of compound **4a** (a) Front view, and (b) Side view, (The alkyl groups have been omitted for clarity).

The crystal packing diagram of the ferrocenyl truxene **4a** reveals intermolecular C-H... π interactions and π - π interaction, between the two adjacent molecules. The study of non-bonding interactions exhibit that two molecules of truxene **4a** are interconnected via C-H... π interactions, involving hydrogen H33 with the cyclopentadienyl ring (C69, C68, C67, C66, C65, 3.01Å) of ferrocene ring, and H32 with alkyl carbon (C16, 2.85Å).

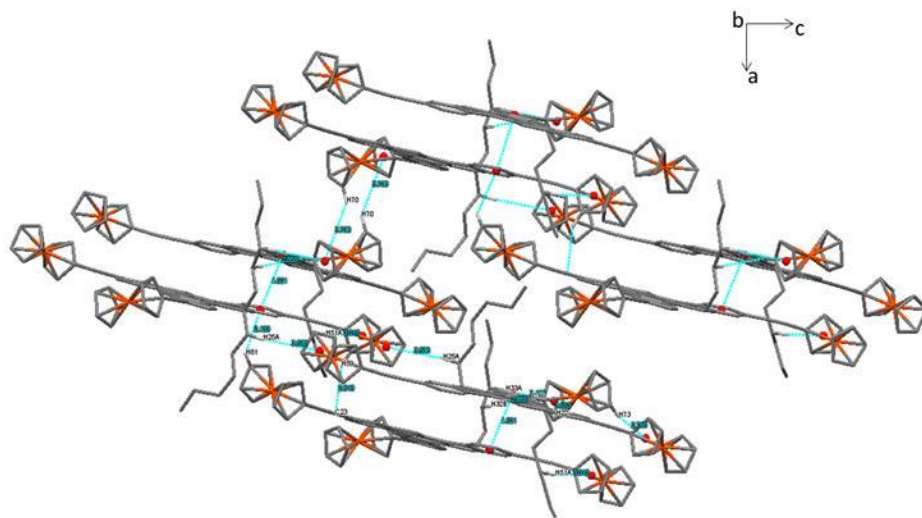


Figure 3.3. The supramolecular structure of compound **4a** along b axis. The secondary interactions are shown by dashed lines. (The hydrogen atoms and alkyl groups have been omitted for clarity).

The π - π interaction between benzene ring of truxene core (C4, C3, C2, C91, C6, C5) and (C12, C13, C14, C93, C10, C11, 4.62Å) leads to the stacking between

two adjacent molecules. These adjacent molecules are further connected to another layer through C-H--- π interactions involving H25 with the cyclopentadienyl ring (C62, C61, C60, C64, C63, 3.63Å) of ferrocene ring, H59 with alkyl carbon (C23, 2.85Å) and H81 with benzene ring (C2, C91, C6, C5, C4, C3, 2.83Å) of the truxene core, leading to the formation of 2-D network (Figure 3.3).

3.5. Photophysical properties

The UV-vis absorption spectra of the truxenes **4a-4c** and **5a** were recorded in dichloromethane at room temperature (Figure 3.4), and the data are listed in Table 3.2. The ferrocenyl truxenes (**4a-4c** and **5a**) show strong absorption band between 333-352 nm, with high extinction coefficient, corresponding to $\pi \rightarrow \pi^*$ transition. The low intensity band at 430 nm is an intramolecular charge transfer from the ferrocenes to the truxene core. The absorption maxima of truxenes **4a-4c** and **5a** show continuous red shift with the enhancement of the conjugation length, and follows the order **5a** > **4c** > **4b** > **4a**. This reflects effective electronic communication between ferrocenyl unit, and the truxene core in compounds **4a-4c**. The TCNE derivative **5a** shows bathochromic shift of the $\pi \rightarrow \pi^*$ transition band and charge transfer band at 618 nm.²⁰ This indicates strong donor-acceptor interaction in truxene **5a**.

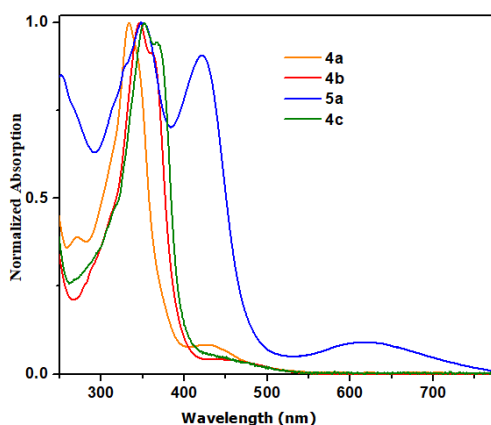


Figure 3.4. Normalized electronic absorption spectra of truxenes **4a-4c** and **5a** (1.0×10^{-6} M concentration) in dichloromethane.

Table 3.1. Crystal data and structure refinement parameter for truxene **4a**.

Compound	4a
Empirical formula	C ₉₉ H ₁₁₄ Fe ₃
Formula weight	1471.45
Temperature	150(2) K
Wavelength	0.71073 Å
Crystal system, space group	Monoclinic, P 21/n
Unit cell dimensions	
a (Å)	16.3107(3)
b (Å)	b = 18.4332(3)
β (°)	90.4590(10)
c (Å)	27.2131(4)
Volume	8181.6(2) Å ³
Z, Calculated density	4, 1.195 Mg/m ³
Absorption coefficient	0.571 mm ⁻¹
F(000)	3144
Crystal size	0.23 x 0.16 x 0.13 mm
Theta range for data collection	3.11 to 25.00 deg.
Limiting indices	-19<=h<=13, -21<=k<=21, -32<=l<=32
Reflections collected / unique	59275 / 14385 [R(int) = 0.0570]
Completeness to theta= 25.00	99.8 %
Absorption correction	Semi-empirical from equivalents
Max. and min. transmission	0.9295 and 0.8799
Refinement method	Full-matrix least-squares on F ²
Data / restraints / parameters	14385 / 0 / 925
Goodness-of-fit on F ²	1.025
Final R indices [I>2sigma(I)]	R1 = 0.0553, wR2 = 0.1455
R indices (all data)	R1 = 0.0721, wR2 = 0.1614
Largest diff. peak and hole	0.940 and -0.511 e.Å ⁻³

3.6. Electrochemical properties.

The electrochemical behavior of the truxene **4a-4c** and **5a** were investigated by the cyclic voltammetric analysis in dry dichloromethane solution at room temperature using tetrabutylammoniumhexafluorophosphate (TBAPF₆) as a supporting electrolyte. The electrochemical data are listed in Table 3.2, and the cyclic voltammogram are shown in Figure 3.5.

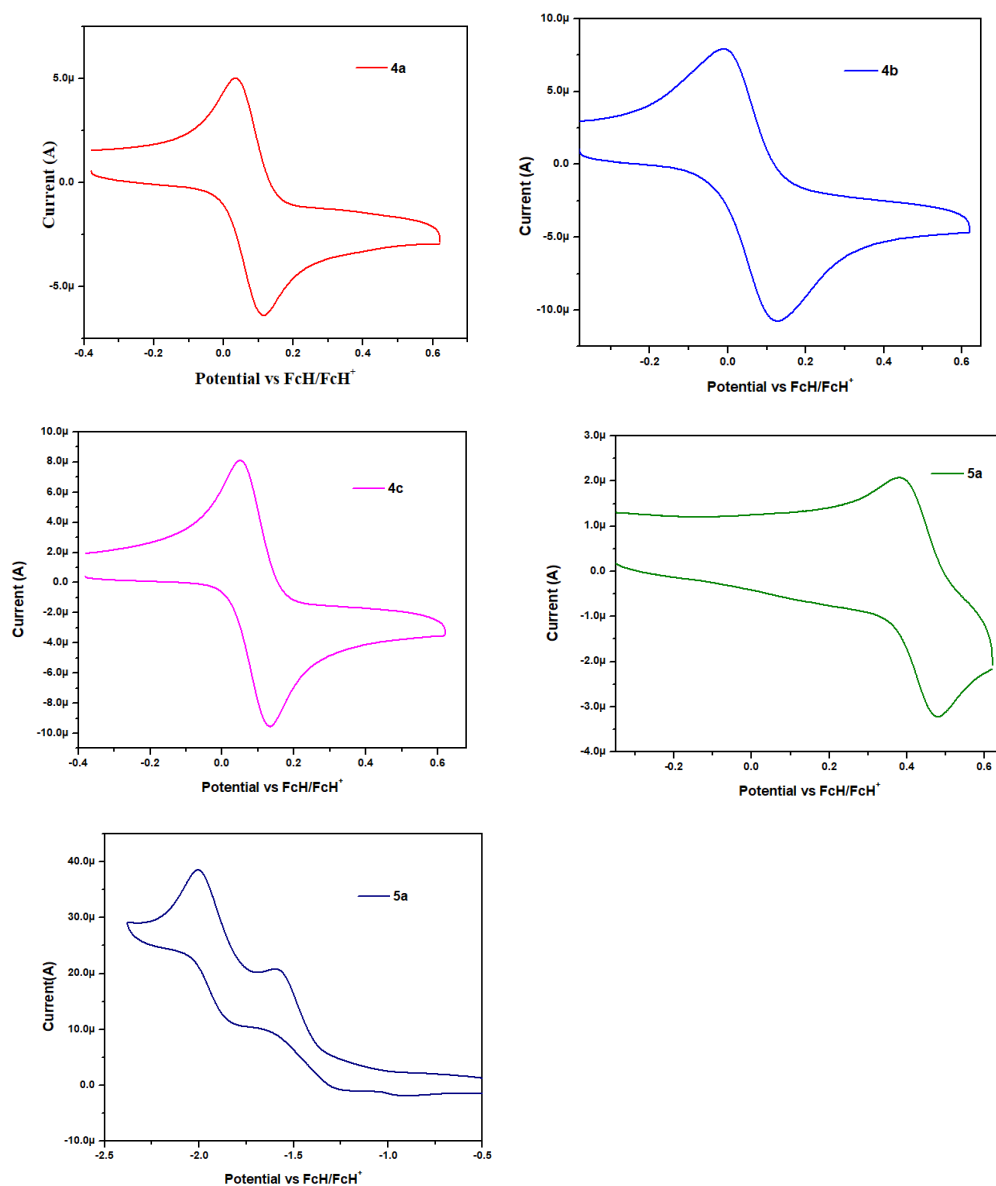


Figure 3.5. Cyclic voltammogram of 1.0×10^{-3} M solutions of compound **4a-4c** and **5a** in CH₂Cl₂ containing 0.1M Bu₄NPF₆ as supporting electrolyte, recorded at a scan speed of 100 mVs⁻¹.

All potentials are corrected to be referenced against Fc/Fc⁺, as required by IUPAC.²² The cyclic voltammogram of the truxene **4a-4c** and **5a** show reversible oxidation wave of ferrocene/ferrocenium. Truxene **5a** shows two irreversible reduction peaks corresponding to the successive one electron reductions of the dicyanovinyl (DCV) groups of the tetracyanoethylene unit.^{14b} The ferrocenyl moieties in the truxene **4a-4c** and **5a** show higher oxidation potential compared to the free ferrocene. This confirms, substantial electronic communication between ferrocene and truxene core. The incorporation of TCNE group, which is a strong electron-acceptor, results in harder oxidation of ferrocene unit in truxene **5a**. The trend in the oxidation potential of the ferrocenyl moiety in the ferrocenyl substituted truxenes follows the order **5a** > **4a** > **4b** > **4c**.

Table 3.2. Photophysical and electrochemical data of ferrocenyl truxenes **4a-4c** and **5a**.

Compound	Photophysical data ^a	Electrochemical ^b data	T _d ^c (°C)
	λ_{max} , [nm] / $\epsilon \times 10^5$ (M ⁻¹ cm ⁻¹)	E _{ox} (V)	
Ferrocene	-	0.38	-
4a	333 (1.1)	0.45	437
4b	346 (2.1)	0.43	393
4c	352 (1.3)	0.46	414
5a	350 (1.9) 421, 618	0.80 -1.05 -1.54	230

^aMeasured in dichloromethane at 1×10^{-6} M concentration. ^bRecorded by cyclic voltammetry using 1.0×10^{-4} M solutions of **4a-4c** and **5a** containing 0.1M solution of Bu₄NPF₆ in DCM at 100 mVs⁻¹ scan rate, vs SCE electrode.

^cDecomposition temperature at 10% weight loss, determined by TGA.

3.7. Experimental section

General Methods

Chemicals were used as received unless otherwise indicated. All oxygen or moisture sensitive reactions were performed under nitrogen/argon atmosphere using standard schlenk method. Triethylamine (TEA) was received from commercial source, and distilled on KOH prior to use. ^1H NMR (400 MHz), and ^{13}C NMR (100MHz) spectra were recorded on the Bruker Avance (III) 400 MHz, using CDCl_3 as solvent. Tetramethylsilane (TMS) was used as reference for recording ^1H (of residual proton; $\delta = 7.26$ ppm), and ^{13}C ($\delta = 77.0$ ppm) spectra in CDCl_3 . UV-visible absorption spectra of all compounds in Dichloromethane were recorded on a Carry-100 Bio UV-visible Spectrophotometer. Cyclic voltamograms (CVs) were recorded on a CHI620D electrochemical analyzer using glassy carbon as a working electrode, Pt wire as the counter electrode, and SCE as the reference electrode. HRMS was recorded on Brucker-Daltonics, micro TOF-Q II mass spectrometer.

Cyclic Voltammetry: Cyclic voltamograms (CVs) were recorded on a CHI620D electrochemical analyzer using a standard three-electrode cell with Glassy carbon as working electrode. The 3 mm diameter glassy carbon working electrode from CH Instruments (CHI 104) were used. The electrode was polished with two different Alpha alumina powder (1.0 and 0.3 micron from CH Instruments) suspended in distilled water on a Microcloth polishing pad, at the end of polishing, the electrodes were thoroughly rinsed with distilled water. Platinum wire was used as the counter electrode and saturated calomel as reference electrode. The scan rate was 100 mVs^{-1} . A solution of tetrabutylammoniumhexafluorophosphate (Bu_4NPF_6) in CH_2Cl_2 (0.1M) was employed as the supporting electrolyte. CH_2Cl_2 was freshly distilled from CaH_2 prior to use. All potentials were experimentally referenced against the saturated calomel electrode couple but were then manipulated to be referenced against Fc/Fc^+ as recommended by IUPAC.²² Under our conditions, the Fc/Fc^+ couple exhibited $E^\circ = 0.38 \text{ V versus SCE}$.

Single crystal X-ray diffraction Studies

Single crystal X-ray structural studies of **4a** were performed on a CCD Agilent Technologies (Oxford Diffraction) SUPER NOVA diffractometer. Data were collected at 293(2) K using graphite-monochromated Mo K α radiation ($\lambda = 0.71073 \text{ \AA}$). The strategy for the Data collection was evaluated by using the CrysAlisPro CCD software. The data were collected by the standard 'phi-omega scan techniques, and were scaled and reduced using CrysAlisPro RED software. The structures were solved by direct methods using SHELXS-97, and refined by full matrix least-squares with SHELXL-97, refining on F². The positions of all the atoms were obtained by direct methods. All non-hydrogen atoms were refined anisotropically. The remaining hydrogen atoms were placed in geometrically constrained positions, and refined with isotropic temperature factors, generally 1.2U_{eq} of their parent atoms. The CCDC number [979595](#) contains the supplementary crystallographic data for **4a**. This data can be obtained free of charge via www.ccdc.cam.ac.uk (or from the Cambridge Crystallographic Data Centre, 12 union Road, Cambridge CB21 EZ, UK; Fax: (+44) 1223-336-033; or deposit@ccdc.cam.ac.uk.

Synthesis and Characterization

The reactant **a** was purchased from Sigma-Aldrich, and the reactants **b-c** were synthesized according to known methods.²¹

General procedure for synthesis of **4a-4c**.

A solution of tri-iodotruxene **3** (250 mg, 0.20 mmol) and the corresponding ethynyl ferrocene (4.5 equivalent) in toluene–triethylamine 5 : 1 (60 mL) was deaerated for 30 min with argon bubbling and then Pd(dba)₂ (40 mg, 0.07 mmol) and AsPh₃ (170 mg, 0.55 mmol) were added. The solution was deaerated for a further 5 min; The mixture was heated at 80 °C for 48 h. The solvent was removed; the remaining residue was suspended in water (50 mL) and extracted with DCM (3 x 20 mL). The combined organic layers were dried (MgSO₄) and concentrated in vacuum. The resulting crude product was purified by column chromatography on silica gel eluting with CH₂Cl₂/hexane (10%). The desired

compounds obtained from the column was recrystallized from DCM/methanol to give compounds **4a-4c** in 70-80% yield.

Synthesis of truxene **5a**

A solution of truxene **4a** (40 mg, 0.03 mmol) and TCNE (15 mg, 0.12mmol) in dichloromethane was heated at 80 °C overnight. After completion of the reaction, solvent was evaporated and the residue was crystallized multiple times with DCM/methanol to afford truxene **5a** as a dark green solid.

Compound 4a: Orange solid (225 mg, 75%) ¹H NMR (400 MHz, CDCl₃): δ (ppm) 8.3(d, 3H, *J* = 8.32 Hz), 7.50-7.59 (m, 6H), 4.54 (t, 7H), 4.21-4.36 (m, 20H), 2.85-2.99 (m, 6H), 2.01-2.16 (m, 6H), 0.71.01(m, 36H), 0.39-0.66(m, 30H)); ¹³C NMR (100 MHz, CDCl₃): δ = 153.69, 145.54, 139.81, 138.06, 129.80, 124.99, 124.44, 121.67, 88.65, 86.55, 71.44, 70.00, 68.88, 65.50, 55.76, 37.00, 31.54, 29.50, 23.96, 22.30, 13.90. HRMS (ESI) *m/z*, calcd for M⁺ (C₉₉H₁₁₄Fe₃): 1471.7000; found: 1471.7006.

Compound 4b: Orange-red solid (199 mg, 72%) ¹H NMR (400 MHz, CDCl₃): δ (ppm) 8.38(d, 3H, *J* = 9.02 Hz), 7.60-7.68 (m, 6H), 7.49-7.58 (m, 12H), 4.72 (t, 7H), 4.39 (t, 7H), 4.06-4.12 (m, 13H), 2.92-3.02 (m, 6H), 2.09-2.19 (m, 6H)) 0.84-1.03 (m, 36H), 0.46-0.48 (m, 30H) ;¹³C NMR (100 MHz, CDCl₃): δ = 153.70, 145.85, 140.22, 139.89, 138.03, 131.66, 129.83, 125.88, 125.21, 124.53, 121.23, 120.49, 90.31, 90.22, 84.28, 69.76, 69.74, 69.39, 66.54, 55.82, 37.02, 31.52, 29.48, 23.98, 22.30, 13.89. HRMS (ESI) *m/z*, calcd for M⁺ (C₁₁₇H₁₂₆Fe₃): 1699.7940; found: 1699.7938.

Compound 4c: Orange solid (200 mg, 70%) ¹H NMR (400 MHz, CDCl₃): δ (ppm) 8.3(d, 3H, *J* = 8.92 Hz), 7.47-7.66 (m, 18H), 4.53 (t, 6H), 4.20-4.32 (m, 21H), 2.87-3.00 (m, 6H), 2.04-2.18 (m, 6H), 0.78-1.02 (m, 36H), 0.40-0.68(m, 30H)); ¹³C NMR (100 MHz, CDCl₃): δ = 152.66, 144.97, 139.36, 136.99, 130.47, 130.31, 128.88, 124.24, 123.53, 122.79, 121.51, 119.91, 90.83, 89.61, 88.77,

84.57, 70.48, 69.00, 68.99, 67.98, 63.93, 54.81, 35.97, 30.47, 28.42, 22.93, 21.25, 12.85 HRMS (ESI) m/z, calcd for M⁺ (C₁₂₃H₁₂₆Fe₃): 1771.7941; found: 1771.7948.

Compound 5a: green solid (30 mg, 60%) ¹H NMR (400 MHz, CDCl₃): δ (ppm) 8.4(d, 3H, J = 7.90 Hz), 7.83-7.99 (m, 3H), 7.43-7.57 (m, 3H), 5.27-5.41 (m, 3H), 5.00(s, 3H), 4.8 (s, 3H) 4.63-4.75 (m, 3H), 4.33-4.48 (m, 15H), 2.73-2.95 (m, 6H), 2.02-2.20 (m, 6H), 0.66-1.00 (m, 36H), 0.25-0.65 (m, 30H)); ¹³C NMR (100 MHz, CDCl₃): δ = 172.40, 166.05, 154.70, 149.61, 144.96, 137.45, 129.93, 127.46, 125.40, 123.06, 113.72, 113.04, 112.09, 111.78, 85.53, 75.87, 74.97, 72.65, 71.25, 56.75, 36.84, 36.71, 36.70, 31.50, 31.44, 31.34, 29.15, 24.10, 22.18, 13.80. HRMS (ESI) m/z, calcd for M⁺ (C₁₁₇H₁₁₄Fe₃N₁₂): 1855.7368; found: 1855.7361.

3.8. Conclusions

In summary, we have synthesized a series of star shaped ferrocenyl substituted truxenes (**4a-4c** and **5a**) by the Pd-catalyzed Sonogashira cross coupling and Cycloaddition reaction in good yields. The electronic absorption and electrochemical studies of these truxenes show effective electronic interaction, which can be tuned by the introduction of different spacers. The enhancement of conjugation leads to red shift of the absorption bands in truxenes **4a-4c**. The compounds **4a-4c** exhibited good thermal stability. The truxenes reported here are potential candidates for opto-electronic applications.

3.9. References

1. (a) Burroughes J. H., Bradley D. D. C., Brown A. R., Marks R. N., Mackay K., Friend R. H., Burns P. L., Holmes A. B. (1990), Light-emitting diodes based on conjugated polymers, *Nature*, 347, 539, (DOI:10.1038/347539a0) (b) Roncali J. (1992), Conjugated poly(thiophenes): synthesis, functionalization, and applications, *J. Chem. Rev.*, 92, 711, (DOI: 10.1021/cr00012a009).

2. (a) Zheng Q., He G. S., Prasad P. N. (2005), π -Conjugated Dendritic Nanosized Chromophore with Enhanced Two-Photon Absorption *Chem.Mater.*, 17, 6004-6011, (DOI: 10.1021/cm051292b). (b) Auger A., Swarts J. C. (2007), Synthesis and Group Electronegativity Implications on the Electrochemical and Spectroscopic Properties of Diferrocenyl meso-Substituted Porphyrins, *Organometallics*, 26, 102, (DOI: 10.1021/om060373u).
3. Hadjichristidis N., Pitsikalis M., Pispas S., Iatrou H. (2001), Polymers with Complex Architecture by Living Anionic Polymerization, *Chem. Rev.*, 101, 3747, (DOI: 10.1021/cr9901337). (b) Zyss J., Ledoux I. (1994), Nonlinear optics in multipolar media: theory and experiments, *Chem. Rev.*, 94, 77, (DOI: 10.1021/cr00025a003).
4. (a) Jiang Y., Lu Y. X., Cui Y. X., Zhou Q. F., Ma Y., Pei J. (2007), Synthesis of Giant Rigid π -Conjugated Dendrimers, *Org. Lett.*, 4539-4542, (DOI: 10.1021/ol702063e). (b) Lo S. C., Burn P. L. (2007), Development of Dendrimers: Macromolecules for Use in Organic Light-Emitting Diodes and Solar Cells, *Chem. Rev.*, 107, 1097-1116, (DOI: 10.1021/cr050136l).
5. Isla H., Grimm B., Perez E. M., Torres M. R., Herranz M. A., Viruela R., Aragón J., Ortí E., Guldi D. M., Martín N. (2012), Bowl-shape electron donors with absorptions in the visible range of the solar spectrum and their supramolecular assemblies with C₆₀, *Chem. Sci.*, 3, 498-508, (DOI:10.1039/C1SC00669J). (b) Pérez E. M., Sierra M., Sánchez L., Torres M. R., Viruela R., Viruela P. M., Ortí E., Martín N. (2007), Self-Organization of Electroactive Materials: A Head-to-Tail Donor-Acceptor Supramolecular Polymer, *Angew. Chem. Int. Ed*, 46, 1847-1851, (DOI: 10.1002/anie.200703049).
6. Ventura B., Barbieri A., Barigelletti F., Diring S. E., Zissel R. (2010), Energy Transfer Dynamics in Multichromophoric Arrays Engineered from Phosphorescent PtII/RuII/OsII Centers Linked to a Central Truxene Platform, *Inorg. Chem.*, 49, 8333-8346, (DOI: 10.1021/ic1008413).

7. Zhang W. B., Jin W. H., Zhou X. H., Pei J. (2007), Star-shaped oligo (pphenylene)-functionalized truxenes as blue-light-emitting materials: synthesis and the structure-property relationship, *Tetrahedron*, 63, 2907–2914, (DOI: org/10.1016/j.tet.2007.01.025).
8. (a) Boorum M. M., Vasil Y. V., Drewello T., Scott L. T. (2001), Groundwork for a Rational Synthesis of C₆₀: Cyclodehydrogenation of a C₆₀H₃₀ Polyarene, *Science*, 294, 828, (DOI: 10.1126/science.1064250). (b) Gomez-Lor B., Frutos O. De, Echavarren A. M. (1999), Synthesis of ‘crushed fullerene’ C₆₀H₃₀, *Chem. Commun.*, 2431, (DOI: 10.1039/A906990I).
9. (a) Yuan M. S., Fang Q., Liu Z. Q., Guo J. P., Chen H. Y., Yu W. T., Xue G. Liu D. S. (2006), Acceptor or Donor (Diaryl B or N) Substituted Octupolar Truxene: Synthesis, Structure, and Charge-Transfer-Enhanced Fluorescence, *J. Org. Chem.*, 71, 7858-7861, (DOI: 10.1021/jo061210i). (b) Duan X. F., Wang J. L., Pei J. (2005), Nanosized π -Conjugated Molecules Based on Truxene and Porphyrin: Synthesis and High Fluorescence Quantum Yields, *Org. Lett.*, 7, 4071, (DOI: 10.1021/ol051221i).
10. (a) Pei J., Wang J., Cao X., Zhou X., Zhang B. (2003), Star-Shaped Polycyclic Aromatics Based on Oligothiophene-Functionalized Truxene: Synthesis, Properties and Facile Emissive Wavelength Tuning, *J. Am. Chem. Soc.*, 125, 9944, (DOI: 10.1021/ja0361650). (b) Cao X. Y., Zhang W. B., Wang J. L., Zhou X. H., Lu H., Pei J. (2003), Extended π -Conjugated Dendrimers Based on Truxene, *J. Am. Chem. Soc.*, 125, 12430, (DOI: 10.1021/ja037723d).
11. Cao X. Y., Liu X. H., Zhou X. H., Zhang Y., Jiang Y., Cao Y., Cui Y. X., Pei J. (2004), Giant Extended π -Conjugated Dendrimers Containing the 10,15-Dihydro-5*H*-diindeno[1,2-*a*;1',2'-*c*]fluorene Chromophore: Synthesis, NMR Behaviors, Optical Properties, and Electroluminescence, *J. Org. Chem.*, 69, 6050, (DOI: 10.1021/jo049268p).
12. Zong X., Liang M., Fan C., Tang K., Li G., Sun Z., S. Xue (2012), Design of Truxene-Based Organic Dyes for High-Efficiency Dye-Sensitized Solar Cells

- Employing Cobalt Redox Shuttle, *J. Phys. Chem. C.*, 116, 11241–11250, (DOI: 10.1021/jp301406x).
13. Xua H. J., Dub B., Gros C. P., Richarda P., Barbea J. M., Pierre D. H. (2013), Shape-persistent poly-porphyrins assembled by a central truxene: synthesis, structure, and singlet energy transfer behaviors, *J. Porphyrins Phthalocyanines*, 17, 44–55, (DOI: org/10.1142/S1088424612501271).
 14. Misra R., Gautam P., Jadhav T., Mobin S. M. (2013), Donor–Acceptor Ferrocenyl-Substituted Benzothiadiazoles: Synthesis, Structure, and Properties, *J. Org. Chem.*, 78, 4940-4948, (DOI:10.1021/jo4005734). (b) Misra R., Gautam P., Mobin S. M. (2013), Aryl-substituted unsymmetrical benzothiadiazoles: synthesis, structure, and properties, *J. Org. Chem.*, 78, 12440-12452, (DOI:10.1021/jo402111q).
 15. (a) Misra R., Maragani R., Jadhav T., Mobin S. M. (2014), Ferrocenyl end capped molecular rods: synthesis, structure, and properties, *New J. Chem.*, 38, 1446-1457, (DOI: 10.1039/C3NJ01244A) (b) Auger A., Muller A. J., Swarts J. C. (2007), Remarkable isolation, structural characterisation and electrochemistry of unexpected scrambling analogues of 5-ferrocenyl-10,20-diphenylporphyrin, *Dalton Trans.*, 3623–3633, (DOI: 10.1039/B706840A).
 16. (a) Kato S., Diederich F. (2010), Non-planar push–pull chromophores, *Chem. Commun.*, 46, 1994–2006, (DOI: 10.1039/B926601A). (b) Tang X., Liu W., J. Wu, Lee C. S., You J., Wang P. (2010), Synthesis, crystal structures, and photophysical properties of triphenylamine-based multicyano derivatives, *J. Org. Chem.*, 75, 7273–7278, (DOI: 10.1021/jo101456v).
 17. Cao X., Zi H., Zhang W., Lu H., Pei J. (2005), Star-Shaped and Linear Nanosized Molecules Functionalized with Hexa-peri-hexabenzocoronene: Synthesis and Optical Properties, *J. Org. Chem.*, 70, 3645-3653, (DOI: 10.1021/jo0480139).
 18. Gompper R., Wagner H. U. (1988), Donor-Acceptor-Substituted Cyclic π -Electron Systems—Probes for Theories and Building Blocks for New Materials, *Angew. Chem. Int. Ed.*, 27, 1437–1455, (DOI: 10.1002/anie.198814371).

19. Wu X., Wu J., Liu Y., Jen A. K. Y. (1999), Highly Efficient, Thermally and Chemically Stable Second Order Nonlinear Optical Chromophores Containing a 2-Phenyl-tetracyanobutadienyl Acceptor *J. Am. Chem. Soc.*, 121, 472 – 473, (DOI: 10.1021/ja983537).
20. Nemykin V. N., Maximov A. Y., Kuposov A. Y. (2007), Mercury-free preparation, characterization, and molecular structure of tricyanovinylferrocene using an unusual reaction between ferrocene and tetracyanoethylene, *Organometallics*, 26, 3138-3148, (DOI: 10.1021/om070160k).
21. Steiner G., Kopacka H., Wurst K., Ongania K. H., Kirchner K. (2001), *J. Organomet. Chem.*, 558–576.
22. Gritzner G., Kuta J. (1984), Recommendations on reporting electrode potentials in nonaqueous solvents: IUPC commission on electrochemistry, *Pure Appl. Chem.*, 56, 461, (DOI: doi.org/10.1016/0013).

Chapter 4

Strategy Towards Tuning Emission of Star Shaped Tetraphenylethene Substituted Truxenes

4.1. Introduction

Organic molecular systems exhibiting aggregation induced emission (AIE) has gained significant attention of the scientific community due to their application in the field of electroluminescent devices.¹ Truxene (10,15-dihydro-5*H*-diindeno[1,2-*a*;10,20-*c*]fluorene) is a planar, C_3 -symmetric polyaromatic hydrocarbon, which is a fusion of three fluorene moieties.² The truxene scaffold is a potential building block for the construction of larger molecular architectures, due to its easy functionalization, rigid structures, and high thermal and chemical stability.³⁻⁴ Jian Pei *et al.* have reported several star shaped π -conjugated molecules based on the truxene core.⁵ Recent reports on truxene based donor-acceptor systems reveal that these molecular systems are potential candidates for application in two-photon absorption, organic light-emitting diodes (OLED), organic solar cells (OSC) and organic fluorescent probes.⁶⁻⁸

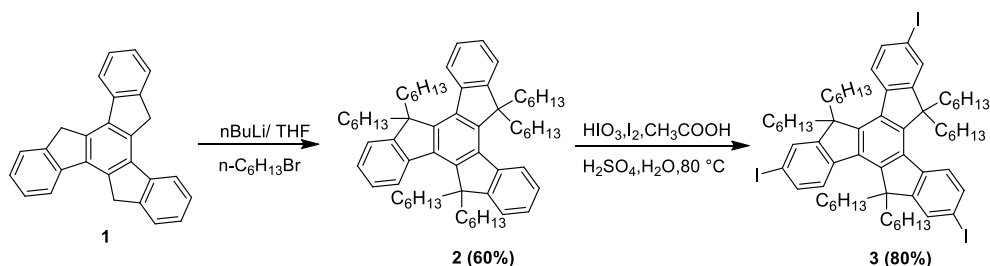
Literature reveals that the conventional fluorophores suffer from aggregation-caused quenching (ACQ) effect. This problem can be overcome by introducing the concept of AIE.⁹⁻¹⁰ Tetraphenylethylene (TPE) and 2,3,3-triphenylacrylonitrile (TPAN) are propeller shaped AIE active molecules, which have the ability to promote aggregation induced emission (AIE) in different fluorophores.¹¹⁻¹² The AIE active molecules are poorly emissive in solutions but highly emissive in solid state.¹³

Our group is involved in the design and synthesis of TPE substituted donor-acceptor systems for their application in aggregation induced emission, mechanochromism and optoelectronic properties. Recently, we have reported the aggregation induced emission and mechanochromic studies of tetraphenylethene substituted pyrenoimidazoles and phenanthroimidazoles.¹⁴ To the best of our

knowledge, there are no reports available on the Tetraphenylethene (TPE) substituted truxenes. Therefore, in the context of our research on the TPE functionalized systems and to study the effect of AIE active TPE unit on the photonic properties of truxene core, the TPE and TPAN substituted truxene **4**, **5** and **6** have been synthesised. Their photophysical and thermal properties were studied and DFT calculations were performed.

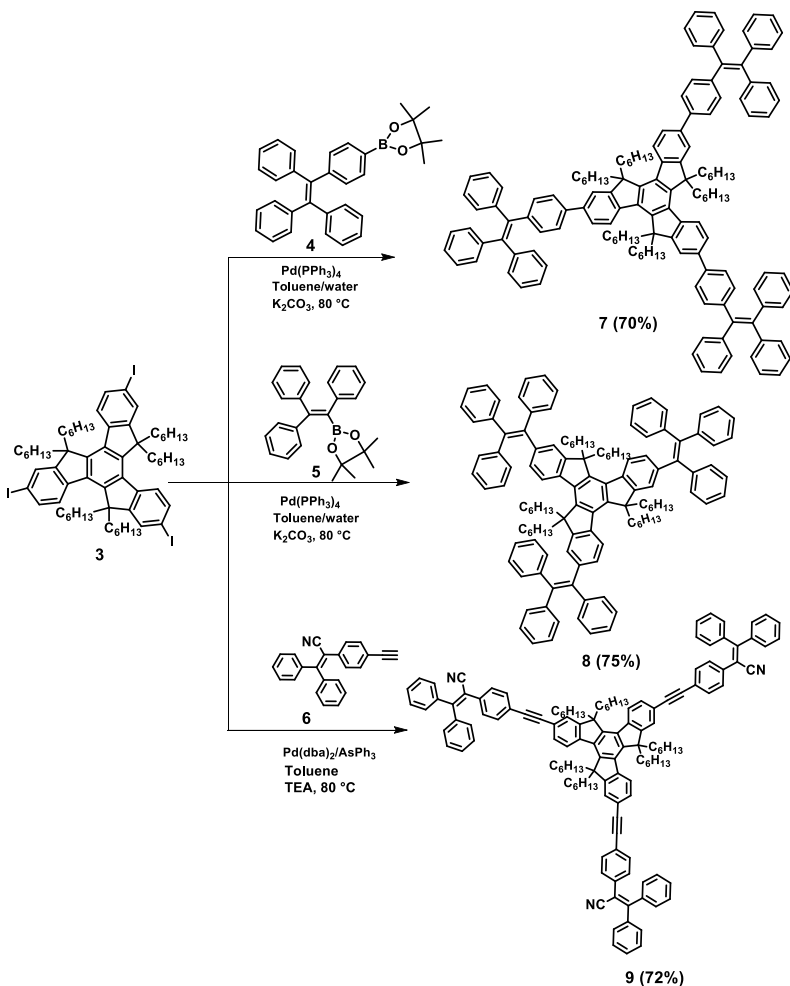
4.2. Results and discussion

TPE and TPAN substituted truxenes **7**, **8** and **9** were synthesized by the Pd-catalyzed Suzuki and Sonogashira cross-coupling reactions of tri-iodotruxene **3** with the corresponding boronic acid and alkyne (Scheme 4.2). The truxene core **1** was synthesized from 1-indanone in the presence of acetic acid and hydrochloric acid (Scheme 4.1).¹⁵ The alkylation reaction of the truxene **1** with bromo-hexane resulted in hexahexylated truxene **2**.¹⁵ The iodination reaction of truxene **2** in the presence of HIO_3 and I_2 resulted in hexahexylated tri-iodo truxene **3** in 80% yield (Scheme 4.1).¹⁶



Scheme 4.1. Synthesis of tri-iodotruxene **3**.

Tetraphenylethene boronic ester (**4**), triphenylethene boronic ester (**5**), were synthesized by reported procedure from corresponding bromo-TPE.^{14c} The TPAN-alkyne (**6**) was synthesized by the Sonogashira cross-coupling reaction of bromo-TPAN with trimethylsilylethyne, followed by deprotection of TMS group by K_2CO_3 in overall 69% yield.¹⁷



Scheme 4.2: Synthesis of TPE and TPAN substituted truxenes **7**, **8** and **9**

The reaction of tri-iodo truxene **3** with tetraphenylethene boronic ester (**4**), triphenylethene boronic ester (**5**) using $\text{Pd}(\text{PPh}_3)_4$ and TPAN-alkyne (**6**), under the catalytic system $\text{Pd}(\text{dba})_2/\text{AsPh}_3$ resulted truxenes **7**, **8** and **9** in 70%, 75% and 72% yields, respectively (Scheme 4.2). Truxenes **7**, **8** and **9** are readily soluble in common organic solvents and were well characterized by ^1H NMR, ^{13}C NMR, and HRMS techniques

Thermal stability is the significant requisite for practical applications of organic chromophores. The thermal properties of the TPE and TPAN substituted truxenes **7**, **8** and **9** were explored using thermogravimetric analysis (TGA) at a heating rate of $10^\circ\text{C min}^{-1}$ under nitrogen atmosphere (Figure 4.1). The truxenes **7**, **8** and **9** showed 10% weight loss at 438°C , 409°C and 413°C respectively. The thermal stability of the TPE and TPAN substituted truxenes follow the order **7** > **9** > **8**.

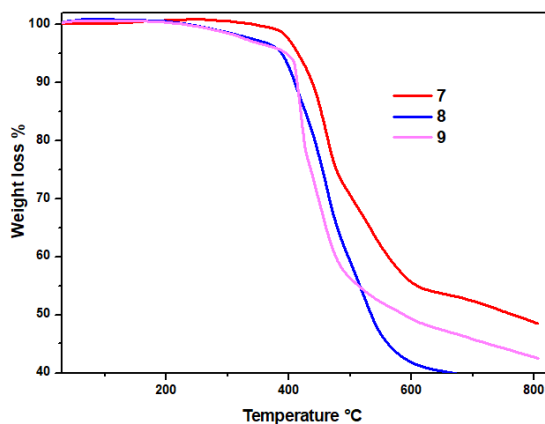


Figure 4.1. TGA plots of truxene 7–9

4.3. Photophysical properties

The electronic absorption spectra of the dilute solutions of TPE and TPAN substituted truxenes **7**, **8** and **9** in tetrahydrofuran (THF) are shown in Figure 4.2, and the data are listed in Table 4.1. The truxenes **7**, **8** and **9** show strong absorption band between 283–285 nm respectively, with high molar extinction coefficient, corresponding to $\pi \rightarrow \pi^*$ transition.¹⁸ The low intensity band between 346–370 nm is caused by intramolecular charge transfer from TPE and TPAN to the truxene core. The emission properties of the TPE and TPAN substituted truxenes **7**, **8** and **9** were studied by steady state and time-resolved fluorescence techniques. Their emission spectra are shown in Figure 4.2(b). The TPE substituted truxene **7** exhibit fluorescence maximum at 487 nm, truxene **8** shows at 512 nm and truxene **9** shows fluorescence maximum at 424 nm (Figure 4.2(b)). The dilute solutions of truxenes **7**, **8** and **9** show fluorescence quantum yields of 0.05, 0.05 and 0.14 respectively.

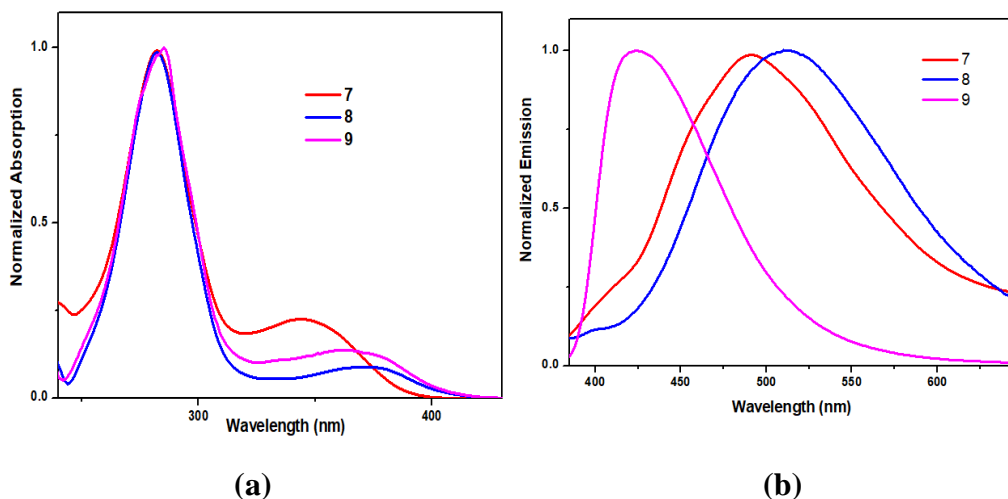


Figure 4.2. (a) Normalized electronic absorption and (b) fluorescence spectra of the solutions of truxenes **7**, **8**, and **9** in tetrahydrofuran at RT.

Table 4.1. Photophysical and thermal properties of truxenes **7**, **8**, and **9**.

Compound	$\lambda_{\text{max}}[\text{nm}]$	Emission	Φ_f^b	T_d °C
	$(\epsilon \times 10^5 [\text{mol}^{-1} \text{cm}^{-1}])^a$	$\lambda_{\text{max}}[\text{nm}]^a$		
7	283(1.1), 346	487	0.05	438
8	283(1.2), 370	512	0.05	409
9	285(2.1), 365	424	0.14	413

^a Measured in THF at T = 25 °C, λ_{obs} (nm): absorption maximum. ϵ , extinction coefficient. ^b Determined by using quinine sulphate as a standard ($\Phi^{\text{st}} = 0.54$)

4.4. Aggregation study:

The aggregation induced emission (AIE) is the characteristic property of TPE containing fluorphores.¹⁶ The aggregation behaviour of truxenes **7**, **8** and **9** were studied with the help of fluorescence spectroscopy in THF–water mixture with varying amount of water fraction. The truxenes **7**, **8** and **9** are readily soluble in tetrahydrofuran (THF) and insoluble in water. The dissolved solute molecules transform into the nano-aggregate particles by increasing the water fraction in the

THF–water mixture. The TPE substituted truxenes **7** and **8** are weakly fluorescent in pure tetrahydrofuran and become highly fluorescent at higher water fraction. The fluorescence intensity of TPE substituted truxenes **7** and **8** continuously increases with increasing water fraction (Figure 4.3 (a & b)). This increase in the fluorescence intensity is attributed to the AIE phenomenon. The quantitative estimation of the AIE process was obtained by calculating the fluorescence quantum yields, in the mixture of water and THF in various proportions, using quinine sulphate as the standard. In the pure THF solution, truxene **7** and **8** exhibit poor fluorescence with quantum yields of 0.05 which was increased to 0.76, 0.75 respectively in the aggregated state (90% aqueous).

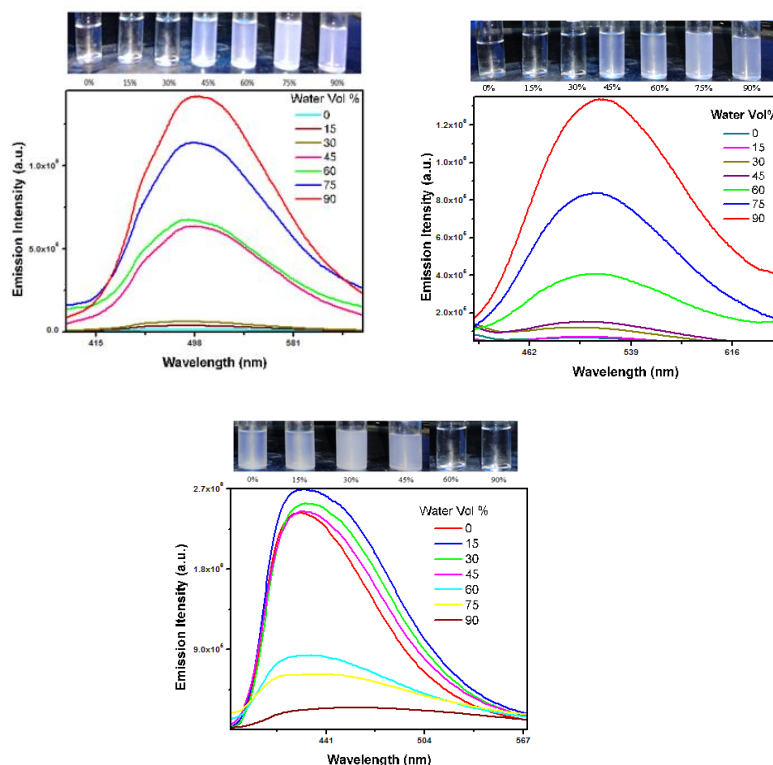


Figure 4.3. Emission spectra of truxenes **7** (a), **8** (b), and **9** (c) (10^{-5} M) in THF/H₂O mixtures with different volume fractions of water. ($\lambda_{\text{ex}} = 283$ nm). Fluorescence color images of the truxenes in the presence of different THF/Water mixtures under UV light are presented above graphs.

The TPAN substituted truxene **9** shows decrease in fluorescence intensity with increasing water fraction (Figure 4.5c). This is attributed to the aggregation-caused quenching (ACQ) effect which can be assigned to the charge transfer from TPAN to the truxene core.¹⁰ The alkyne linkage increases the distance between TPE and truxene core, which gives sufficient space for planarization and π - π stacking.¹⁷ Which favours the aggregation-caused fluorescence quenching and makes TPAN substituted truxene **9** AIE inactive. The truxene **9** shows 0.14 quantum yield in pure THF which was decreased to 0.06 in the aggregated state.

4.5. Computational calculations

In order to gain insight into the electronic structures of truxenes and to understand the photophysical properties of the TPE and TPAN substituted truxenes **7**, **8** and **9** the density functional theory (DFT) and time dependent density functional (TD-DFT) calculations were performed. The structures of **7**, **8** and **9** were optimized using Gaussian 09W program at the B3LYP/6-31G** level. The TD-DFT calculations were carried out in tetrahydrofuran (THF) using the polarized continuum model (CPCM) of Gaussian 09 software. The 6-31G** basis set was used for all the calculations.¹⁹⁻²²

The truxene core of TPE and TPAN substituted truxenes **7**, **8** and **9** show planar geometry while TPE units show twisted geometry (Figure 4.4). The interplanar angles between the truxene core and the plane of TPE units in truxene **7** are 35.6°, 35.6° and 35.7°. In truxene **8** the dihedral angles between truxene core and TPE units are 46.9°, 46.7° and 46.8°. The truxene core of TPAN substituted truxene **9** and phenyl ring of TPAN is in same plane, which reflects stronger electronic communication compared to truxene **7** and **8**.

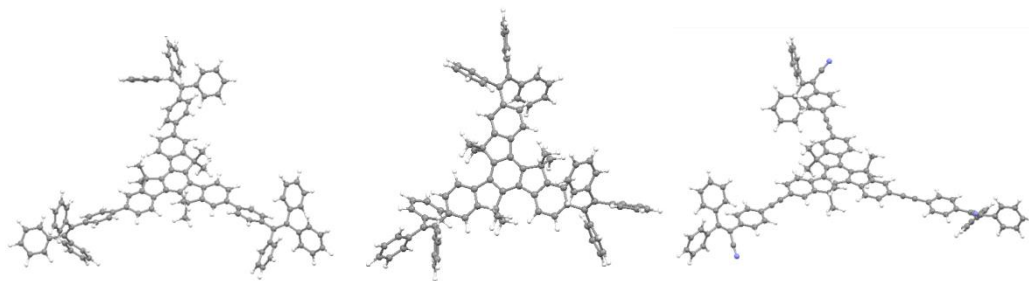


Figure 4.4. The DFT optimized structures of the truxenes **7**, **8** and **9** with Gaussian 09 at the B3LYP/6-31G** level of theory.

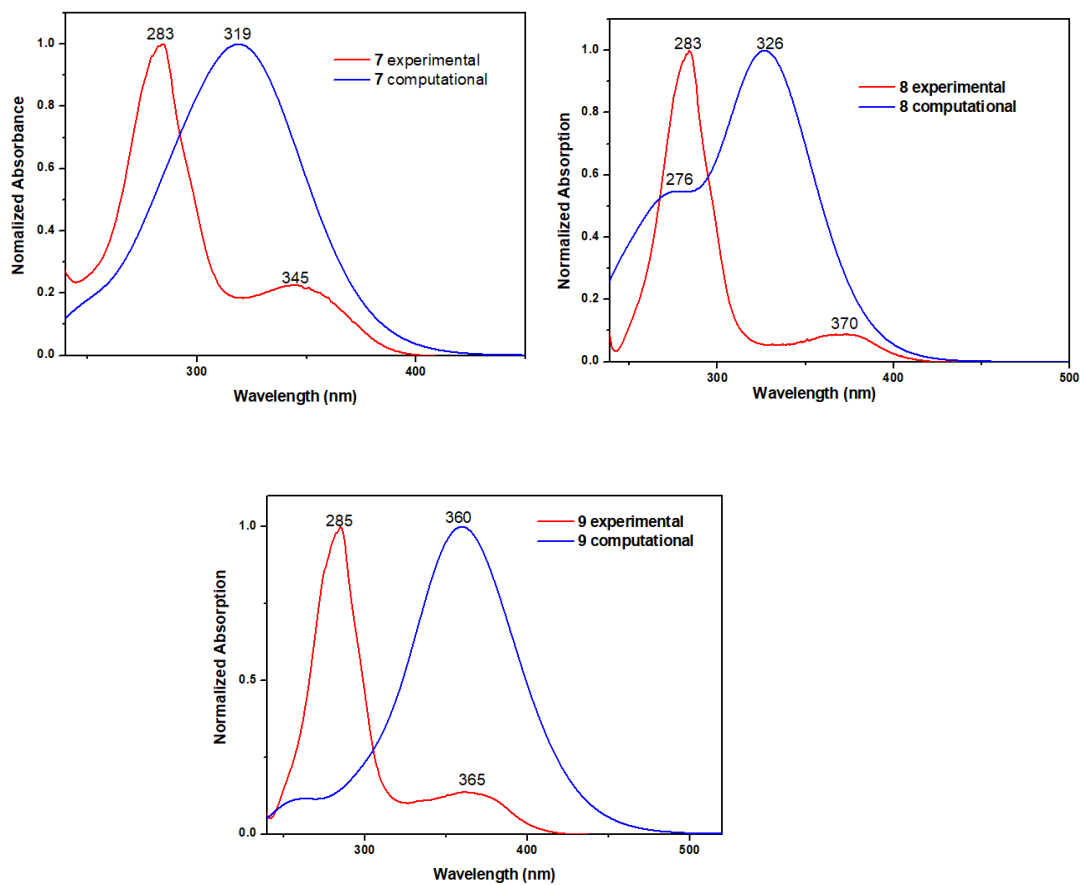


Figure 4.5. The comparison of experimental and calculated (TD-DFT) at CAMB3LYP absorption spectrum the truxenes **7**, **8** and **9** in THF solution.

The TD-DFT predicted vertical excitation energies for truxenes **7**, **8** and **9** are shown in Figure 4.5 along with experimental UV-vis spectra and data are listed in Table 4.2. The major intense transition in the truxenes **7**, **8** and **9** is π - π^* in nature. The strong absorption bands calculated at CAM-B3LYP level are at 319 nm, and 326 nm for truxenes **7** and **8** respectively. The experimental values for these transitions are 283 nm for **7** and **8**. The TPAN substituted truxene **9** show calculated band at 360 nm which perfectly matches with the ICT band. This reveals that electron density transfers from truxene core (donor) to TPAN (acceptor) unit.

Figure 4.6 shows the electron density distribution of the HOMO and LUMO of the TPE and TPAN substituted truxenes **7**, **8** and **9**. The HOMO and LUMO in TPE substituted truxenes **7** and **8** are delocalized over the truxene and TPE unit. The TPAN substituted truxene **9** shows HOMO delocalized over the truxene core while the LUMO is exclusively located on the TPAN units, which indicates charge transfer from HOMO to LUMO. The HOMO-LUMO gap is lower for TPAN substituted truxene **9** as compared to truxene **7** and **8**, due to the incorporation of TPAN alkyne as a strong acceptor.

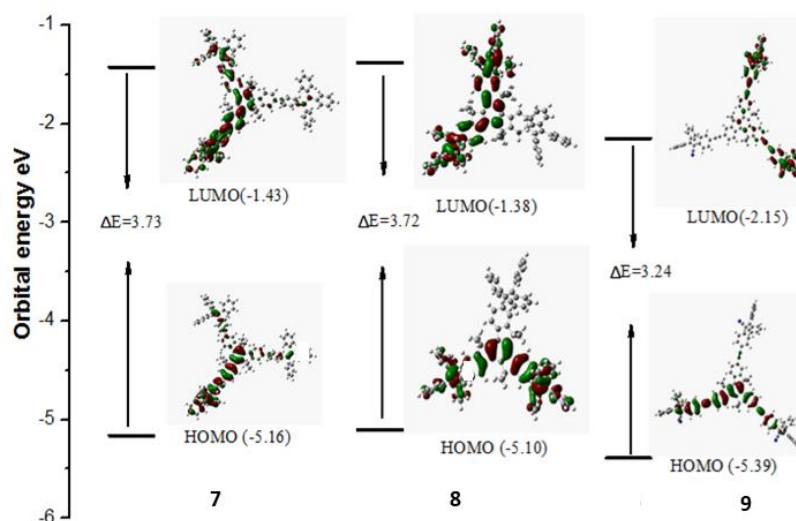


Figure 4.6. The energy level diagram of the frontier molecular orbitals of the TPE and TPAN substituted truxenes **7**, **8** and **9** using B3LYP/6-31G(d,p) level of DFT theory.

Table 4.2. Computed vertical transition energies and their Oscillator strengths (*f*) and major contributions for the truxene **7–9**.

Compound	TD-DFT/ CAM-B3LYP (THF)		
	λ_{max}	f^a	Major contribution (%)
7	319 nm	2.88	HOMO-2→LUMO+1(18%)
			HOMO-1→LUMO (10%)
			HOMO-1→LUMO+2 (11%)
			HOMO→LUMO+2 (14%)
8	326 nm	1.89	HOMO-2→LUMO (18%)
			HOMO-2→LUMO (18%),
			HOMO-1→LUMO+1 (16%),
			HOMO-1→LUMO+2 (25%),
			HOMO→LUMO (17%)
9	360 nm	3.30	HOMO-2→LUMO (24%)
			HOMO→LUMO (11%),
			HOMO→LUMO+2 (14%)
			HOMO-1→LUMO (8%),

^a*f* is Oscillator strengths

4.6. Experimental section

General: Chemicals were used as received unless otherwise indicated. All oxygen or moisture sensitive reactions were performed under nitrogen/argon atmosphere using standard Schlenk method. Triethylamine (TEA) was received from commercial source, and distilled on KOH prior to use. ^1H NMR (400 MHz), and ^{13}C NMR (100MHz) spectra were recorded on the Bruker Avance (III) 400 MHz, using CDCl_3 as solvent. Tetramethylsilane (TMS) was used as reference for recording ^1H (of residual proton; $\delta = 7.26$ ppm), and ^{13}C ($\delta = 77.0$ ppm) spectra in CDCl_3 . UV-visible absorption spectra of all compounds in chloroform were recorded on a Carry-100 Bio UV-visible Spectrophotometer. HRMS was recorded on Bruker-Daltonics, micrO TOF-Q II mass spectrometer.

4.7. Synthesis and Characterization

The reactant **4**, **5**, **6** were synthesized according to known methods.^{14c,17}

Synthesis of truxenes **7** and **8**.

A solution of tri-iodotruxene **3** (200 mg, 0.16 mmol) and the corresponding TPE boronic ester (4.5 equivalent) in toluene–water 3 : 1 (60 mL) was deaerated for 30 min with argon bubbling and then $\text{Pd}(\text{PPh}_3)_4$ (40 mg, 0.07 mmol) were added. The solution was deaerated for further 5 min. The mixture was heated at 80 °C for 48 h. The solvent was removed; the remaining residue was suspended in water (50 mL) and extracted with DCM (3 x 20 mL). The combined organic layers were dried (MgSO_4) and concentrated in vacuum. The resulting crude product was purified by column chromatography on silica gel eluting with CH_2Cl_2 /hexane (10%). The desired compounds obtained from the column was recrystallized from DCM/methanol to give compounds **7** and **8** in 70-75% yield.

Synthesis of truxenes **9**

A solution of tri-iodotruxene **3** (250 mg, 0.20 mmol) and the TPAN alkyne (4.5 equivalent) in toluene–triethylamine 5 : 1 (60 mL) was deaerated for 30 min with argon bubbling and then $\text{Pd}(\text{dba})_2$ (40 mg, 0.07 mmol) and AsPh_3 (170 mg, 0.55 mmol) were added. The solution was deaerated for a further 5 min. The mixture was heated at 80 °C for 48 h. The solvent was removed; the remaining residue

was suspended in water (50 mL) and extracted with DCM (3 x 20 mL). The combined organic layers were dried (MgSO₄) and concentrated in vacuum. The desired compounds obtained from the column was recrystallized from DCM/methanol to give compound **9** in 75% yield.

Compound 7:

white solid (yield: 70%) ¹H NMR (400 MHz, CDCl₃): δ (ppm) 8.3(d, 3H, *J* = 8.70 Hz), 7.58-7.68 (m, 6H), 7.53 (d, 6H, *J* = 7.50 Hz), 7.01-7.21 (m, 51H), 2.87-3.01 (m, 6H), 2.02-2.17 (m, 6H), 0.75-0.99 (m, 36H), 0.45-0.63 (m, 30H)); ¹³C NMR (100 MHz, CDCl₃): δ = 154.2, 145.0, 143.8, 142.7, 141.0, 140.6, 139.6, 138.8, 138.3, 138.0, 131.8, 131.4, 131.4, 131.3, 127.8, 127.7, 127.6, 126.4, 126.4, 126.0, 127.8, 124.7, 120.0, 55.0, 37.7, 31.5, 29.5, 23.9, 22.2, 13.8, HRMS (ESI) *m/z*, calcd for M⁺ (C₁₄₁H₁₄₄): 1838.1296; found: 1838.1608.

Compound 8:

white solid (yield: 75%) ¹H NMR (400 MHz, CDCl₃): δ (ppm) 7.96(d, 3H, *J* = 8.58 Hz), 6.72-7.51 (m, 51H), 2.57-2.79 (m, 6H), 1.54-1.69 (m, 6H), 0.59-1.00 (m, 66H)); ¹³C NMR (100 MHz, CDCl₃): δ = 152.7, 144.9, 144.0, 143.9, 143.8, 141.7, 141.3, 140.5, 138.6, 137.9, 131.5, 131.4, 131.3, 129.9, 129.3, 129.0, 127.6, 127.5, 126.4, 126.3, 125.1, 123.9, 55.2, 36.5, 31.5, 29.7, 29.2, 23.6, 22.3, 13.9. HRMS (ESI) *m/z*, calcd for M⁺ (C₁₂₃H₁₃₂): 1610.0357; found: 1610.0355.

Compound 9:

yellow solid (yield: 72%) ¹H NMR (400 MHz, CDCl₃): δ (ppm) 8.33(d, 3H, *J* = 9.20 Hz), 7.52-7.63 (m, 6H), 7.39-7.51 (m, 20H), 7.18-7.34 (m, 16H), 7.04 (d, 6H, *J* = 7.36), 2.85-2.99 (m, 6H), 2.00-2.16 (m, 6H), 0.77-0.99 (m, 36H)), 0.39-0.67 (m, 30H); ¹³C NMR (100 MHz, CDCl₃): δ = 158.3, 153.6, 146.0, 140.4, 140.2, 138.9, 137.9, 134.6, 131.6, 130.8, 130.0, 129.9, 129.7, 129.2, 128.5, 128.4, 125.3, 124.5, 123.4, 120.7, 119.8, 110.9, 91.7, 89.3, 55.84, 36.9, 31.4, 29.6, 29.4, 23.9, 22.2, 13.8. HRMS (ESI) *m/z*, calcd for M⁺ (C₁₃₂H₁₂₉N₃): 1756.0214; found: 1757.0510.

4.8. Conclusions

In summary, the tetraphenylethylene (TPE) substituted truxene **7**, **8** and 2,3,3-triphenyl acrylonitrile (TPAN) substituted truxene **9** were designed and

synthesized by the Pd-catalyzed Suzuki and Sonogashira cross-coupling reactions. Their photonic and thermal properties were studied. The TPE substituted truxene **7** and **8** show aggregation-induced emission behaviour and TPAN substituted truxene **9** shows aggregation-caused quenching effect in THF/water medium. The computational calculations of truxenes **7–9** are in good agreement with the experimental data.

4.9. References:

1. Chi Z., Zhang X., Xu B., Zhou X., Ma C., Zhang Y., Liua S., Xu J. (2012), Recent advances in organic mechanofluorochromic materials, *Chem. Soc. Rev.*, 41, 3878–3896, (DOI: 10.1039/C2CS35016E).
2. Ventura B., Barbieri A., Barigelletti F., Diring S. E., Ziesel R. (2010), Energy Transfer Dynamics in Multichromophoric Arrays Engineered from Phosphorescent PtII/RuII/OsII Centers Linked to a Central Truxene Platform, *Inorg. Chem.*, 49, 8333–8346, (DOI: 10.1021/ic1008413).
3. Zhang W. B., Jin W. H., Zhou X. H., Pei J. (2007), Star-shaped oligo(p-phenylene)- functionalized truxenes as blue-light-emitting materials: synthesis and the structure-property relationship, *Tetrahedron*, 63, 2907–2914, (doi.org/10.1016/j.tet.2007.01.025).
4. (a) Boorum M. M., Vasil Y. V., Drewello T., Scott L. T. (2001), Groundwork for a rational synthesis of C₆₀: cyclodehydrogenation of a C₆₀H₃₀ polyarene, *Science*, 294, 828, (DOI: 10.1126/science.1064250). (b) Gomez-Lor B., De Frutos O., Echavarren A. M. (1999), Synthesis of ‘crushed fullerene’ C₆₀H₃₀, *Chem. Commun.*, 2431, (DOI: 10.1039/A906990I). (c) Rabideau P. W., Abdourazak A. H., Marcinow Z., Sygula R., Sygula A. (1995), Buckybowls 2. Toward the Total Synthesis of Buckminsterfullerene (C₆₀): Benz[5,6]-as-indaceno[3,2,1,8,7-mnopqr]indeno[4,3,2,1-cdef]chrysene, *J. Am. Chem. Soc.*, 117, 6410, (DOI: 10.1021/ja00128a052).
5. Zong X., Liang M., Fan C., Tang K., Li G., Sun Z., Xue S. (2012), Design of truxene-based organic dyes for high-efficiency dye-sensitized solar

- cells employing cobalt redox shuttle, *J. Phys. Chem. C.*, 116, 11241–11250, (DOI: 10.1021/jp301406x).
6. Xua H. J., Dub B., Gros C. P., Richarda P., Barbea J. M., Pierre D. H. (2013), Shape-persistent poly-porphyrins assembled by a central truxene: synthesis, structure, and singlet energy transfer behaviors, *J. Porphyrins Phthalocyanines*, 17, 44–55, (doi.org/10.1142/S1088424612501271).
 7. Huang W., Smarsly E., Han J., Bender M., Seehafer K., Wacker I., Schröder R. R., Bunz U. H. F. (2017), Truxene-Based Hyperbranched Conjugated Polymers: Fluorescent Micelles Detect Explosives in Water, *ACS Appl. Mater. Interfaces*, 9, 3068–3074, (DOI: 10.1021/acsami.6b12419).
 8. Yao C., Yu Y., Yang X., Zhang H., Huang Z., Xu X., Zhou G., Yue L., Wu Z. (2015), Effective blocking of the molecular aggregation of novel truxene-based emitters with spirobifluorene and electron-donating moieties for furnishing highly efficient non-doped blue-emitting OLEDs, *J. Mater. Chem. C*, 3, 5783, (DOI: 10.1039/C5TC01018G).
 9. Luo J., Zhou Y., Niu Z. Q., Zhou Q.-F., Ma Y., Pei. J. (2007), Three-Dimensional Architectures for Highly Stable Pure Blue Emission, *J. Am. Chem. Soc.*, 129, 11314–11315, (DOI: 10.1021/ja073466r).
 10. Raksasorn D., Namuangruk S., Prachumrak N., Sudyoasuk T., Promarak V., Sukwattanasinitt M., Rashatasakhon P. (2015), Synthesis and characterization of hole-transporting star-shaped carbazolyl truxene derivatives, *RSC Adv.*, 5, 72841, (DOI: 10.1039/C5RA12011J).
 11. Luo J. D., Xie Z. L., Lam J. W. Y., Cheng L., Chen H. Y., Qiu C. F., Kwok H. S., Zhan X. W., Liu Y. Q., Zhu D. B., Tang B. Z. (2001), Aggregation-induced emission of 1-methyl-1,2,3,4,5-pentaphenylsilole, *Chem. Commun.*, 1740, (DOI: 10.1039/B105159H).
 12. Liu H., Xu J., Li Y. (2010), Aggregate Nanostructures of Organic Molecular Materials, *Acc. Chem. Res.*, 43, 1496–1508, (DOI: 10.1021/ar100084y).

13. Dong Y., Lam J., Liu A. J., Tang B. Z., Sun J., Kwok H. S. (2007), Aggregation-induced emissions of tetraphenylethene derivatives and their utilities as chemical vapor sensors and in organic light-emitting diodes, *Appl. Phys. Lett.*, 91, 011111., (doi.org/10.1063/1.2753723).
14. (a) Misra R., Jadhav T., Dhokale B., Mobin S. M. (2014), Reversible mechanochromism and enhanced AIE in tetraphenylethene substituted phenanthroimidazoles, *Chem. Commun.*, 50, 9076, (DOI: 10.1039/C4CC02824D). (b) Jadhav T., Dhokale B., Mobin S. M., Misra R. (2015), Mechanochromism and aggregation induced emission in benzothiazole substituted tetraphenylethylenes: a structure function correlation, *RSC Adv.*, 5, 29878, (DOI: 10.1039/C5RA04881H).
15. Luo J. D., Xie Z. L., Lam J. W. Y., Cheng L., Chen H. Y., Qiu C. F., Kwok H. S., Zhan X. W., Liu Y. Q., Zhu D. B., Tang B. Z. (2001), Aggregation-induced emission of 1-methyl-1,2,3,4,5-pentaphenylsilole, *Chem. Commun.*, 1740, (DOI: 10.1039/B105159H).
16. (a) Jadhav T., Dhokale B., Mobin S. M., Misra R. (2015), Aggregation induced emission and mechanochromism in pyrenoimidazoles, *J. Mater. Chem. C*, 3, 9981, (DOI: 10.1039/C5TC02181B). (b) Jadhav T., Dhokale B., Misra R. (2015), Effect of the cyano group on solid state photophysical behavior of tetraphenylethene substituted benzothiadiazoles, *J. Mater. Chem. C*, 3, 9063, (DOI: 10.1039/C5TC01871D).
17. Kanibolotsky A. L., Berridge R., Skabara P. J., Perepichka I. F., Bradley D. D. C., Koeberg M. (2004), Synthesis and properties of monodisperse oligofluorene-functionalized truxenes: highly fluorescent star-shaped architectures, *J. Am. Chem. Soc.*, 126, 13695, (DOI: 10.1021/ja039228n).
18. Cao X., Zi H., Zhang W., Lu H., Pei J. (2005), Star-Shaped and Linear Nanosized Molecules Functionalized with Hexa-peri-hexabenzocoronene: Synthesis and Optical Properties, *J. Org. Chem.*, 70, 3645-3653, (DOI: 10.1021/jo0480139).
19. Dhokale B., Jadhav T., Mobin S. M., Misra R. (2015), Meso Alkynylated Tetraphenylethylene (TPE) and 2,3,3-Triphenylacrylonitrile (TPAN)

- Substituted BODIPYs, *J. Org. Chem.*, 80, 8018–8025, (DOI:10.1021/acs.joc.5b01117).
20. Becke A. D. (1993), Density-functional thermochemistry. III. The role of exact exchange, *J. Chem. Phys.*, 98, 5648–5652, (doi.org/10.1063/1.464913).
21. (a) Maragani R., Gautam P., Mobin S. M., Misra R. (2016), C_2 -Symmetric ferrocenyl bisthiazoles: synthesis, photophysical, electrochemical and DFT studies, *Dalton Trans.*, 45, 4802–4809, (10.1039/C5DT04988A). (b) Pedone A. (2013), Role of Solvent on Charge Transfer in 7-Aminocoumarin Dyes: New Hints from TD-CAM-B3LYP and State Specific PCM Calculations, *J. Chem. Theory Comput.*, 9, 4087–4096 (DOI: /abs/10.1021/ct4004349).
22. Gusev D. G. (2013), Assessing the Accuracy of M06-L Organometallic Thermochemistry, *Organometallics*, 32, 4239–4243 (DOI: 10.1021/om400412p).

Chapter 5

C₃-Symmetric Star Shaped Donor-Acceptor Truxenes: Synthesis, Photophysical, Electrochemical and Computational Studies

5.1. Introduction

The development of novel π -conjugated donor–acceptor (D–A) molecular systems have drawn immense attention of the scientific community due to their potential applications in multi-photon absorption, organic light emitting diodes (OLEDs) and organic field effect transistors (OFETs), organic photovoltaics (OPVs).^{1,2} The electronic and photonic properties of the π -conjugated D–A molecular systems can be tuned by altering the HOMO-LUMO gap.³ The HOMO-LUMO gap in D– π –A molecular systems can be tuned either by altering the strength of D/A units or by varying the π -bridge.^{4,5}

The D–A systems incorporating the cyano-based acceptors such as tetracyanoethylene (TCNE) and 7,7,8,8-tetracyanoquinodimethane (TCNQ) are potential candidates for dye-sensitized solar cells (DSSCs), organic photovoltaics and non-linear optics.^{6–8} Diederich and others have reported the synthesis and properties of various TCNE and TCNQ substituted derivatives using [2+2] cycloaddition–retroelectrocyclization reaction.^{9a–c} Michinobu *et al.* have explored the TCNE and TCNQ substituted polymers which are promising materials for photovoltaic applications.^{9d,e} Shoji *et al.* have reported donor–acceptor based TCNE and TCNQ molecules as a redox active ICT chromophores.^{9f,g} Butenschoen *et al.* have synthesized a variety of 1,1'-disubstituted ferrocenyl TCBD derivatives.^{9h} Our group is interested in the design and synthesis of novel D–A molecular systems for optoelectronic applications.¹⁰

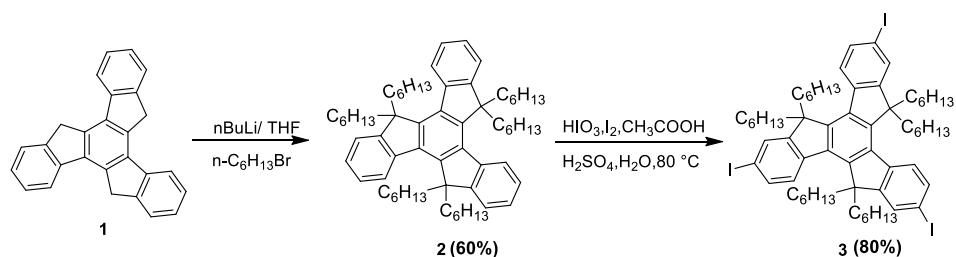
The star-shaped truxene is a rigid building block for constructing extended π -conjugated molecular systems due to its easy functionalization, excellent solubility, high thermal and chemical stability.^{11–13} Jian Pei *et al.* have explored

various star shaped π -conjugated molecules based on the truxene core for optoelectronic applications.^{12,14} Literature reveals that truxene based donor–acceptor systems have potential applications in organic light-emitting diodes (OLED), organic solar cells (OSC) and organic fluorescent probes.^{15–17}

Recently, we have explored the reaction pathway and tuning of HOMO-LUMO gap of TCNE functionalized bithiazole based donor-acceptor systems.²¹ We were further interested to study the [2+2] cycloaddition-retroelectrocyclization reaction pathway and tuning of HOMO-LUMO energy gap of triphenylamine (donor), naphthalimide (acceptor) substituted truxene and their TCNE and TCNQ derivatives. The triphenylamine and naphthalimide substituted truxenes were synthesized by the Pd-catalyzed Sonogashira cross-coupling reaction and their photophysical, electrochemical and computational studies were performed. The triphenylamine (donor) substituted truxene **7** was further subjected to the [2+2] cycloaddition–retroelectrocyclization reaction with tetracyanoethylene (TCNE) and 7,7,8,8-tetracyanoquinodimethane (TCNQ), which resulted in truxenes **10** and **11**. On the other hand the naphthalimide (acceptor) substituted truxene **6** does not undergo the cycloaddition retroelectrocyclization reaction due to the lower HOMO and higher LUMO energy level of TCNE.¹⁸

5.2. Results and discussion

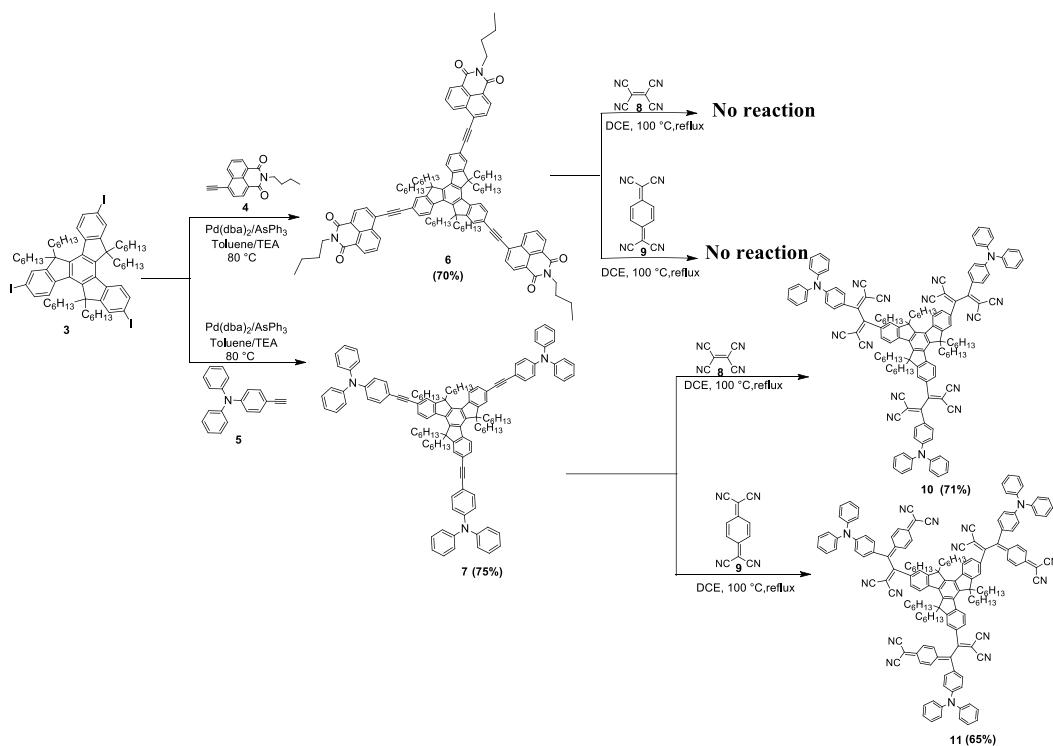
The donor (TPA) and acceptor (NDI) substituted substituted truxenes **6**, **7**, **10** and **11** were synthesized by the Pd-catalyzed Sonogashira cross-coupling reaction and [2+2] cycloaddition-retroelectrocyclization reactions (Scheme 5.2). The truxene **1** was synthesized by 1-indanone in the presence of acetic acid and hydrochloric acid.¹⁹ Truxene exhibits poor solubility due to its flat disc like conformation. Therefore, in order to improve the solubility six hexyl groups were attached to the C-5, C-10, and C-15 positions of the truxene moiety by alkylation reaction using bromo-hexane, which resulted readily soluble hexahexylated truxene **2** (Scheme 1).¹⁹ The iodination reaction of truxene **2** in the presence of HIO₃ and I₂ resulted in tri-iodo truxene **3** in 80% yield (Scheme 5.1).²⁰



Scheme 5.1. Synthesis of tri-iodotruxene **3**.

The intermediates 4-ethynyl-N,N-diphenylaniline (**5**), 4-ethynyl-1,8-naphthalimide (**4**) were synthesized by reported procedure.²¹ To overcome the solubility problem n-butyl group was attached at the N-position of 4-ethynyl-1,8-naphthalimide. The reaction of tri-iodo truxene **3** with 4-ethynyl-1,8-naphthalimide **4**, 4-ethynyl-N,N-diphenylaniline **5** under the catalytic system Pd(dba)₂/AsPh₃ resulted truxene **6** and **7** in 70% and 75% yield respectively (Scheme 5.2). The triphenylamine substituted truxene **7** was further subjected to the [2+2] cycloaddition-retroelectrocyclization reactions with TCNE and TCNQ at 100 °C for 16 h, which resulted truxene **10** and **11** in 71%, and 65% yield respectively. The reaction of naphthalimide substituted truxene **6** with TCNE and TCNQ did not lead to the product formation (Scheme 5.2). The truxenes **6**, **7**, **10** and **11** showed good solubility in common organic solvents and were well characterized by ¹H NMR, ¹³C NMR, and HRMS techniques.

The triphenylamine substituted truxene **7** undergoes cycloaddition reaction with TCNE as shown by negative Gibbs free energy -0.14 kcal/mol calculated by computational studies, shown in Figure 5.1. In case of naphthalimide substituted truxene **6** the cycloaddition reaction was unsuccessful as shown by positive Gibbs free energy (0.59 kcal/mol).²² This confirms that donor substituted truxenes are favourable for cycloaddition reaction, whereas truxenes substituted by electron withdrawing groups are not favourable (Figure 5.1). In triphenylamine substituted truxene (**7**) the HOMO energy level (-4.99 eV) is closer to the LUMO level of TCNE (-4.56 eV) as compared to HOMO energy level of truxene **6** (-5.68 eV) (Figure 5.2). Therefore overlapping of HOMO orbital of truxene **7** and LUMO orbital of TCNE is feasible in cycloaddition reaction whereas the overlapping of orbitals between TCNE and truxene **6** is not favourable.²³



Scheme 5.2: Synthesis of donor/acceptor substituted truxenes **6**, **7**, **10** and **11**.

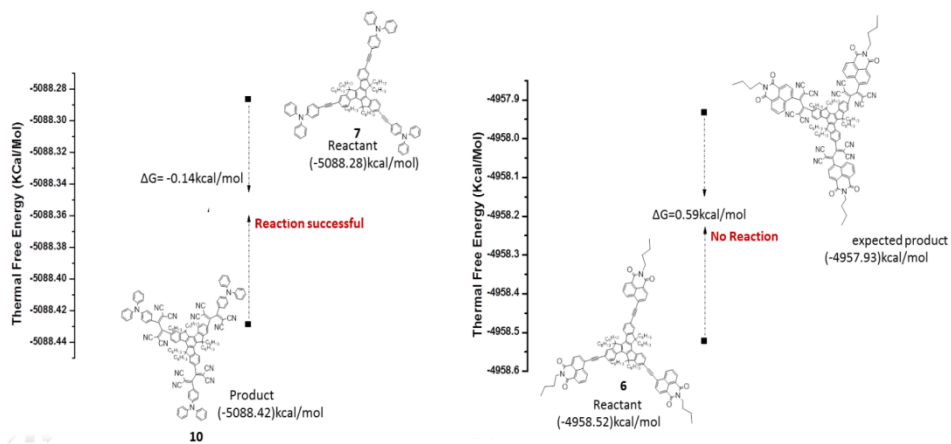


Figure 5.1. The Gibbs free energy differences of the truxenes **6** and **7** by using 6-311+ g(d,p)/B3LYP at 100°C in 1,2-dichloroethane solvent.

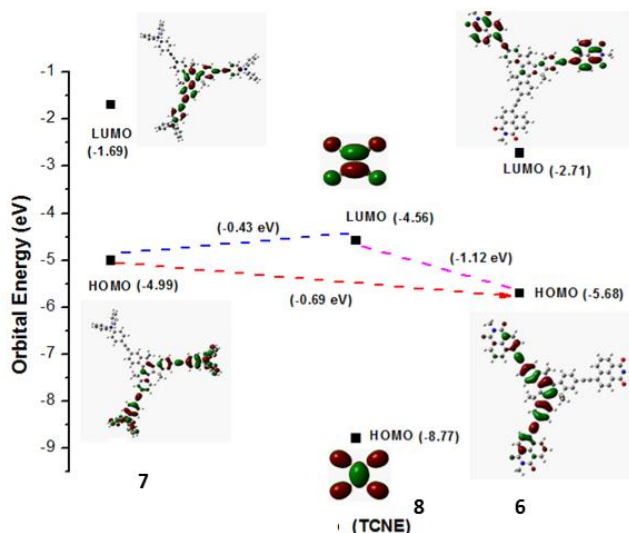


Figure 5.2. The HOMO and LUMO molecular orbitals of truxene **7**, TCNE and truxene **6**.

5.3. Thermal stability: The thermal stability of the donor and acceptor substituted truxenes **6**, **7**, **10** and **11** were explored using thermogravimetric analysis (TGA) at a heating rate of $10\text{ }^{\circ}\text{C min}^{-1}$ under nitrogen atmosphere (Figure 5.3). The decomposition temperature for 10% weight loss in truxenes **6**–**11** were above $370\text{ }^{\circ}\text{C}$. The naphthalimide substituted truxene **6** showed better thermal stability, as the 10% weight loss is at higher temperature ($426\text{ }^{\circ}\text{C}$) as compared to other truxenes (Table 1). The overall thermal stability of truxenes follow the order **6** > **7** > **11** > **10**.

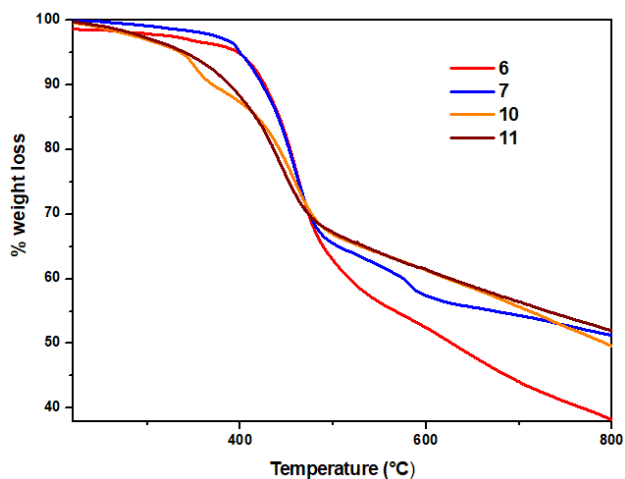


Figure 5.3. TGA plots of truxenes **6**, **7**, **10** and **11**

5.4. Photophysical properties:

The UV-vis absorption spectra of the truxenes **6**, **7**, **10** and **11** were recorded in dichloromethane at room temperature (Figure 5.4), and the data are listed in Table 5.1. The truxenes exhibit absorption band between 273–320 nm corresponding to π - π^* transition. The absorption spectra of truxene **6** and **7** exhibit charge transfer (CT) band at 418 nm and 383 nm respectively. In truxene **10**, the incorporation of TCNE unit results in red shifted strong charge transfer band at 433 nm whereas TCNQ acceptor unit result in multi-CT bands in truxene **11**.²⁴ This indicates strong donor–acceptor interaction in truxene **10** and **11** with TCNE and TCNQ linkers. The presence of strong CT transition results in intense colour solution of truxenes **6–11** in dichloromethane (Figure 5.5).

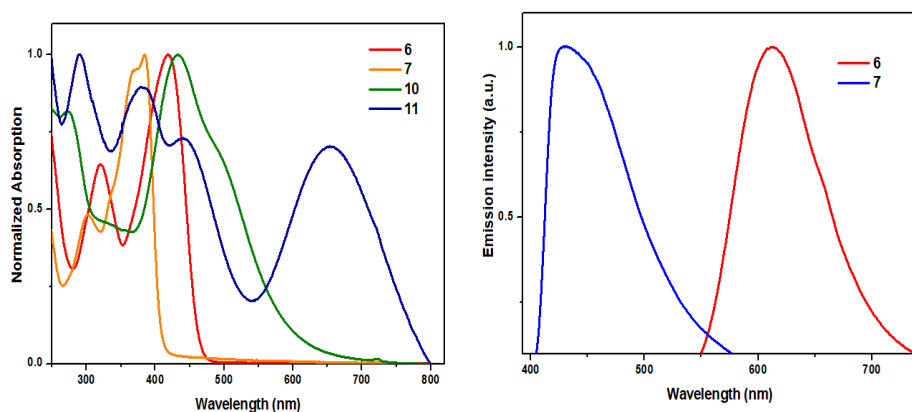


Figure 5.4. Normalized electronic absorption spectra of truxene **6**, **7**, **10** and **11** and fluorescence spectra of truxenes **6** and **7** (1.0×10^{-5} M concentration) in dichloromethane.

The trend observed in the HOMO–LUMO gap values exhibit the order $7 > 6 > 10 > 11$. This reveals that the HOMO–LUMO gap values were considerably lowered in the TCNQ linked truxene **11** followed by the TCNE substituted truxene **10** and naphthalimide substituted truxene **6**. Hence, HOMO-LUMO gap in these truxene derivatives are function of the acceptor strength. The fluorescence emission wavelengths for truxenes **6** and **7** were observed at 611 nm

and 430 nm respectively (Table 5.1). The TCNE and TCNQ linked truxenes **10** and **11** are non-emissive in nature.^{25,26}

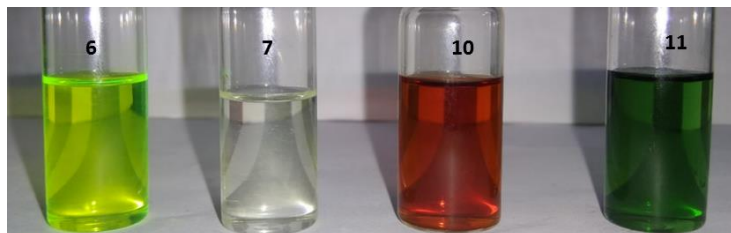


Figure 5.5: Truxenes **6**, **7**, **10** and **11** at 1×10^{-5} M concentration in dichloromethane in day light.

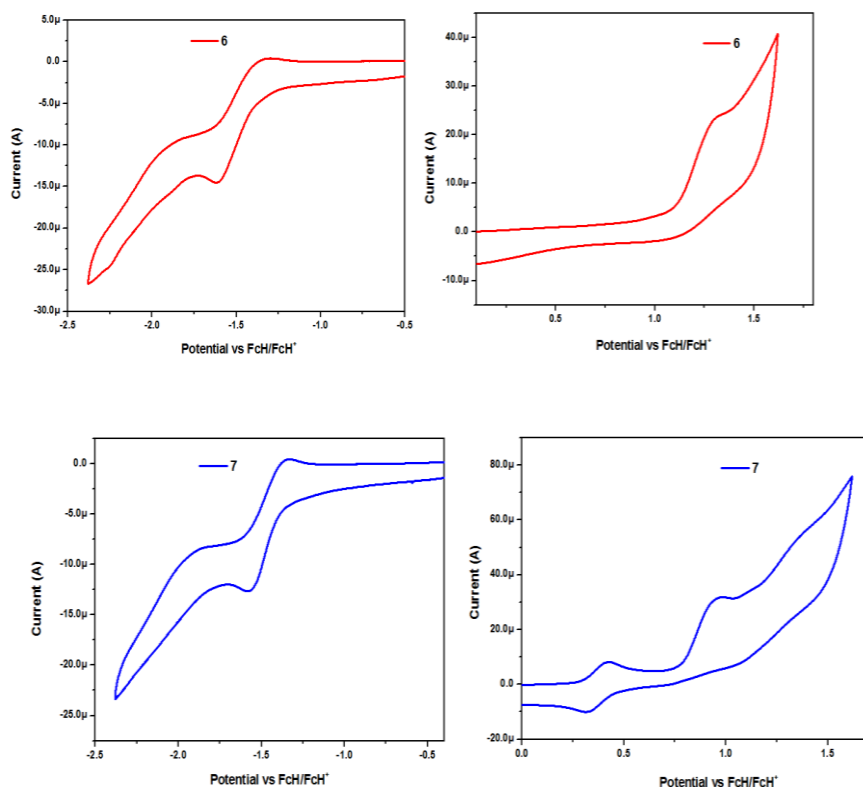
Table 5.1. Photophysical and electrochemical data of truxenes **6**, **7**, **10** and **11**

Compound	Photophysical data ^a	Emission $\lambda_{\text{max}}[\text{nm}]^a$	Φ_f^b	Electro-chemical data ^c		Theoretical HOMO-LUMO gap (eV)	^d T _d °C
	λ_{max} , [nm] ($\epsilon \times 10^5 [\text{mol}^{-1} \text{cm}^{-1}]$)			E _{ox} (V)	E _{red} (V)		
Ferrocene	-	-	-	0.00	-		
6	320(1.1), 418	611	0.42	1.31	-1.47	2.98	426
7	300(1.2), 383	430	0.54	0.37 0.96	-1.44	3.31	424
10	273(1.5), 433	-	-	1.30	-1.49	2.34	370
11	290(1.8), 380, 440, 655	-	-	1.25	-1.46	1.92	388

^aMeasured in DCM at T = 25 °C, λ_{max} (nm): absorption maximum. ϵ , extinction coefficient. ^b Determined by using quinine sulphate as a standard ($\Phi^{\text{st}} = 0.54$). ^cRecorded by cyclic voltammetry using 1.0×10^{-3} M solutions of **6–11** containing 0.1 M solution of Bu₄NPF₆ in DCM at 100 mV s⁻¹ scan rate, vs. FcH/FcH⁺. ^dDecomposition temperature at 10% weight loss, determined by TGA.

5.5. Electrochemical properties: The electrochemical behaviour of the truxenes **6**, **7**, **10** and **11** were investigated by the cyclic voltammetric analysis in dry dichloromethane solution at room temperature (25 °C) using tetrabutylammoniumhexafluorophosphate (TBAPF₆) as a supporting electrolyte.

The electrochemical data are listed in Table 5.1. The cyclic voltammograms of the truxenes **6**, **7**, **10** and **11** are shown in the Figure 5.6. All potentials are corrected to be referenced against FcH/FcH⁺, as required by IUPAC.²⁷ The cyclic voltammogram of the truxenes **6**, **10** and **11** show one irreversible oxidation wave in the range of 1.25–1.31 V (Figure 5.6). The triphenylamine substituted truxene **7** shows one reversible oxidation peak and one quasireversible peak. The first oxidation potentials of truxene **7** is at $E_{1/2} = 0.37$ V, and the second oxidation potential at $E_{1/2} = 0.96$ V, suggesting a successive formation of the monocation and then dication radical, which is attributed to the removal of electrons from the triphenylamine moiety.²⁸ The truxenes **6**, **7**, **10** and **11** exhibit one reversible reduction wave in the range of -1.44 to -1.49 V. The acceptor substituted truxenes **6**, **10**, and **11** exhibit harder oxidation and reduction as compared to donor substituted truxene **7**. This reflects strong donor-acceptor interaction in truxene **6**, **10** and **11**.



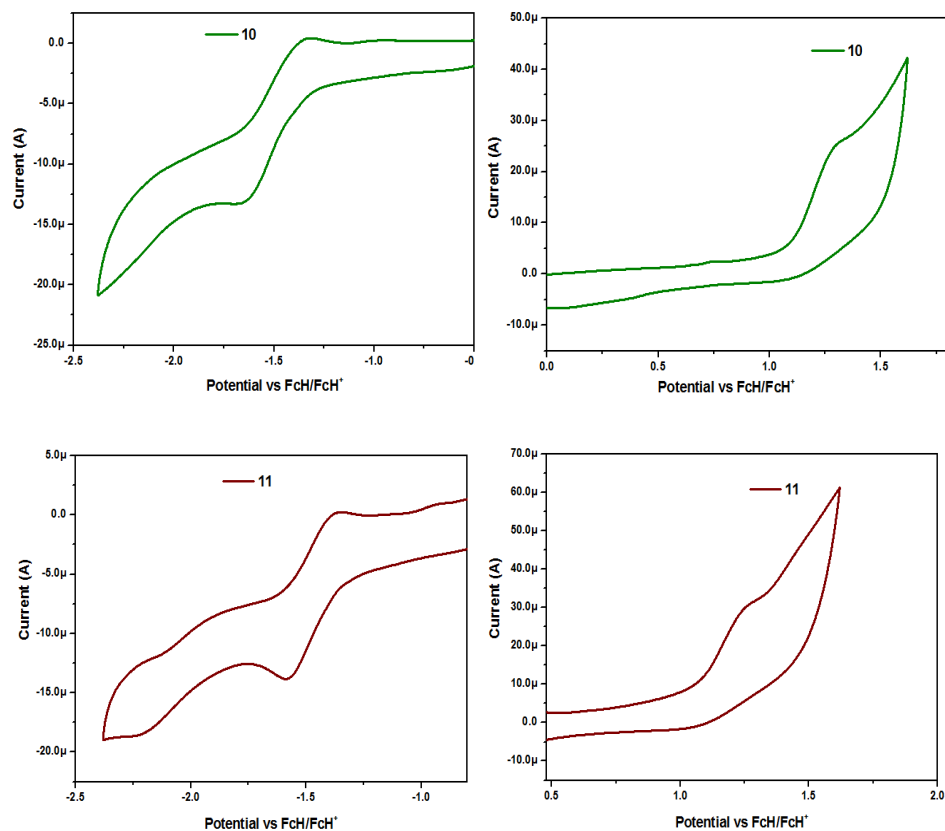


Figure 5.6. Cyclic voltammogram of 1.0×10^{-4} M solutions of truxenes **6**, **7**, **10** and **11** in CH_2Cl_2 containing 0.1M Bu_4NPF_6 as supporting electrolyte, recorded at a scan speed of 100 mV s^{-1} .

5.6. Time dependent density functional (TD-DFT) studies:

To understand the photophysical and electrochemical properties of donor-acceptor substituted truxenes **6**, **7**, **10** and **11** the density functional theory (DFT) and time dependent density functional (TD-DFT) calculations were performed. The structures **6**, **7**, **10** and **11** were optimized using Gaussian 09 program at the B3LYP/6-31G** level.²⁹ The TD-DFT calculations were carried out in the 1,2-dichloroethane (DCE) using the polarized continuum model (CPCM) of Gaussian 09 software. The 6-31G**/CAM-B3LYP basis set was used for all the calculations.²⁹

The TD-DFT predicted vertical excitation energies of truxene **6** and **7** are shown in Figure 5.7 along with experimental UV-vis spectra and data are listed in Table 5.2. The truxene **6** shows absorption bands calculated at CAM-B3LYP level at 284 nm and 389 nm. The experimental values for these transitions are 320 nm and

418 nm respectively. The truxene **7** shows calculated band at 272 nm and 355 nm which corresponds to experimental bands at 300 nm and 383 nm (Figure 6). The incorporation of TCNE (truxene **10**) results major intense transitions at 383 nm and TCNQ (truxene **11**) results bands at 370 nm and 570 nm, which belongs to intramolecular charge transfer (ICT), this is in accordance with the experimental values (Figure 5.7). These bands are supported by the frontier molecular orbitals, which show that intramolecular charge transfer (ICT) takes place from triphenylamine (donor) to TCNE or TCNQ (acceptor) as shown in 5.8.

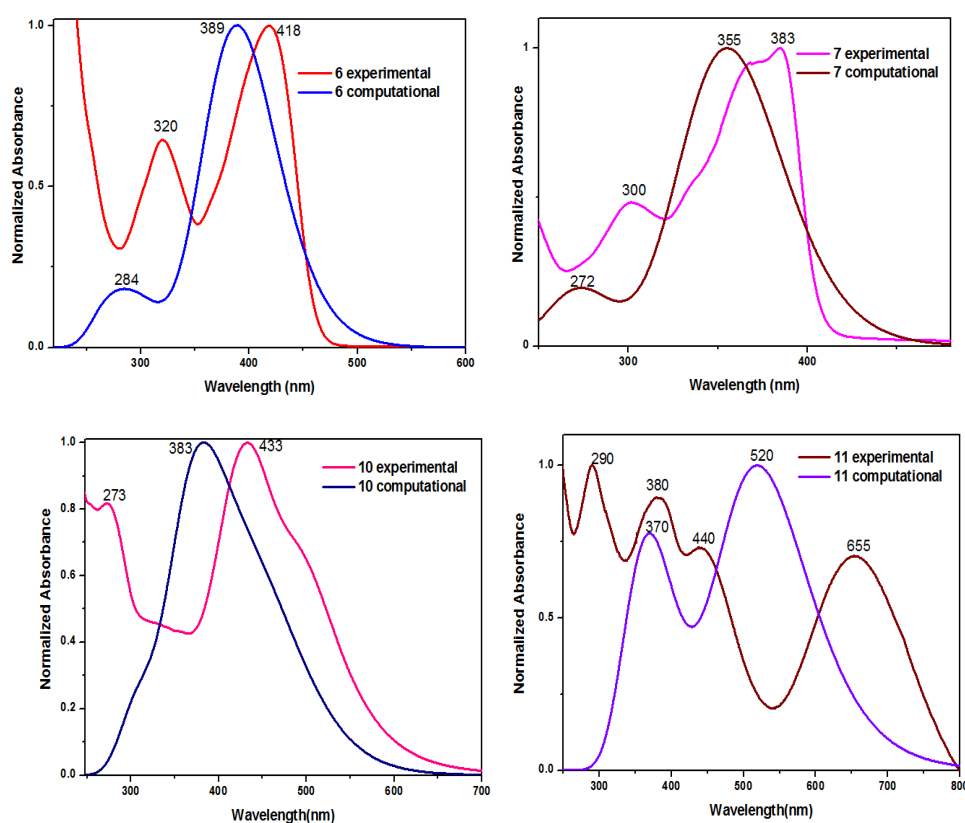


Figure 5.7. The comparison of experimental and calculated (TD-DFT at CAM-B3LYP level) absorption spectrum of truxene **6**, **7** in 1,2-dichloroethane solution.

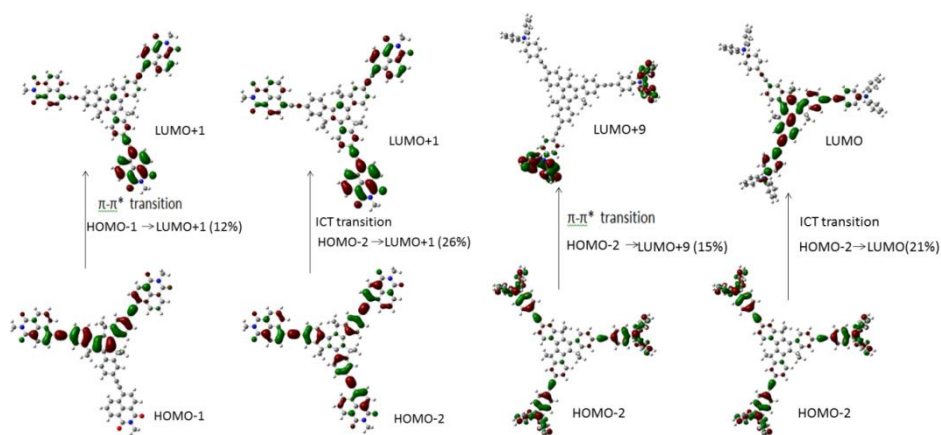


Figure 5.8. The major transitions in truxene **6** and **7**

The optimized structures of truxene **6** and **7** exhibit planar conformation with respect to truxene core. The incorporation of the TCNE and TCNQ groups results in loss of planarity in truxene **10** and **11**. The dihedral angle between the triphenylamine groups and truxene core is 76.1° , 89.6° , 74.9° in truxene **10**, and 74.0° , 74.8° , 74.8° in truxene **11** (Figure 5.9).

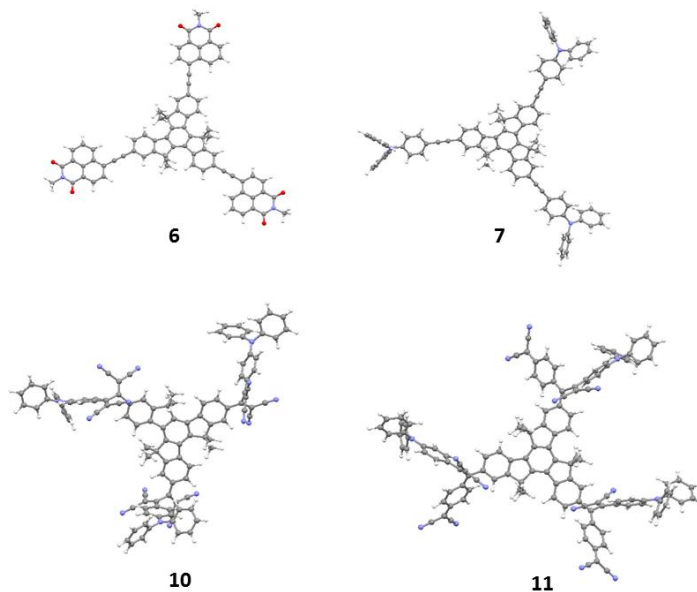


Figure 5.9. The DFT optimized structures of the truxenes **6**, **7**, **10** and **11** with Gaussian 09 at the B3LYP/6-31G** level of theory.

Table 5.2. Computed vertical transition energies and their Oscillator strengths (f) and major contributions for the truxenes **6**, **7**, **10** and **11**

Truxenes	TD-DFT/ CAM-B3LYP (DCE)		
	λ_{max}	f^a	Major contribution (%)
6	284 nm	0.0087	HOMO-1→LUMO+1(12%)
	389 nm	2.29	HOMO-2→LUMO+1(26%)
7	272 nm	0.352	HOMO-2→LUMO+9 (15%)
	355 nm	3.369	HOMO-2→LUMO (21%)
10	383 nm	0.6231	HOMO-4→LUMO+2 (12%)
11	370 nm	0.2677	HOMO-1→LUMO (27%)
	520 nm	0.7923	HOMO-5→LUMO (11%)

^a f is Oscillator strengths

Figure 5.10 shows the electron density distribution of the HOMO and LUMO of the truxenes **6**, **7**, **10** and **11**. In truxene **6** the HOMO is delocalized on the truxene core and LUMO is on the naphthalimide unit, this separation of HOMO and LUMO results in strong charge transfer and low energy gap (2.98 eV). The truxene **7** shows that, the HOMO is delocalized over the triphenylamine groups, whereas the LUMO is delocalized on the truxene core. In case of TCNE and TCNQ substituted truxene **10** and **11** the HOMO is delocalized over the triphenylamine group and LUMO is on TCNE and TCNQ acceptor unit respectively. Thus, the electron density transfers from triphenylamine groups (HOMO) to TCNE (LUMO) and TCNQ groups in truxene **10** and **11**. The HOMO-LUMO gap is lowest in truxene **11** as compared to other truxenes due to the incorporation of TCNQ as a strong acceptor.

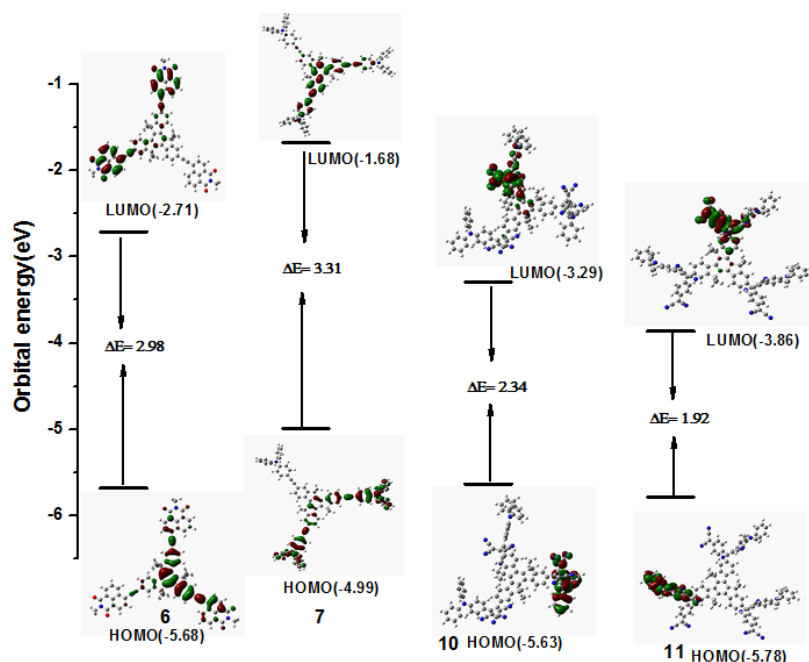


Figure 5.10. The energy level diagram of the frontier molecular orbitals of the truxenes **6**, **7**, **10** and **11** calculated using B3LYP/6-31G(d,p) level of DFT theory.

5.7. Experimental section

General experimental. All reagents were obtained from commercial sources, and used as received unless otherwise stated. ^1H NMR (400 MHz) and ^{13}C NMR (100 MHz) spectra were recorded on a Bruker Avance (III) 400 MHz instrument by using CDCl_3 as solvent. ^1H NMR chemical shifts are reported in parts per million (ppm) relative to the solvent residual peak (CDCl_3 , 7.26 ppm). Multiplicities are given as s (singlet), d (doublet), t (triplet), q (quartet), and m (multiplet), and the coupling constants, J , are given in Hz. ^{13}C NMR chemical shifts are reported relative to the solvent residual peak (CDCl_3 , 77.36 ppm). Thermogravimetric analyses were performed on the Mettler Toledo Thermal Analysis system. UV–visible absorption spectra were recorded on a Cary-100 Bio UV–visible spectrophotometer. Cyclic voltamograms (CVs) were recorded on a CHI620D electrochemical analyser using glassy carbon as the working electrode, Pt wire as the counter electrode, and the saturated calomel electrode (SCE) as the reference electrode. The scan rate was 100 mVs^{-1} . A solution of tetrabutylammonium

hexafluorophosphate (TBAPF₆) in CH₂Cl₂ (0.1 M) was employed as the supporting electrolyte. DCM was freshly distilled from CaH₂ prior to use. All potentials were experimentally referenced against the saturated calomel electrode couple but were then manipulated to be referenced against FcH/FcH⁺ as recommended by IUPAC. Under our conditions, the FcH/FcH⁺ couple exhibited E° = 0.38 V versus SCE. HRMS was recorded on Bruker-Daltonics micrOTOF-Q II mass spectrometer.

Synthesis and Characterization

The reactants **4** and **5** were synthesized according to known methods.²¹

Procedure for the preparation of truxenes **6** and **7**.

A solution of tri-iodotruxene **3** (250 mg, 0.20 mmol) and the corresponding alkyne (4.5 equivalent) in toluene–triethylamine 5 : 1 (60 mL) was deaerated for 30 min with argon bubbling and then Pd(dba)₂ (40 mg, 0.07 mmol) and AsPh₃ (170 mg, 0.55 mmol) were added. The solution was deaerated for a further 5 min. The mixture was heated at 80 °C for 48 h. The solvent was removed; the remaining residue was suspended in water (50 mL) and extracted with DCM (3 x 20 mL). The combined organic layers were dried (MgSO₄) and concentrated in vacuum. The resulting crude product was purified by column chromatography on silica gel eluting with CH₂Cl₂/hexane (10%). The desired compounds obtained from the column was recrystallized from DCM/methanol to give compound **6** and **7** in 70% and 75% yield respectively.

Procedure for the preparation of truxenes **10** and **11**.

A solution of alkyne derivative (40 mg) and TCNE/TCNQ (5 equivalent) in 1,2-dichloroethane was refluxed for 24 h at 100 °C. After completion of the reaction, the reaction mixture was concentrated under reduced pressure. The crude compound was purified by column chromatography on silica eluting with CH₂Cl₂/hexane (10%) and crystallized multiple times with DCM/methanol to afford truxene **10** and **11** in 71% and 65% yield.

Truxene 6: yellow solid (yield: 70%), M. P. above 280 °C. IR data (KBr, cm^{-1})- 754, 815, 854, 1083, 1381, 1661, 1701, 2159. ^1H NMR (400 MHz, CDCl_3): δ (ppm) 8.86 (d, 3H, $J = 8.18$ Hz, -naphthalimide core protons), 8.69 (d, 3H, $J = 7.36$ Hz, -naphthalimide core protons), 8.61 (d, 3H, $J = 7.77$ Hz, -naphthalimide core protons), 8.46 (d, 3H, $J = 8.45$ Hz, -naphthalimide core protons), 8.05 (d, 3H, $J = 7.77$ Hz, -truxene core protons), 7.90 (t, 3H, -naphthalimide core protons), 7.76-7.82 (m, 6H, truxene core protons), 4.21 (t, 6H, N-butyl chain protons), 2.94-3.01 (m, 6H, truxene hexyl chain protons), 2.14-2.25 (m, 6H, truxene hexyl chain protons), 1.70-1.80 (m, 6H, N-butyl chain protons), 1.41-1.51 (m, 6H, N-butyl chain protons), 0.80-1.05 (m, 45H, truxene hexyl chain and methyl protons of butyl chain), 0.47-0.68 (m, 30H, truxene hexyl chain protons) ^{13}C NMR (100 MHz, CDCl_3): $\delta = 164.0, 163.8, 153.9, 146.6, 141.1, 138.0, 132.4, 131.6, 130.8, 130.5, 130.4, 128.2, 127.7, 127.4, 125.5, 124.7, 123.1, 122.1, 120.3, 99.9, 87.0, 56.07, 40.0, 37.0, 31.5, 30.2, 29.7, 29.4, 24.0, 22.2, 20.4, 13.9, 13.8$. HRMS (ESI) m/z , calcd for M^+ ($\text{C}_{117}\text{H}_{129}\text{N}_3\text{O}_6$): 1671.9981; found: 1671.9994.

Truxene 7: brown solid (yield: 75%), M.P. 130 °C, IR data (KBr, cm^{-1})- 617, 648, 695, 2160. ^1H NMR (400 MHz, CDCl_3): δ (ppm) 8.31 (d, 3H, $J = 8.91$ Hz, truxene core protons), 7.52-7.61 (m, 6H, truxene core protons), 7.44 (d, 6H, $J = 7.80$ Hz, triphenyl amine core protons), 7.24-7.32 (m, 12H, triphenyl amine core protons), 7.01-7.06 (m, 24H, triphenyl amine core protons), 2.85-2.91 (m, 6H, hexyl chain protons), 2.00-2.15 (m, 6H, hexyl chain protons), 0.77-0.91 (m, 36H, hexyl chain protons), 0.39-0.66 (m, 30H, hexyl chain protons).

^{13}C NMR (100 MHz, CDCl_3): $\delta = 153.6, 147.9, 147.2, 145.7, 140.0, 138.0, 132.5, 129.4, 129.7, 125.0, 124.4, 123.5, 122.3, 121.2, 116.2, 99.0, 89.4, 55.7, 36.9, 31.5, 29.6, 29.4, 23.9, 22.2, 13.8$. HRMS (ESI) m/z , calcd for M^+ ($\text{C}_{123}\text{H}_{129}\text{N}_3$): 1649.0214; found: 1649.0620.

Truxene 10: Reddish brown solid (yield: 71%), M. P. above 280 °C. IR data (KBr, cm^{-1})- 803, 748, 1185, 1337, 1466, 1443, 2158, 2221. ^1H NMR (400 MHz, CDCl_3): δ (ppm) 8.44 (d, 3H, $J = 8.01$ Hz, TPA core protons), 8.17 (s, 3H, truxene core protons), 7.77 (d, 6H, $J = 9.01$ Hz, truxene core protons), 7.37-7.50 (m, 13H, Triphenyl amine core protons), 7.20-7.32 (m, 20H, Triphenyl amine

core protons), 6.99 (d, 6H, $J = 10.01$ Hz, Triphenyl amine core protons), 2.79-2.91 (m, 6H, hexyl chain protons), 2.11-2.24 (m, 6H, hexyl chain protons), 0.74-0.98 (m, 36H, hexyl chain protons), 0.35-0.60 (m, 30H, hexyl chain protons). ^{13}C NMR (100 MHz, CDCl_3): $\delta = 168.6, 163.8, 154.6, 153.9, 150.0, 145.3, 144.4, 137.5, 132.0, 130.5, 130.1, 128.3, 126.9, 126.8, 125.5, 124.0, 121.7, 118.0, 113.6, 112.6, 112.4, 111.4, 86.3, 78.0, 56.8, 36.7, 31.4, 29.1, 24.0, 22.1, 13.8$. HRMS (ESI) m/z , calcd for M^+ ($\text{C}_{141}\text{H}_{129}\text{N}_{15}$): 2032.0555; found: 2032.1007.

Truxene 11: Black solid (yield: 65%), M. P. above 280 °C. IR data (KBr, cm^{-1})-695, 755, 815, 1177, 1575, 2209. ^1H NMR (400 MHz, CDCl_3): δ (ppm) 8.37 (d, 3H, $J = 9.23$ Hz, TPA core protons), 7.90 (s, 3H, truxene core protons), 7.65 (d, 3H, $J = 9.80$ Hz, truxene core protons), 7.58 (d, 3H, $J = 9.80$ Hz, triphenyl amine core protons), 7.29-7.38 (m, 15H, triphenyl amine core protons), 7.19-7.25 (m, 12H, triphenyl amine core protons), 7.13-7.19 (m, 15H, triphenyl amine core protons), 7.04 (d, 3H, $J = 10.38$ Hz, triphenyl amine core protons), 6.97 (d, 6H, $J = 9.23$ Hz, triphenyl amine core protons), 2.74-2.86 (m, 6H, hexyl chain protons), 1.99-2.10 (m, 6H, hexyl chain protons), 0.72-0.91 (m, 36H, hexyl chain protons), 0.32-0.56 (m, 30H, hexyl chain protons).

^{13}C NMR (100 MHz, CDCl_3): $\delta = 171.4, 154.5, 153.7, 151.6, 150.5, 149.5, 145.2, 140.6, 137.5, 135.2, 134.0, 133.4, 133.0, 132.7, 129.9, 128.5, 127.1, 126.5, 126.0, 125.4, 123.7, 119.1, 114.0, 113.8, 113.3, 112.3, 86.6, 74.8, 56.5, 53.4, 36.5, 31.2, 28.9, 23.9, 22.0, 13.8$. HRMS (ESI) m/z , calcd for M^+ ($\text{C}_{159}\text{H}_{141}\text{N}_{15}$): 2261.1521; found: 2261.2406.

5.8. Conclusions

In summary, we have described the synthesis of star shaped donor-acceptor substituted truxenes **6**, **7**, **10** and **11**. Their photophysical, electrochemical properties, thermal stability and HOMO-LUMO gap can be tuned by varying the strength of donor and acceptor groups. The optical properties of the truxenes **6**, **7**, **10** and **11** were explained from the TD-DFT calculations. The computational calculation show significant lowering of the HOMO-LUMO gap by the incorporation of TCNE and TCNQ groups in truxene **7**. The truxene **10** and **11** are

non-emissive in nature which further supports strong donor–acceptor interaction. The thermal stability can be improved by the incorporation of planar naphthalimide unit on truxene core. The [2+2] cycloaddition retroelectrocyclization reaction pathway was studied by computational calculations. These studies show that, the donor substituted truxenes are favorable for the cycloaddition reaction whereas truxene substituted by acceptor groups are not favourable for [2+2] cycloaddition-retroelectrocyclization reactions. The results obtained here, provide a new avenue for the design and synthesis of organic molecules with low HOMO-LUMO gap and enhanced thermal stability for various optoelectronic applications. The study on photovoltaic properties of truxenes **6**, **7**, **10** and **11** are currently in progress in our laboratory.

5.9. References

- (a) Sonar P., Singh S. P., Li Y., Soh M. S., Dodabalapur A. (2010), A Low-Bandgap Diketopyrrolopyrrole Benzothiadiazole Based Copolymer for High-Mobility Ambipolar Organic Thin-Film Transistors, *Adv. Mater.*, 22, 5409–5413, (DOI: 10.1002/adma.201002973) (b) Kato S., Furuya T., Kobayashi A., Nitani M., Ie Y., Aso Y., Yoshihara T., Tobita S., Nakamura Y. (2012), Synthesis of Ladder-Type π -Conjugated Heteroacenes via Palladium-Catalyzed Double N-Arylation and Intramolecular O-Arylation, *J. Org. Chem.*, 77, 7595–7606, (DOI: 10.1021/jo070427p). (c) Omer K. M., Ku S. Y., Wong K. T., Bard A. J. (2009), Green Electrogenated Chemiluminescence of Highly Fluorescent Benzothiadiazole and Fluorene Derivatives, *J. Am. Chem. Soc.*, 131, 10733–10741, (DOI: 10.1021/ja904135y). (d) Wang J. L., Tang Z.-M., Xiao Q., Ma Y., Pei J. (2009), Star-Shaped D- π -A Conjugated Molecules: Synthesis and Broad Absorption Bands, *Org. Lett.*, 11, 863–866, (DOI: 10.1021/ol802845w). (e) Sharma R., Maragani R., Mobin S. M., Misra R. (2013), Ferrocenyl substituted calixarenes: synthesis, structure and properties, *RSC Adv.*, 3, 5785-5788 (DOI: 10.1039/C3RA00146F). (f) Singh C. P., Sharma R., Shukla V., Khundrakpam P., Misra R., Bindra K. S., Chari R. (2014), Optical limiting

- and nonlinear optical studies of ferrocenyl substituted calixarenes, *Chem. Phys. Lett.*, 616, 189–195, (doi.org/10.1016/j.cplett.2014.10.030).
2. (a) Kato S., Matsumoto T., Ishi-I T., Thiemann T., Shigeiwa M., Gorohmaru H., Maeda S., Yamashita Y., Mataka S., (2004), Strongly red-fluorescent novel donor– π -bridge–acceptor– π -bridge–donor (D– π -A– π -D) type 2,1,3-benzothiadiazoles with enhanced two-photon absorption cross-sections, *Chem. Commun.*, 2342–2343, (DOI:10.1039/B410016F). (b) Neto B. A. D., Lapis A. A. M., Júnior E. N., da S., Dupont J. (2013), 2,1,3-Benzothiadiazole and derivatives: synthesis, properties, reactions, and applications in light technology of small molecules, *Eur. J. Org. Chem.*, 228-255 (DOI: 10.1002/ejoc.201201161). (c) Kato S., Matsumoto T., Shigeiwa M., Gorohmaru H., Maeda S., Ishi-I T., Mataka S. (2006), Novel 2,1,3-benzothiadiazole-based red-fluorescent dyes with enhanced two-photon absorption cross-sections *Chem.-Eur. J.*, 12, 2303-2317 (DOI: 10.1002/chem.200500921). (d) Kobayashi N., Inagaki S., Nemykin V. N., Nonomura T. (2001), A novel hemiporphyrine comprising three isoindoleimine and three thiadiazole units, *Angew. Chem., Int. Ed.*, 40, 2710–2712. (e) Lindner B. D., Engelhart J. U., Märken M., Tverskoy O., Appleton A. L., Rominger F., Hardcastle K. I., Enders M., Bunz U. H. F. (2012), *Chem. Eur. J.*, 18, 4627–4633. (f) Aviram A., Ratner M. A. (1974), Molecular rectifiers, *Chem. Phys. Lett.*, 29, 277–283, (doi.org/10.1016/0009) (g) Sharma R., Gautam P., Mobin S. M., Misra R. (2013), β -Substituted ferrocenyl porphyrins: synthesis, structure, and properties, *Dalton Trans.*, 42, 5539-5545 (DOI: 10.1039/C3DT00003F). (h) Sharma R., Gautam P., Misra R. Shukla S. K. (2015), β -Substituted triarylborane appended porphyrins: photophysical properties and anion sensing, *RSC Adv.*, 5, 27069, (DOI: 10.1039/C5RA03931B).
3. (a) Zhang Q. T., Tour J. M. (1998), Alternating Donor/Acceptor Repeat Units in Polythiophenes. Intramolecular Charge Transfer for Reducing Band Gaps in Fully Substituted Conjugated Polymers, *J. Am. Chem. Soc.*, 120, 5355–5362, (DOI: 10.1021/ja972373e). (b) Gohier F., Frère P. R.

- (2013), 3-Fluoro-4-hexylthiophene as a Building Block for Tuning the Electronic Properties of Conjugated Polythiophenes, *J. Org. Chem.*, 78, 1497–1503, (DOI:10.1021/jo302571u). (c) Sharma R., Maragani R., Misra R. (2016), Ferrocenyl aza-dipyrromethene and aza-BODIPY: Synthesis and properties, *J. Organomet. Chem.*, 825, 8–14, (doi.org/10.1016/j.jorganchem.2016.10.019).
4. (a) Štefko M., Tzirakis M. D., B. Breiten, M.-O. Ebert, O. Dumele, Schweizer W. B., Gisselbrecht J.-P., Boudon C., Beels M. T., Biaggio I., Diederich F. (2013), Donor–acceptor (D–A)-substituted polyyne chromophores: modulation of their optoelectronic properties by varying the length of the acetylene spacer, *Chem. –Eur. J.*, 19, 12693-12704 (DOI: 10.1002/chem.201301642). (b) Van Mullekom H. A. M., Vekemans J. A. J. M., Meijer E. W. (1998), Band-gap engineering of donor–acceptor-substituted π -conjugated polymers, *Chem. -Eur. J.*, 4, 1235–1243 (DOI: 10.1002/(SICI)1521-3765(19980710)4:7<1235::AID. (c) Wang J.-L., Xiao Q., Pei J. (2010), Benzothiadiazole-based D– π –A– π –D organic dyes with tunable band gap: synthesis and photophysical properties, *Org. Lett.*, 12, 4164-4167 (DOI: 10.1021/ol101754q). (d) Bures F., Schweizer W. B., May J. C., Boudon C., Gisselbrecht J. -P., Gross M., Biaggio I., Diederich F. (2007), Property tuning in charge-transfer chromophores by systematic modulation of the spacer between donor and acceptor, *Chem.-Eur. J.*, 13, 5378-5387 (DOI: 10.1002/chem.200601735). (e) Moonen N. N. P., Pomerantz W. C., Gist R., Boudon C., Gisselbrecht J.-P., Kawai T., Kishioka A., Gross M., Irie M., Diederich F. (2005), Donor-substituted cyanoethynylethenes: π -conjugation and band-gap tuning in strong charge-transfer chromophores, *Chem. -Eur. J.*, 11, 3325-3341 (DOI: 10.1002/chem.200500082).
5. Gautam P., Misra R., Siddiqui S. A., Sharma G. D. (2015), Unsymmetrical Donor–Acceptor–Acceptor– π –Donor Type Benzothiadiazole-Based Small Molecule for a Solution Processed Bulk Heterojunction Organic Solar

- Cell, *ACS Appl. Mater. Interfaces*, 7, 10283–10292 (DOI: 10.1021/acsami.5b02250)
6. (a) Kivala M., Diederich F. (2009), Acetylene-derived strong organic acceptors for planar and nonplanar push–pull chromophores, *Acc. Chem. Res.*, 42, 235-248 (DOI: 10.1021/ar8001238). (b) Kato S., Diederich F. (2010), Non-planar push–pull chromophores, *Chem. Commun.*, 46, 1994-2006 (DOI: 10.1039/B926601A). (c) Kivala M., Stanoeva T., Michinobu T., Frank B., Gescheidt G., Diederich F. (2008), One-electron-reduced and -oxidized stages of donor-substituted 1,1,4,4-tetracyanobuta-1,3-dienes of different molecular architectures, *Chem.–Eur. J.*, 14, 7638-7647 (DOI: 10.1002/chem.200800716).
7. (a) Michinobu T., May J. C., Lim J. H., Boudon C., Gisselbrecht J.-P., Seiler P., Gross M., Biaggio I., Diederich, F. (2005), A new class of organic donor–acceptor molecules with large third-order optical nonlinearities, *Chem. Commun.*, 737-739 (DOI: 10.1039/B417393G); (b) Michinobu T., Boudon I., Gisselbrecht J.-P., Seiler P., Frank B., Moonen N. N. P., Gross M., Diederich F. (2006), Donor-substituted 1,1,4,4-tetracyanobutadienes (TCBDs): new chromophores with efficient intramolecular charge-transfer interactions by atom-economic synthesis, *Chem.–Eur. J.*, 12, 1889-1905 (DOI: 10.1002/chem.200501113). (c) Leliège A., Blanchard P., Rousseau T., Roncali J. (2011), Triphenylamine/Tetracyanobutadiene-based D-A-D π -conjugated systems as molecular donors for organic solar cells, *Org. Lett.*, 13, 3098-3101 (DOI: 10.1021/ol201002j).
8. (a) Michinobu T., Satoh N., Cai J., Li Y., Han L. (2014), Novel design of organic donor–acceptor dyes without carboxylic acid anchoring groups for dye-sensitized solar cells, *J. Mater. Chem. C*, 2, 3367-3372 (DOI: 10.1039/C3TC32165G). (b) Esembeson B., Scimeca M. L., Michinobu T., Diederich F., Biaggio I. (2008), A high-optical quality supramolecular assembly for third-order integrated nonlinear optics, *Adv. Mater.*, 2008, 20, 4584-4587 (DOI: 10.1002/adma.200801552).

9. (a) Yamada M., Schweizer W. B., Schoenebeck F., Diederich F. (2010), Unprecedented thermal rearrangement of push–pull-chromophore–[60]fullerene conjugates: formation of chiral 1,2,9,12-tetrakis-adducts, *Chem. Commun.*, 46, 5334-5336 (DOI: 10.1039/C0CC00881H). (b) Jordan M., Kivala M., Boudon C., Gisselbrecht J.-P., Schweizer W. B., Seiler P., Diederich F. (2011), Switching the regioselectivity in cycloaddition-retro-electrocyclizations between donor-activated alkynes and the electron-accepting olefins TCNE and TCNQ, *Chem.–Asian J.*, 6, 396-401 (DOI: 10.1002/asia.201000539). (c) Kivala M., Boudon C., Gisselbrecht J.-P., Seiler P., Gross M., Diederich, F. (2007), A novel reaction of 7,7,8,8-tetracyanoquinodimethane (TCNQ): charge-transfer chromophores by [2 + 2] cycloaddition with alkynes, *Chem. Commun.* 2007, 4731-4733 (DOI: 10.1039/B713683H). (d) Michinobu T. (2008), Click-type reaction of aromatic polyamines for improvement of thermal and optoelectronic properties, *J. Am. Chem. Soc.* 130, 14074–14075, (DOI: 10.1021/ja8061612). (e) Li Y., Michinobu T. (2010), Double click synthesis and second-order nonlinearities of polystyrenes bearing donor–acceptor chromophores, *Macromolecules*, 43, 5277–5286, (DOI: 10.1021/ma100869m). (f) Shoji T., Ito S., Okujimac T., Moritad N. (2012), Synthesis of push–pull chromophores by the sequential [2 + 2] cycloaddition of 1-azulenylbutadiynes with tetracyanoethylene and tetrathiafulvalene, *Org. Biomol. Chem.*, 10, 8308-8313 (DOI: 10.1039/C2OB26028J). (g) Shoji T., Ito S., Toyota K., Iwamoto T., Yasunami M., Morita N. (2009), Reactions between 1-ethynylazulenes and 7,7,8,8-tetracyanoquinodimethane (TCNQ): preparation, properties, and redox behavior of novel azulene-substituted redox-active chromophores, *Eur. J. Org. Chem.*, 4316-4324 (DOI: 10.1002/ejoc.200900539). (h) Krauß N., Kielmann M., Ma J., Butenschön H. (2015), Reactions of Alkynyl-and 1, 1'-Dialkynylferrocenes with Tetracyanoethylene–Unanticipated Addition at

- the Less Electron-Rich of Two Triple Bonds, *Eur. J. Org. Chem.* 2622–2631, (DOI: 10.1002/ejoc.201500105).
10. (a) Jadhav T., Maragani R., Misra R., Sreeramulu V., Rao D. N., Mobin S. M. (2013), Design and synthesis of donor–acceptor pyrazabole derivatives for multiphoton absorption, *Dalton Trans.*, 42, 4340-4342 (DOI: 10.1039/C3DT33065F). (b) Gautam P., Dhokale B., Mobin S. M., Misra R. (2012), Ferrocenyl BODIPYs: synthesis, structure and properties, *RSC Adv.*, 2, 12105-12107 (DOI: 10.1039/C2RA21964F). (c) Misra R., Sharma R., Mobin S. M. (2014), Star shaped ferrocenyl truxenes: synthesis, structure and properties, *Dalton Trans.*, 43, 6891-6896, (DOI: 10.1039/C4DT00210E).
11. (a) Ventura B., Barbieri A., Barigelletti F., Diring S. E., Ziesel R. (2010), Energy Transfer Dynamics in Multichromophoric Arrays Engineered from Phosphorescent PtII/RuII/OsII Centers Linked to a Central Truxene Platform, *Inorg. Chem.*, 49, 8333–8346, (DOI: 10.1021/ic1008413). (b) Goubard F., Dumur F. (2015), Truxene: a promising scaffold for future materials, *RSC Adv.*, 5, 3521–3551, (DOI:10.1039/C4RA11559G).
12. (a) Zhang W. B., Jin W. H., Zhou X. H., Pei J. (2007), Star-shaped oligo (pphenylene)-functionalized truxenes as blue-light-emitting materials: synthesis and the structure-property relationship, *Tetrahedron*, 63, 2907–2914, (DOI: org/10.1016/j.tet.2007.01.025). (b) Huang J., Xu B., Su J. H., Chin H., Tian H. (2010), Efficient blue lighting materials based on truxene-cored anthracene derivatives for electroluminescent devices, *Tetrahedron*, 66, 7577–7582, (doi.org/10.1016/j.tet.2010.07.039).
13. (a) Boorum M. M., Vasil Y. V., Drewello T., Scott L. T. (2001), Groundwork for a Rational Synthesis of C60: Cyclodehydrogenation of a C60H30 Polyarene, *Science*, 294, 828, (DOI: 10.1126/science.1064250). (b) Gomez-Lor B., Frutos O. De, Echavarren A. M. (1999), Synthesis of ‘crushed fullerene’ C60H30, *Chem. Commun.*, 2431, (DOI: 10.1039/A906990I).

14. (a) Pei J., Wang J., Cao X. , Zhou X., Zhang B. (2003), Star-Shaped Polycyclic Aromatics Based on Oligothiophene-Functionalized Truxene: Synthesis, Properties and Facile Emissive Wavelength Tuning, *J. Am. Chem. Soc.*, 125, 9944, (DOI: 10.1021/ja0361650). (b) Cao X. Y., Zhang W. B., Wang J. L., Zhou X. H., Lu H., Pei J. (2003), Extended π -Conjugated Dendrimers Based on Truxene, *J. Am. Chem. Soc.*, 125, 12430, (DOI: 10.1021/ja037723d).
15. (a) Zong X., Liang M., Fan C., Tang K., Li G., Sun Z., Xue S. (2012), Design of truxene-based organic dyes for high-efficiency dye-sensitized solar cells employing cobalt redox shuttle, *J. Phys. Chem. C.*, 116, 11241–11250, (DOI: 10.1021/jp301406x). (b) Xie Y., Zhang X., Xiao Y., Zhang Y., Zhou F., Qib J., Qu J. (2012), Fusing three perylenebisimide branches and a truxene core into a star-shaped chromophore with strong two-photon excited fluorescence and high photostability, *Chem. Commun.*, 48, 4338–4340, (DOI: 10.1039/C2CC31261A).
16. (a) Xua H. J., Dub B., Gros C. P., Richarda P., Barbea J. M., Pierre D. H. (2013), Shape-persistent poly-porphyrins assembled by a central truxene: synthesis, structure, and singlet energy transfer behaviors, *J. Porphyrins Phthalocyanines*, 17, 44–55, DOI: (10.1142/S1088424612501271). (b) Kimura M., Kuwano S., Sawaki Y., Fujikawa H., Noda K., Taga Y., Takagi K. (2005), New 9-fluorene-type trispirocyclic compounds for thermally stable hole transport materials in OLEDs, *J. Mater. Chem.*, 15, 2393–2398, (DOI: 10.1039/B502268A).
17. (a) Huang W., Smarsly E., Han J., Bender M., Seehafer K., Wacker I., Schröder R. R., Bunz U. H. F. (2017), Truxene-Based Hyperbranched Conjugated Polymers: Fluorescent Micelles Detect Explosives in Water, *ACS Appl. Mater. Interfaces*, 9, 3068–3074, (DOI: 10.1021/acsami.6b12419). (b) Misra R., Gautam P. (2014), Tuning of the HOMO–LUMO gap of donor-substituted symmetrical and unsymmetrical benzothiadiazoles, *Org. Biomol. Chem.*, 12, 5448–5457, (DOI: 10.1039/C4OB00629A).

18. Lehnherr D., Adam M., Murray A. H., McDonald R., Hampel F., Tykwinski R. R. (2017), Synthesis, physical properties, and chemistry of donor–acceptor-substituted pentacenes, *Canadian Journal of Chemistry*, 95, 303-314 (DOI: 10.1139/cjc-2016-0450).
19. Kanibolotsky A. L., Berridge R., Skabara P. J., Perepichka I. F., Bradley D. D. C., Koeberg M. (2004), Synthesis and properties of monodisperse oligofluorene-functionalized truxenes: highly fluorescent star-shaped architectures, *J. Am. Chem. Soc.*, 126, 13695, (DOI: 10.1021/ja039228n).
20. Cao X., Zi H., Zhang W., Lu H., Pei J. (2005), Star-Shaped and Linear Nanosized Molecules Functionalized with Hexa-peri-hexabenzocoronene: Synthesis and Optical Properties, *J. Org. Chem.*, 70, 3645-3653, (DOI: 10.1021/jo0480139).
21. Maragani R., Bijesh S., Sharma R., Misra R. (2017), C_s-Symmetric Donor-Acceptor Bisthiazoles: Synthesis, Photophysical, Electrochemical and Computational Studies, *Asian J. Org. Chem.*, 6, 1408-1414, (DOI: 10.1002/ajoc.201700274).
22. Benin V., Yeates A. T., Dudis D. (2008), Preparation of halogenated derivatives of thiazolo [5, 4-d] thiazole via direct electrophilic aromatic substitution, *J. Heterocyclic Chem.*, 45, 811, (DOI: 10.1002/jhet.5570450328).
23. Reutenauer P., Kivala M., Jarowski P. D., Boudon C., Gisselbrecht J.-P., Gross M., Diederich, F. (2007), New strong organic acceptors by cycloaddition of TCNE and TCNQ to donor-substituted cyanoalkynes, *Chem. Commun.*, 4898-4900 (DOI: 10.1039/B714731G).
24. Chen S., Li Y., Liu C., Yang W., Li Y. (2011), Strong Charge-Transfer Chromophores from [2+ 2] Cycloadditions of TCNE and TCNQ to Peripheral Donor-Substituted Alkynes, *Eur. J. Org. Chem.*, 32, 6445–6451, (DOI: 10.1002/ejoc.201101009).
25. (a) Dhokale, B., Gautam, P., & Misra, R. (2012). Donor–acceptor perylenediimide–ferrocene conjugates: synthesis, photophysical, and electrochemical properties, *Tetrahedron Letters*, 53(18), 2352–2354,

- <http://doi.org/http://dx.doi.org/10.1016/j.tetlet.2012.02.107>; (b) Rochford J., Rooney M. T. P. (2007), Redox Control of meso-Zinc(II) Ferrocenylporphyrin Based Fluorescence Switches, *Inorg. Chem.*, 46, 7247, (DOI: 10.1021/ic0703326). (c) Rao M. R., Pavan K. V., Ravikanth M. (2010), Synthesis of boron-dipyrromethene–ferrocene conjugates, *J. Organomet. Chem.*, 695, 863–869, (doi.org/10.1016/j.jorganchem.2010.01.009).
26. (a) Fery-Forgues, S., Delavaux-Nicot, B., (2000), Ferrocene and ferrocenyl derivatives in luminescent systems, *J. Photochem. Photobiol., A*, 132, 137–159, (DOI: [http://dx.doi.org/10.1016/S1010-6030\(00\)00213-6](http://dx.doi.org/10.1016/S1010-6030(00)00213-6)); (b) Barlow, S., Marder, S. R., (2000), Electronic and optical properties of conjugated group 8 metallocene derivatives, *Chem. Commun.*, 1555–1562, (DOI: 10.1039/B004907G).
27. (a) Francl F., Pietro W. J., Hehre W. J., Binkley J. S., Gordon M. S., Defrees D. J., Pople J. A. (1982), Self-consistent molecular orbital methods. XXIII. A polarization-type basis set for second-row elements, *J. Chem. Phys.*, 77, 3654–3665, (doi.org/10.1063/1.444267). (b) Ding F., Chen S., Wang H. (2010), Computational study of ferrocene-based molecular frameworks with 2, 5-diethynylpyridine as a chemical bridge, *Materials*, 3, 2668–2683, (doi:10.3390/ma3042668).
28. Yang Z., Xu B., He J., Xue L., Guo Q., Xia H., Tian W. (2009), Solution-processable and thermal-stable triphenylamine-based dendrimers with truxene cores as hole-transporting materials for organic light-emitting devices, *Organic Electronics*, 10 (2009) 954–959, (DOI:org/10.1016/j.orgel.2009.04.024).
29. Pedone A. (2013), Role of Solvent on Charge Transfer in 7-Aminocoumarin Dyes: New Hints from TD-CAM-B3LYP and State Specific PCM Calculations, *J. Chem. Theory Comput.*, 9, 4087–4096 (DOI: /abs/10.1021/ct4004349).

Chapter 6

Phenothiazene Based 1,1,4,4-Tetracyanobuta-1,3-Diene (TCBD) Substituted Donor-Acceptor Truxenes: Synthesis, Photophysical and Electrochemical Properties

6.1. Introduction

There has been a continuous growing interest in the development of novel π -conjugated donor-acceptor (D-A) systems, because of their applications in the field of non-linear optics organic light emitting diodes (OLEDs) and electroluminescent devices.^{1,2} The photonic properties of the π -conjugated donor-acceptor systems can be tuned by altering the strength of donor or acceptor units, and by varying the connecting π -linker.^{3,4}

The star-shaped truxene is a planar C_3 -symmetric, fused fluorene trimer, which provides easy functionalization, high thermal and chemical stability.⁵ Truxene has a large π -conjugated system and multi reactive sites which can further offer the extension of π -conjugation which leads to diverse derivatives.^{6,7} Jian Pei *et al.* and others have devoted considerable synthetic effort on various star shaped π -conjugated truxene based molecular systems, which are useful for optoelectronic applications.⁸⁻¹⁰ Recently, Guijiang Zhou *et al.* have reported spirobifluorene substituted truxene based emitters for blue-emitting OLEDs.^{6c}

Phenothiazine is a well-known heterocyclic compound with electron-rich sulfur and nitrogen heteroatoms, exhibits butterfly shaped nonplanar geometry, high electron-donating ability, good thermal and electrochemical stability.¹¹ The molecules containing phenothiazine exhibit unique optoelectronic properties and are useful in various applications such as organic field-effect transistors (OFETs), chemiluminescence and light-emitting diodes.^{12,13}

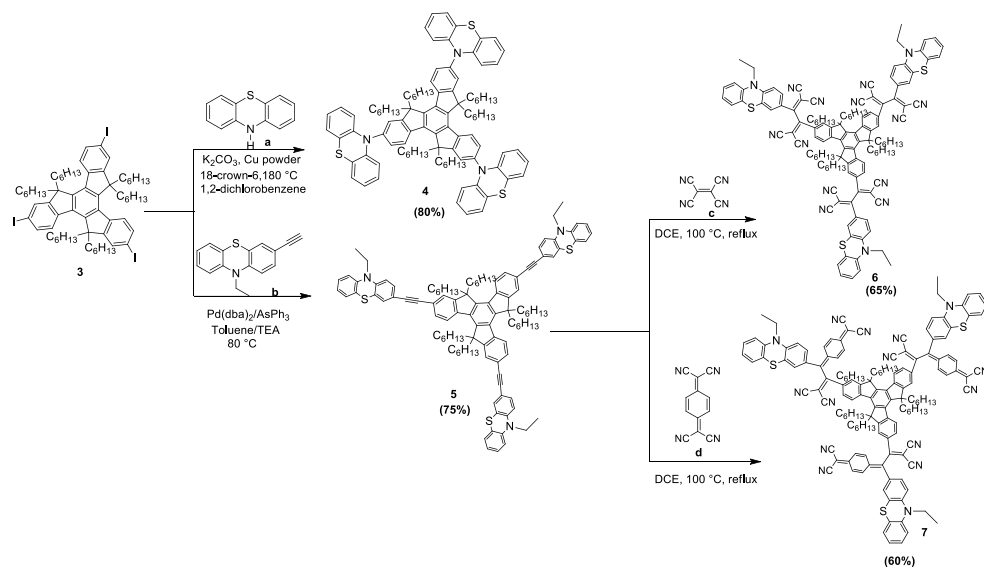
Diederich and co-workers have reported the synthesis of various TCNE and TCNQ substituted derivatives using [2+2] cycloaddition-retroelectrocyclization reaction.¹⁴ Shoji *et al.* have explored donor-acceptor based TCBD and

cyclohexa-2,5-diene-1,4-ylidene-expanded TCBD molecules as a redox active chromophores.¹⁵ Butenschoen *et al.* have synthesized a variety of 1,1'-disubstituted ferrocenyl TCBD derivatives.^{15c} Our group has reported a vast variety of TCBD functionalized chromophores for optoelectronic applications.¹⁶⁻¹⁸ We have explored the ferrocenyl substituted truxene based donor-acceptor systems.^{16e} In continuation of our work on truxene based donor-acceptor systems herein we report the design and synthesis of phenothiazine substituted truxenes **4-7**. In this manuscript our aim was- (i) To study the effect of substitution of phenothiazine unit through different positions *i.e.* through N-substitution (10-position) and 3-position. (ii) To improve the photonic and electronic properties of phenothiazine substituted truxene **5** by incorporating TCNE and TCNQ acceptors in between phenothiazine and truxene.

To the best of our knowledge, there are no reports available on phenothiazene substituted truxenes. Therefore, to study the effect of phenothiazine unit, the truxene **4** and **5** were synthesized using the Ullmann and Sonogashira cross-coupling reactions. The [2+2] cycloadditions of tetracyanoethylene (TCNE) and 7,7,8,8-tetracyanoquinodimethane (TCNQ) with the phenothiazine substituted truxene **5** followed by the electrocyclic ring-opening resulted in donor-acceptor truxene **6** and **7**. Their photophysical, electrochemical and thermal properties were studied and DFT calculations were performed.

6.2. Results and discussion

The synthesis of phenothiazene substituted truxenes **4-7** are shown in Scheme **6.1**. The truxene core **1** was synthesized by 1-indanone in the presence of acetic acid and hydrochloric acid followed by the alkylation reaction of the truxene **1** with bromo-hexane and further iodination reaction in the presence of HIO₃ and I₂ resulted in hexahexylated tri-iodo truxene **3** in 80% yield.^{19,20} The intermediate ethynyl phenothiazine (b) was synthesized by reported procedure.²¹ The Ullmann and Pd-catalyzed Sonogashira cross-coupling reaction reaction of tri-iodo truxene **3** with phenothiazine and ethynyl phenothiazine resulted truxene **4** and **5** in 80% and 75% yields respectively (Scheme **6.1**).



Scheme 6.1. Synthesis of phenothiazine substituted truxenes **4–7**.

The tetracyanobutadiene (TCBD) and 7,7,8,8-tetracyanoquinodimethane (TCNQ) linked truxene **6** and **7** were synthesized via [2 + 2] cycloaddition–retroelectrocyclization reaction of the truxene **5** with tetracyanoethene (TCNE) and 7,7,8,8-tetracyanoquinodimethane (TCNQ). The reaction of truxene **5** with three equivalents of TCNE and TCNQ resulted truxene **6** and **7** in 65% and 60% yields respectively (Scheme 6.1). The truxenes **4–7** are readily soluble in common organic solvents. The truxenes **4–7** were well characterized by ^1H NMR, ^{13}C NMR, HRMS and MALDI techniques.

6.3. Thermal stability.

The thermal stability of the truxenes **4–7** were explored using thermogravimetric analysis (TGA) at a heating rate of $10\text{ }^\circ\text{C min}^{-1}$ under nitrogen atmosphere. The decomposition temperature for 10% weight loss in phenothiazine substituted truxenes **4** and **5** was above $400\text{ }^\circ\text{C}$, whereas TCNE and TCNQ substituted truxenes **6** and **7** show 10% weight loss at $376\text{ }^\circ\text{C}$ and $335\text{ }^\circ\text{C}$ respectively (Table 6.1). The overall thermal stability of truxenes **4–7** follows the order $\mathbf{4} > \mathbf{5} > \mathbf{6} > \mathbf{7}$ (Figure 6.1). The TGA results indicate that the materials are thermally stable enough to be used as a organic optoelectronic materials.

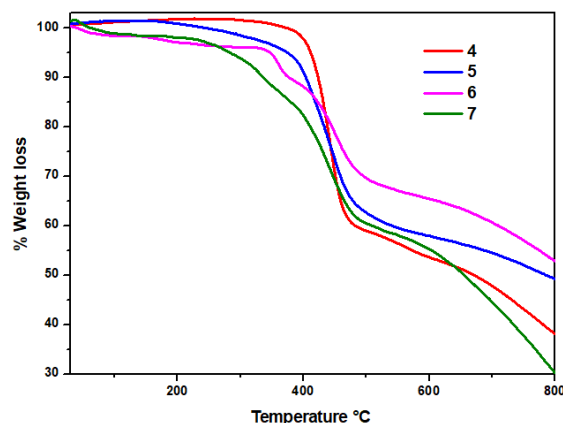


Figure 6.1. TGA plots of truxenes **4–7**.

6.4. Photophysical properties:

The UV-vis absorption spectra of the truxenes **4–7** were recorded in dichloromethane at room temperature (Figure **6.2**), and data are listed in Table **1**. The truxenes **4–7** exhibit absorption band between 258–392 nm corresponding to π - π^* transition. The truxene substituted by phenothiazine through 3-position (**5**) shows bathochromic shift of the π - π^* transition band compared to truxene substituted through N-position of phenothiazine (**4**). Truxene **5** exhibits strong charge transfer band at 374 nm, reflecting effective electronic communication between phenothiazene unit and truxene core. The incorporation of the tetracyanobutadiene (TCBD) and tetracyanoquinodimethane (TCNQ) acceptor unit result in multi-CT bands²² in truxene **6** and **7**. This indicates strong donor–acceptor interaction in the truxene **6** and **7** with TCNE and TCNQ linkers. The effect of donor–acceptor interaction is also displayed in the photograph of the truxenes **4–7** in dichloromethane solvent in day light (Figure **6.3**).

The emission properties of the truxene **4** and **5** were studied by steady state fluorescence technique. Their emission spectra are shown in Figure **6.2b**. The phenothiazine substituted truxene **4** exhibit fluorescence maxima at 453 nm. The truxene **5** shows red shifted fluorescence maxima at 579 nm. This reflects better electronic communication in truxene **5** compared to truxene **4**. The TCNE and

TCNQ linked truxene **6** and **7** are non-emissive in nature due to the fast non-radiative deactivation of the excited state with intramolecular charge transfers.^{23,24}

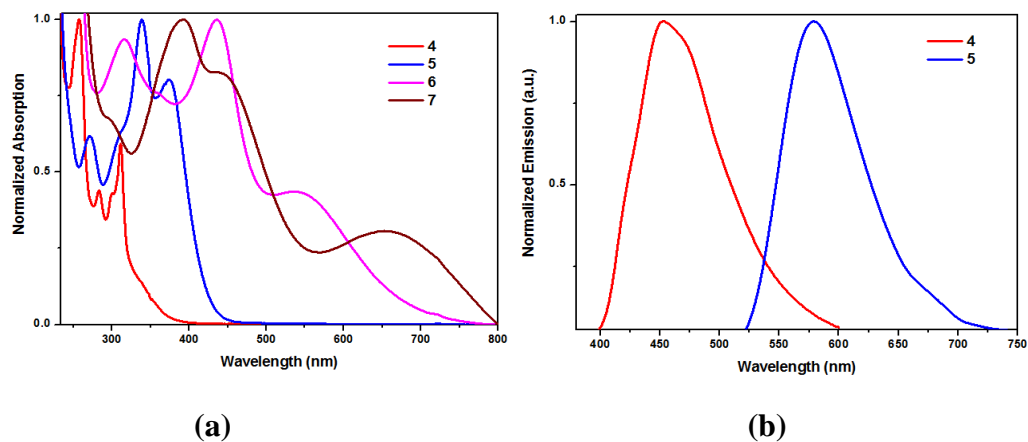


Figure 6.2: (a) Normalized electronic absorption spectra of truxene **4–7** and (b) fluorescence spectra of truxenes **4** and **5** (1.0×10^{-5} M concentration) in dichloromethane.

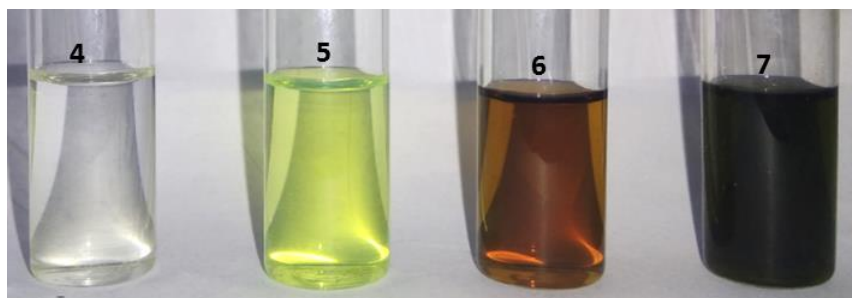
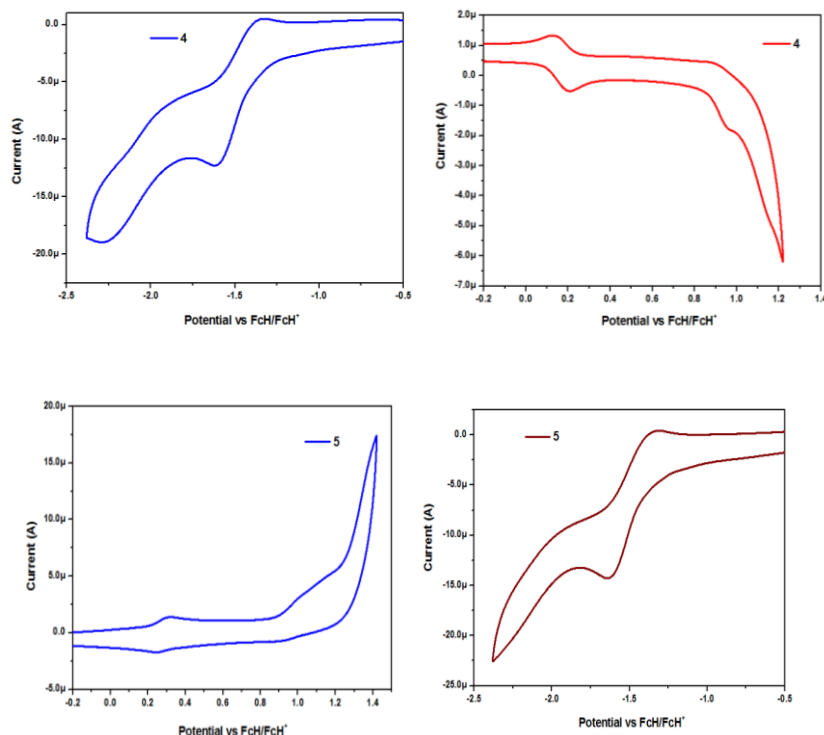


Figure 6.3: Truxenes **4–7** at 1×10^{-5} M concentration in dichloromethane in day light.

6.5. Electrochemical properties.

The electrochemical behaviour of the truxenes **4–7** were investigated by the cyclic voltammetric analysis in dry dichloromethane solution at room temperature using tetrabutylammoniumhexafluorophosphate (TBAPF₆) as a supporting electrolyte. The electrochemical data are listed in Table **6.1** and the cyclic voltammograms of the truxenes **5–7** are shown in Figure **6.4**. All potentials are corrected to be referenced against FcH/FcH⁺, as required by IUPAC.²⁵ Generally phenothiazine exhibits one reversible oxidation, as this is electron-rich tricyclic heterocycle.²⁶ The phenothiazine substituted truxenes **4–7** undergo reversible oxidation in the range of 0.16–0.51 V due to the presence of phenothiazine donor unit. The truxene **5** exhibits harder oxidation of phenothiazine as compared to N-substituted phenothiazine truxene **4**, which indicates better electronic communication in truxene **5**. Further incorporation of TCNE and TCNQ units results much harder oxidation of phenothiazine in truxene **6** and **7**. This reflects strong donor-acceptor interaction in phenothiazine substituted truxene **6** and **7**. The trend in the first oxidation potential of the truxenes **4–7** follows the order **6**>**7**>**5**>**4**. The truxenes **4–7** exhibit one reversible reduction wave between -1.46 V and -1.47 V.



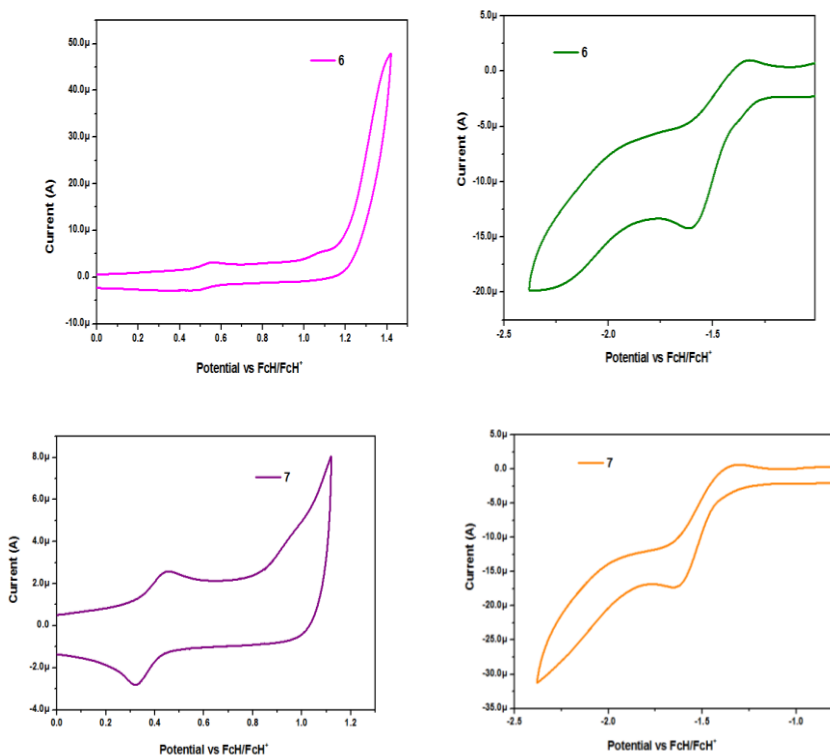


Figure 6.4. Cyclic voltammogram of 1.0×10^{-4} M solutions of truxene **4** in CH_2Cl_2 containing 0.1M Bu_4NPF_6 as supporting electrolyte, recorded at a scan speed of 100 mV s^{-1}

6.6. Computational Studies:

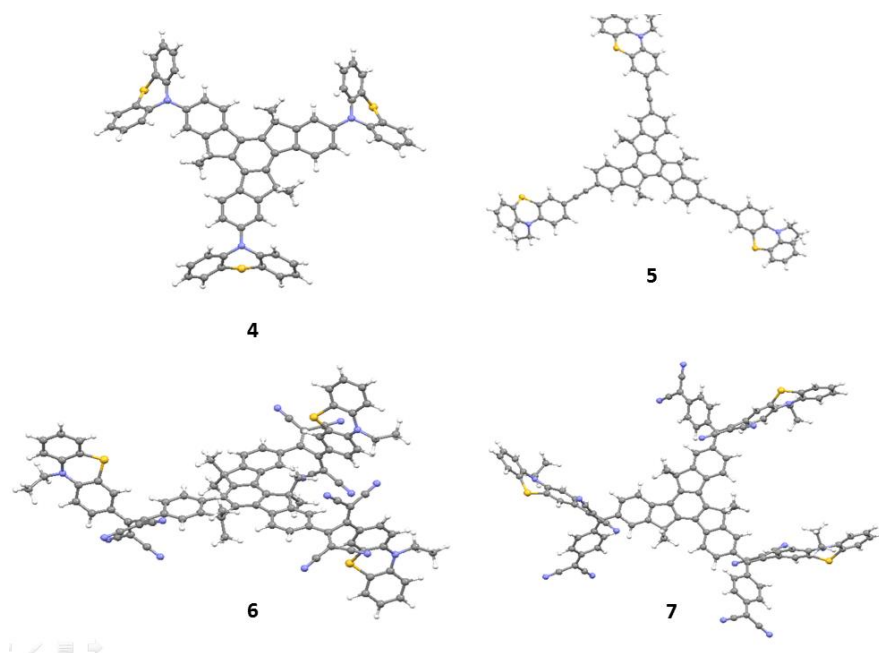
To gain insight into the photophysical and electrochemical properties of truxenes **4–7** the density functional theory (DFT) and time dependent density functional (TD-DFT) calculation was performed. The geometries of truxenes **4–7** were optimized using Gaussian 09 program at the B3LYP/6-31G** level.²⁷ The TD-DFT calculations were carried out in the dichloromethane (DCM) using the polarized continuum model (CPCM) of Gaussian 09 software. The 6-31G**/CAM-B3LYP basis set was used for all the calculations.²⁷

In phenothiazine substituted truxenes **4–7**, the truxene core shows planar conformation and phenothiazine exhibits butterfly shaped non planar geometry (Figure 6.5).

Table 6.1. Photophysical and electrochemical data of truxenes **4–7**

Compound	Photophysical data ^a λ_{\max} [nm] ($\epsilon \times 10^4$ [mol ⁻¹ cm ⁻¹])	Emission λ_{\max} [nm] ^b	Electro-chemical data ^b		^c T _d °C
			E _{ox} (V)	E _{red} (V)	
Ferrocene	-	-	0.00	-	-
4	258 (1.1), 311	453	0.16, 0.94	-1.46	424
5	340 (1.2), 374	579	0.28 1.08	-1.47	404
6	317(1.4), 436, 545	-	0.51 1.07	-1.46	376
7	392 (1.2), 444, 659	-	0.38	-1.47	335

^aMeasured in DCM at T = 25 °C, λ_{\max} (nm): absorption maximum. ϵ , extinction coefficient. ^b Recorded by cyclic voltammetry using 1.0×10^{-3} M solutions of **4–7** containing 0.1 M solution of Bu₄NPF₆ in DCM at 100 mV s⁻¹ scan rate, vs. FcH/FcH⁺. ^c Decomposition temperature at 10% weight loss, determined by TGA.

**Figure 6.5.** The DFT optimized structures of the truxenes **4–7** with Gaussian 09 at the B3LYP/6-31G** level of theory.

In truxene **4** the dihedral angle between truxene core and phenothiazine units are 40.4° , 40.3° , 40.2° respectively whereas in truxene **5** the truxene core and phenyl ring of phenothiazine is in same plane, which results stronger electronic communication compared to truxene **4**. The incorporation of the TCNE and TCNQ groups result in loss of planarity in truxene **6** and **7**. The dihedral angle between truxene core and phenothiazine units are 75.1° , 81.0° , 81.2° in truxene **6** and 74.3° , 75.7° , 72.3° in truxene **7**.

The TD-DFT predicted theoretical UV-vis absorption spectra of the truxenes **4–7** are shown in Figure **6.6** along with experimental UV-vis spectra and the composition of the electronic transitions and oscillator strength values are compiled in Table **6.2**.

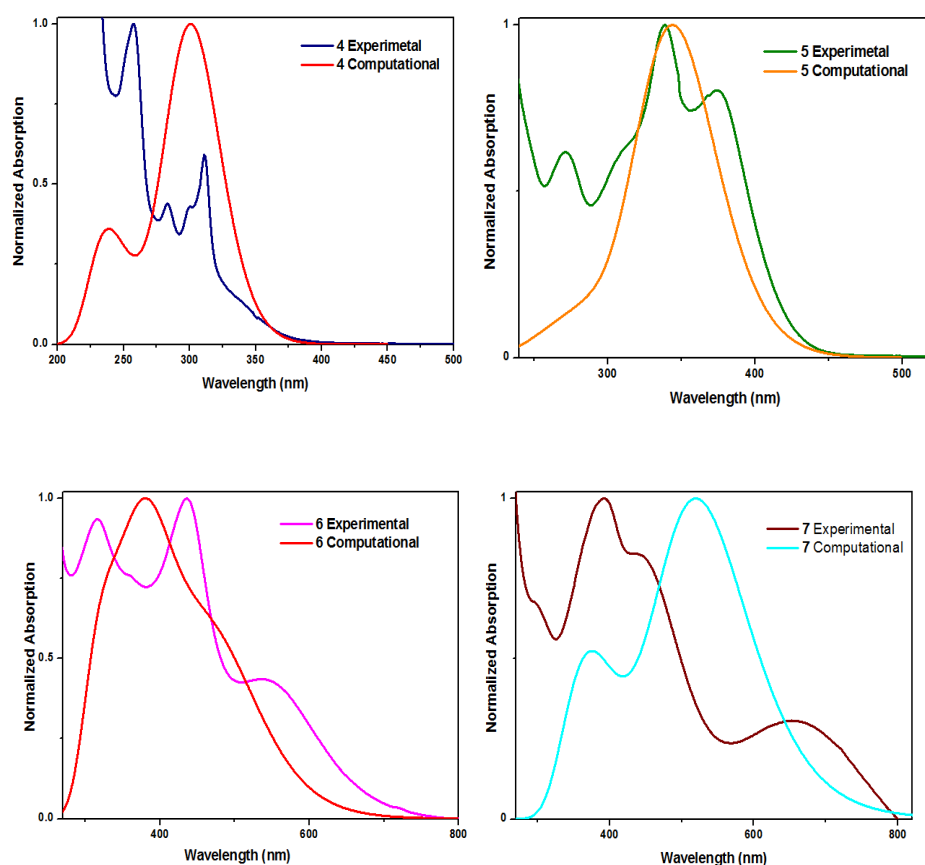


Figure 6.6. The comparison of experimental and calculated (TD-DFT at CAM-B3LYP level) absorption spectrum of truxene **4–7** in DCM solution.

The truxene **4** and **5** show absorption band calculated at CAM-B3LYP level at 301nm 343 nm respectively, which corresponds to π - π^* and ICT band respectively as shown by molecular orbitals (Figure 6.7). The incorporation of TCNE (truxene **6**) results in major intense transitions at 379 nm and TCNQ (truxene **7**) results bands at 375 nm and 517 nm, which belongs to intramolecular charge transfer (ICT).

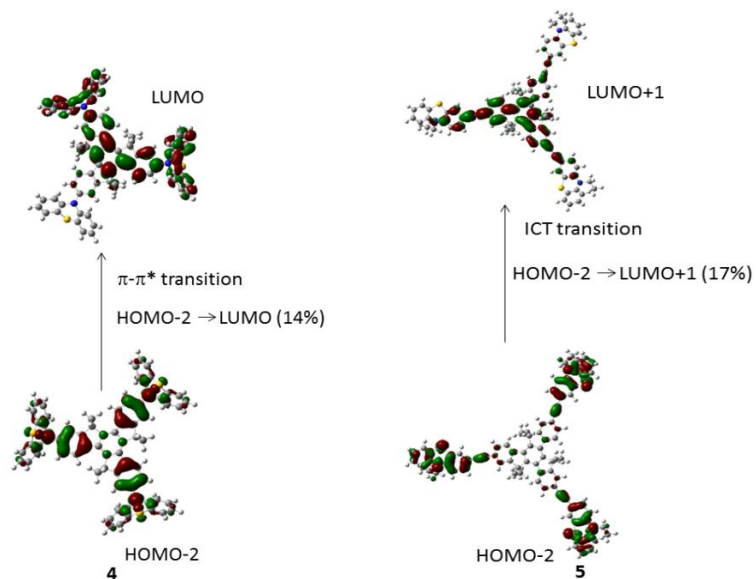


Figure 6.7. The major transitions in truxene **4** and **5**

Table 6.2. Computed vertical transition energies and their Oscillator strengths (f) and major contributions for the truxene **4–7**

Truxenes	TD-DFT/ CAM-B3LYP (THF)		
	λ_{max}	f^a	Major contribution (%)
4	301 nm	1.51	HOMO-2→LUMO (14%)
5	343 nm	2.97	HOMO-2→LUMO+1 (17%)
6	379 nm	0.72	HOMO-4→LUMO+1 (16%)
7	517 nm	0.66	HOMO-4→LUMO+1 (11%)

^a f is Oscillator strengths

Figure 6.8 shows the electron density distribution of the HOMO and LUMO of the truxenes **4–7**. In truxene **4** the HOMO is mainly localized on the truxene core and LUMO is on the phenothiazene unit whereas in truxene **5** HOMO is mainly delocalized over phenothiazene unit and LUMO is delocalized on the tuxene core. In truxene **6** and **7** the HOMO is delocalized over the phenothiazene unit and LUMO is on TCNE and TCNQ acceptor unit respectively. Thus, the electron density transfers from phenothiazene (HOMO) to TCNE (LUMO) and TCNQ (LUMO) groups in truxene **6** and **7**. The HOMO-LUMO gap is lowest in truxene **7** as compared to other truxenes due to the incorporation of TCNQ as a strong acceptor.

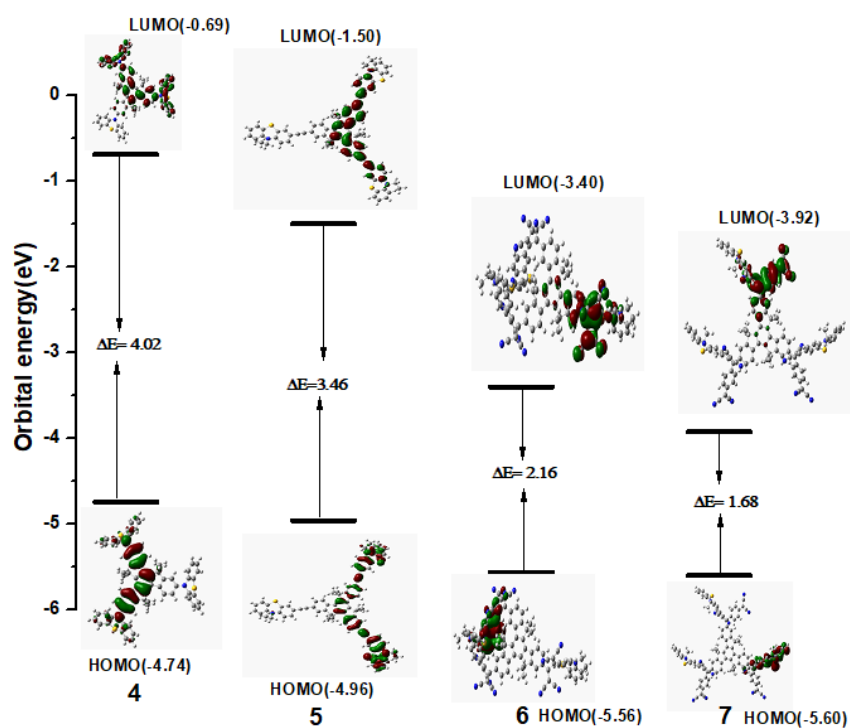


Figure 6.8. The energy level diagram of the frontier molecular orbitals of the truxenes **4–7** using B3LYP/6-31G(d,p) level of DFT theory.

6.7. Experimental section

General experimental. All reagents were obtained from commercial sources, and used as received unless otherwise stated. ^1H NMR (400 MHz) and ^{13}C NMR (100 MHz) spectra were recorded on a Bruker Avance (III) 400 MHz instrument by using CDCl_3 as solvent. ^1H NMR chemical shifts are reported in parts per million (ppm) relative to the solvent residual peak (CDCl_3 , 7.26 ppm). Multiplicities are given as s (singlet), d (doublet), t (triplet), q (quartet), and m (multiplet), and the coupling constants, J , are given in Hz. ^{13}C NMR chemical shifts are reported relative to the solvent residual peak (CDCl_3 , 77.36 ppm). Thermogravimetric analyses were performed on the Mettler Toledo Thermal Analysis system. UV–visible absorption spectra were recorded on a Cary-100 Bio UV–visible spectrophotometer. Cyclic voltamograms (CVs) were recorded on a CHI620D electrochemical analyser using glassy carbon as the working electrode, Pt wire as the counter electrode, and the saturated calomel electrode (SCE) as the reference electrode. The scan rate was 100 mV s^{-1} . A solution of tetrabutylammonium hexafluorophosphate (TBAPF_6) in CH_2Cl_2 (0.1 M) was employed as the supporting electrolyte. DCM was freshly distilled from CaH_2 prior to use. All potentials were experimentally referenced against the saturated calomel electrode couple but were then manipulated to be referenced against FcH/FcH^+ as recommended by IUPAC. Under our conditions, the FcH/FcH^+ couple exhibited $E^\circ = 0.38\text{ V}$ versus SCE. HRMS was recorded on a Bruker-Daltonics micrOTOF-Q II mass spectrometer.

Synthesis and Characterization

The intermediate **b** was synthesized according to known methods.²¹

Procedure for the preparation of truxenes **4** and **5**.

Truxene 4: Phenothiazene (**a**) (0.325 g, 1.63 mmol), iodo-truxene **3** (0.500 g, 0.40 mmol), anhydrous potassium carbonate (3.18 g, 23 mmol), 18-crown-6 (0.10g, 0.38mmol), cupric sulfate (83 mg), and 1,2-dichlorobenzene (30 mL) were added to a round bottom flask, degassed, and flushed with N_2 . The reaction

mixture was heated at 180 °C for 2 days, and then cooled to room temperature. After that dichloromethane and water were added. The organic phase was washed with water and then dried over Na₂SO₄. After removal of the solvent, the residue was purified by silica column chromatography, using DCM:hexane (10%) mixture as eluent to afford compound **4** in 80% yield.

Truxene 5: A solution of tri-iodotruxene **3** (250 mg, 0.20 mmol) and the phenothiazene alkyne (4.5 equivalent) in toluene–triethylamine 5 : 1 (60 mL) was deaerated for 30 min with argon bubbling and then Pd(dba)₂ (40 mg, 0.07 mmol) and AsPh₃ (170 mg, 0.55 mmol) were added. The solution was deaerated for a further 5 min. The mixture was heated at 80 °C for 48 h. The solvent was removed; the remaining residue was suspended in water (50 mL) and extracted with DCM (3 x 20 mL). The combined organic layers were dried (MgSO₄) and concentrated in vacuum. The resulting crude product was purified by column chromatography on silica gel eluting with CH₂Cl₂/hexane (10%). The desired compound obtained from the column was recrystallized from DCM/methanol to give compound **5** in 75% yield.

Procedure for the preparation of truxenes 6 and 7.

A solution truxene **5** (40 mg) and TCNE/TCNQ (5 equivalent) in dichloroethane was stirred for 24 h at 100 °C reflux condition. After completion of the reaction, the reaction mixture was concentrated under reduced pressure. The crude compound was purified by column chromatography on silica and crystallized multiple times with DCM/methanol to afford truxene **6** and **7** in 65% and 60% yield.

Truxene 4: white solid (yield: 80%) ¹H NMR (400 MHz, CDCl₃): δ (ppm) 8.56 (d, 3H, *J* = 8.80 Hz), 7.52 (s, 3H), 7.41 (d, 3H, *J* = 8.80 Hz), 7.02-7.10 (m, 6H), 6.79-6.89 (m, 12H), 6.27-6.36 (m, 6H), 2.97-3.10 (m, 6H), 2.05-2.18 (m, 6H), 0.86-1.05 (m, 36H), 0.59-0.73 (m, 30H). ¹³C NMR (100 MHz, CDCl₃): δ = 156.4, 146.0, 139.8, 137.9, 126.7, 115.7, 56.1, 36.6, 31.4, 29.2, 24.0, 22.2. HRMS (ESI) *m/z*, calcd for M⁺ (C₉₉H₁₁₁S₃N₃): 1437.7935; found: 1437.7970.

Truxene 5: Greenish yellow solid (yield: 75%) ¹H NMR (400 MHz, CDCl₃): δ

(ppm) 8.32 (d, 3H, $J = 9.19$ Hz), 7.49-7.61 (m, 6H), 7.30-7.43 (m, 6H), 7.08-7.20 (m, 6H), 6.76-6.98 (m, 6H), 3.83-4.09 (m, 6H), 2.84-2.99 (m, 6H), 2.01-2.14 (m, 6H), 1.44 (t, 9H), 0.74-1.01 (m, 36H), 0.38-0.65 (m, 30H). ^{13}C NMR (100 MHz, CDCl_3): $\delta = 153.6, 145.7, 144.9, 144.2, 140.1, 138.0, 130.8, 130.0, 129.6, 127.4, 127.3, 125.0, 124.5, 124.3, 123.7, 122.6, 121.1, 117.1, 115.2, 114.7, 90.0, 89.2, 55.7, 41.9, 37.0, 31.4, 29.7, 29.4, 23.9, 22.2, 13.8, 12.9$. MALDI calcd for M^+ ($\text{C}_{105}\text{H}_{108}\text{S}_3\text{N}_3$): 1595.379 found: 1595.589.

Truxene 6: Red solid (yield: 65%) ^1H NMR (400 MHz, CDCl_3): δ (ppm) 8.47 (d, 3H, $J = 6.86$ Hz), 8.15 (s, 3H), 7.82 (d, 3H, $J = 9.79$ Hz), 7.41-7.49 (m, 6H), 7.19(t, 3H), 6.90-7.07 (m, 12H), 3.96-4.05 (m, 6H), 2.80-2.93 (m, 6H), 2.10-2.23 (m, 6H), 1.48 (t, 9H), 0.74-1.00 (m, 36H), 0.34-0.63 (m, 30H). ^{13}C NMR (100 MHz, CDCl_3): $\delta = 129.8, 129.5, 127.4, 127.44, 127.2, 126.9, 126.8, 126.7, 126.3, 123.7, 123.6, 122.6, 122.6, 122.3, 116.1, 115.7, 115.2, 114.4, 53.4, 41.9, 31.9, 29.7, 29.3, 22.7, 14.1, 12.9, 12.8$.

MALDI calcd for M^+ ($\text{C}_{123}\text{H}_{108}\text{S}_3\text{N}_{15}$): 1979.652; found: 1979.232.

Truxene 7: Greenish black solid (yield: 60%) ^1H NMR (400 MHz, CDCl_3): δ (ppm) 8.37 (d, 3H, $J = 8.52$ Hz), 7.88 (s, 3H), 7.62 (d, 3H, $J = 7.61$ Hz), 7.52 (d, 3H, $J = 8.52$ Hz), 7.34 (d, 3H, $J = 10.84$ Hz), 7.06-7.25 (m, 12H), 6.98-7.03 (m, 6H), 6.94 (t, 3H), 6.82-6.90 (m, 6H), 3.87-3.97 (m, 6H), 2.71-2.89 (m, 6H), 1.96-2.14 (m, 6H), 1.42 (t, 9H), 0.69-0.92 (m, 36H), 0.26-0.58 (m, 30H). ^{13}C NMR (100 MHz, CDCl_3): $\delta = 170.6, 154.5, 153.7, 149.6, 148.9, 148.2, 144.7, 142.2, 137.5, 134.7, 133.8, 133.5, 132.5, 132.0, 128.9, 128.4, 127.9, 127.4, 126.4, 126.1, 125.4, 125.1, 123.9, 123.7, 122.0, 115.6, 114.6, 113.6, 113.5, 113.1, 112.3, 86.5, 56.5, 42.6, 36.6, 31.9, 31.2, 29.6, 29.3, 29.0, 23.8, 22.6, 22.0, 14.1, 13.8, 12.7$. MALDI calcd for M^+ ($\text{C}_{141}\text{H}_{120}\text{S}_3\text{N}_{15}$): 2207.640 found: 2207.512.

6.8. Conclusions

In summary, C_3 symmetric, star shaped phenothiazene based 1,1,4,4-Tetracyanobuta-1,3-diene (TCBD) and cyclohexa-2,5-diene-1,4-ylidene-expanded TCBD substituted donor-acceptor truxenes **4-7** were designed and synthesized by using the Ullmann, Pd-catalyzed Sonogashira cross-coupling and [2+2] Cycloaddition-retroelectrocyclization reactions. Their photophysical,

electrochemical, thermal properties were explored. The truxenes **4–7** exhibited good thermal stability. The substitution of phenothiazine through N-position at truxene core enhances the thermal stability compared to the 3-position substitution. The electronic absorption spectra reveals that the incorporation of TCBD and cyclohexa-2,5-diene-1,4-ylidene-expanded TCBD acceptor group results strong ICT at longer wavelength, donor-acceptor interactions and lower HOMO-LUMO gap. The optical and electrochemical properties of the truxenes **4–7** were explained from the TD-DFT calculations. The computational calculation show significant lowering of the HOMO-LUMO gap by the incorporation of TCNE and TCNQ groups. The truxene **6** and **7** are non-emissive in nature which further supports strong donor-acceptor interaction. The truxenes reported here are potential candidates for organic photovoltaic applications and their detailed study is currently on going in our laboratory.

6.9. References:

1. (a) Sonar P., Singh S. P., Li Y., Soh M. S., Dodabalapur A. (2010), A Low-Bandgap Diketopyrrolopyrrole Benzothiadiazole Based Copolymer for High-Mobility Ambipolar Organic Thin-Film Transistors, *Adv. Mater.*, 22, 5409–5413, (DOI: 10.1002/adma.201002973) (b) Kato S., Furuya T., Kobayashi A., Nitani M., Ie Y., Aso Y., Yoshihara T., Tobita S., Nakamura Y. (2012), Synthesis of Ladder-Type π -Conjugated Heteroacenes via Palladium-Catalyzed Double N-Arylation and Intramolecular O-Arylation, *J. Org. Chem.*, 77, 7595–7606, (DOI: 10.1021/jo070427p). (c) Omer K. M., Ku S. Y., Wong K. T., Bard A. J. (2009), Green Electrogenerated Chemiluminescence of Highly Fluorescent Benzothiadiazole and Fluorene Derivatives, *J. Am. Chem. Soc.*, 131, 10733–10741, (DOI: 10.1021/ja904135y). (d) Wang J. L., Tang Z.-M., Xiao Q., Ma Y., Pei J. (2009), Star-Shaped D- π -A Conjugated Molecules: Synthesis and Broad Absorption Bands, *Org. Lett.*, 11, 863–866, (DOI: 10.1021/ol802845w). (e) Sharma R., Maragani R., Mobin S. M., Misra R. (2013), Ferrocenyl substituted calixarenes: synthesis,

- structure and properties, *RSC Adv.*, 3, 5785-5788 (DOI: 10.1039/C3RA00146F). (f) Singh C. P., Sharma R., Shukla V., Khundrakpam P., Misra R., Bindra K. S., Chari R. (2014), Optical limiting and nonlinear optical studies of ferrocenyl substituted calixarenes, *Chem. Phys. Lett.*, 616, 189–195, (doi.org/10.1016/j.cplett.2014.10.030).
2. (a) Kato S., Matsumoto T., Ishi-I T., Thiemann T., Shigeiwa M., Gorohmaru H., Maeda S., Yamashita Y., Mataka S., (2004), Strongly red-fluorescent novel donor- π -bridge-acceptor- π -bridge-donor (D- π -A- π -D) type 2,1,3-benzothiadiazoles with enhanced two-photon absorption cross-sections, *Chem. Commun.*, 2342–2343, (DOI:10.1039/B410016F). (b) Neto B. A. D., Lapis A. A. M., Júnior E. N., da S., Dupont J. (2013), 2,1,3-Benzothiadiazole and derivatives: synthesis, properties, reactions, and applications in light technology of small molecules, *Eur. J. Org. Chem.*, 228-255 (DOI: 10.1002/ejoc.201201161). (c) Kato S., Matsumoto T., Shigeiwa M., Gorohmaru H., Maeda S., Ishi-I T., Mataka S. (2006), Novel 2,1,3-benzothiadiazole-based red-fluorescent dyes with enhanced two-photon absorption cross-sections *Chem.-Eur. J.*, 12, 2303-2317 (DOI: 10.1002/chem.200500921). (d) Kobayashi N., Inagaki S., Nemykin V. N., Nonomura T. (2001), A novel hemiporphyrine comprising three isoindoleimine and three thiadiazole units, *Angew. Chem., Int. Ed.*, 40, 2710–2712. (e) Lindner B. D., Engelhart J. U., Märken M., Tverskoy O., Appleton A. L., Rominger F., Hardcastle K. I., Enders M., Bunz U. H. F. (2012), *Chem. Eur. J.*, 18, 4627–4633. (f) Aviram A., Ratner M. A. (1974), Molecular rectifiers, *Chem. Phys. Lett.*, 29, 277–283, (doi.org/10.1016/0009) (g) Sharma R., Gautam P., Mobin S. M., Misra R. (2013), β -Substituted ferrocenyl porphyrins: synthesis, structure, and properties, *Dalton Trans.*, 42, 5539-5545 (DOI: 10.1039/C3DT00003F). (h) Sharma R., Gautam P., Misra R. Shukla S. K. (2015), β -Substituted triarylborane appended porphyrins: photophysical properties and anion sensing, *RSC Adv.*, 5, 27069, (DOI: 10.1039/C5RA03931B).

3. (a) Zhang Q. T., Tour J. M. (1998), Alternating Donor/Acceptor Repeat Units in Polythiophenes. Intramolecular Charge Transfer for Reducing Band Gaps in Fully Substituted Conjugated Polymers, *J. Am. Chem. Soc.*, 120, 5355–5362, (DOI: 10.1021/ja972373e). (b) Gohier F., Frère P. R. (2013), 3-Fluoro-4-hexylthiophene as a Building Block for Tuning the Electronic Properties of Conjugated Polythiophenes, *J. Org. Chem.*, 78, 1497–1503, (DOI:10.1021/jo302571u).
4. (a) Štefko M., Tzirakis M. D., B. Breiten, M.-O. Ebert, O. Dumele, Schweizer W. B., Gisselbrecht J.-P., Boudon C., Beels M. T., Biaggio I., Diederich F. (2013), Donor–acceptor (D–A)-substituted polyynene chromophores: modulation of their optoelectronic properties by varying the length of the acetylene spacer, *Chem. –Eur. J.*, 19, 12693-12704 (DOI: 10.1002/chem.201301642). (b) Van Mullekom H. A. M., Vekemans J. A. J. M., Meijer E. W. (1998), Band-gap engineering of donor–acceptor-substituted π -conjugated polymers, *Chem. -Eur. J.*, 4, 1235–1243 (DOI: 10.1002/(SICI)1521-3765(19980710)4:7<1235::AID. (c) Wang J.-L., Xiao Q., Pei J. (2010), Benzothiadiazole-based D– π -A– π -D organic dyes with tunable band gap: synthesis and photophysical properties, *Org. Lett.*, 12, 4164-4167 (DOI: 10.1021/ol101754q). (d) Bures F., Schweizer W. B., May J. C., Boudon C., Gisselbrecht J. -P., Gross M., Biaggio I., Diederich F. (2007), Property tuning in charge-transfer chromophores by systematic modulation of the spacer between donor and acceptor, *Chem.-Eur. J.*, 13, 5378-5387 (DOI: 10.1002/chem.200601735). (e) Moonen N. N. P., Pomerantz W. C., Gist R., Boudon C., Gisselbrecht J.-P., Kawai T., Kishioka A., Gross M., Irie M., Diederich F. (2005), Donor-substituted cyanoethynylethenes: π -conjugation and band-gap tuning in strong charge-transfer chromophores, *Chem. -Eur. J.*, 11, 3325-3341 (DOI: 10.1002/chem.200500082).
5. (a) Ventura B., Barbieri A., Barigelletti F., Diring S. E., Ziessel R. (2010), Energy Transfer Dynamics in Multichromophoric Arrays Engineered from Phosphorescent PtII/RuII/OsII Centers Linked to a Central Truxene

- Platform, *Inorg. Chem.*, 49, 8333–8346, (DOI: 10.1021/ic1008413). (b) Goubard F., Dumur F. (2015), Truxene: a promising scaffold for future materials, *RSC Adv.*, 5, 3521–3551, (DOI:10.1039/C4RA11559G).
6. (a) Zhang W. B., Jin W. H., Zhou X. H., Pei J. (2007), Star-shaped oligo (pphenylene)-functionalized truxenes as blue-light-emitting materials: synthesis and the structure-property relationship, *Tetrahedron*, 63, 2907–2914, (DOI: org/10.1016/j.tet.2007.01.025). (b) Huang J., Xu B., Su J. H., Chin H., Tian H. (2010), Efficient blue lighting materials based on truxene-cored anthracene derivatives for electroluminescent devices, *Tetrahedron*, 66, 7577–7582, (doi.org/10.1016/j.tet.2010.07.039).
7. (a) Boorum M. M., Vasil Y. V., Drewello T., Scott L. T. (2001), Groundwork for a Rational Synthesis of C₆₀: Cyclodehydrogenation of a C₆₀H₃₀ Polyarene, *Science*, 294, 828, (DOI: 10.1126/science.1064250). (b) Gomez-Lor B., Frutos O. De, Echavarren A. M. (1999), Synthesis of ‘crushed fullerene’ C₆₀H₃₀, *Chem. Commun.*, 2431, (DOI: 10.1039/A906990I).
8. Huang W., Smarsly E., Han J., Bender M., Seehafer K., Wacker I., Schröder R. R., Bunz U. H. F. (2017), Truxene-Based Hyperbranched Conjugated Polymers: Fluorescent Micelles Detect Explosives in Water, *ACS Appl. Mater. Interfaces*, 9, 3068–3074, (DOI: 10.1021/acsami.6b12419).
9. (a) Rabideau P. W., Abdourazak A. H., Marcinow Z., Sygula R., Sygula A. (1995), Buckybowls 2. Toward the Total Synthesis of Buckminsterfullerene (C₆₀): Benz[5,6]-as-indaceno[3,2,1,8,7-mnopqr]indeno[4,3,2,1-cdef]chrysene, *J. Am. Chem. Soc.*, 117, 6410, (DOI: 10.1021/ja00128a052). (b) Demlow E. V., Kelle T. (1997), Synthesis of New Truxene Derivatives: Possible Precursors of Fullerene Partial Structures, *Synth. Commun.*, 27, 2021, (DOI: 10.1080/00397919708006804). (c) Gomez-Lor B., Gonzalez-Cantalapiedra E., DeFrutos O., Ardenas C., Santos D. J., Echavarren A. M. (2004), Synthesis of C₃ Benzo[1,2-e:3,4-e':5,6-

- e']tribenzo[1]acephenanthrylenes (“Crushed Fullerene” Derivatives) by Intramolecular Palladium-Catalyzed Arylation, *Chem. Eur. J.*, 10, 2601, (DOI: 10.1002/chem.200306023).
10. (a) Pei J., Wang J., Cao X. , Zhou X., Zhang B. (2003), Star-Shaped Polycyclic Aromatics Based on Oligothiophene-Functionalized Truxene: Synthesis, Properties and Facile Emissive Wavelength Tuning, *J. Am. Chem. Soc.*, 125, 9944, (DOI: 10.1021/ja0361650). (b) Cao X. Y., Zhang W. B., Wang J. L., Zhou X. H., Lu H., Pei J. (2003), Extended π -Conjugated Dendrimers Based on Truxene, *J. Am. Chem. Soc.*, 125, 12430, (DOI: 10.1021/ja037723d).
11. Sang G., Zou Y., Li Y. (2008), Two Polythiophene Derivatives Containing Phenothiazine Units: Synthesis and Photovoltaic Properties, *J. Phys. Chem. C.*, 112, 12058–12064, (DOI: 10.1021/jp803187u).
12. (a) Fang J. (2013), Solution-Processed Hybrid Cathode Interlayer for Inverted Organic Solar Cells, *ACS Appl. Mater. Interfaces.*, 5, 10428–10432 (b) Wan Z., Jia C., Duan Y., Zhou L., Lin Y., Shi Y. (2012), Phenothiazine–triphenylamine based organic dyes containing various conjugated linkers for efficient dye-sensitized solar cells, *J. Mater. Chem.*, 22, 25140, (DOI: 10.1039/C2JM34682F).
13. Zhang G., Sun J., Xue P., Zhang Z., Gong P., Peng J., Lu R. (2015), Phenothiazine modified triphenylacrylonitrile derivatives: AIE and mechanochromism tuned by molecular conformation, *J. Mater. Chem. C*, 3, 2925–2932, (DOI: 10.1039/C4TC02925A).
14. (a) Yamada M., Schweizer W. B., Schoenebeck F., Diederich F. (2010), Unprecedented thermal rearrangement of push–pull-chromophore–[60]fullerene conjugates: formation of chiral 1,2,9,12-tetrakis-adducts, *Chem. Commun.*, 46, 5334-5336 (DOI: 10.1039/C0CC00881H). (b) Jordan M., Kivala M., Boudon C., Gisselbrecht J.-P., Schweizer W. B., Seiler P., Diederich F. (2011), Switching the regioselectivity in cycloaddition-retro-electrocyclizations between donor-activated alkynes and the electron-accepting olefins TCNE and TCNQ, *Chem.–Asian J.*, 6,

- 396-401 (DOI: 10.1002/asia.201000539). (c) Kivala M., Boudon C., Gisselbrecht J.-P., Seiler P., Gross M., Diederich, F. (2007), A novel reaction of 7,7,8,8-tetracyanoquinodimethane (TCNQ): charge-transfer chromophores by [2 + 2] cycloaddition with alkynes, *Chem. Commun.* 2007, 4731-4733 (DOI: 10.1039/B713683H).
15. (a) Shoji T., Ito S., Toyota K., Yasunami M., Morita N. (2008), Synthesis, Properties, and Redox Behavior of Mono-, Bis-, and Tris[1,1,4,4-tetracyano-2-(1-azulenyl)-3-butadienyl] Chromophores Binding with Benzene and Thiophene Cores, *Chem.–Eur. J.*, 14, 8398–8408, (DOI: 10.1002/chem.200701981). (b) Shoji T., Ito S., Toyota K., Iwamoto T., Yasunami M., Morita N. (2009), Reactions between 1-ethynylazulenes and 7,7,8,8-tetracyanoquinodimethane (TCNQ): preparation, properties, and redox behavior of novel azulene-substituted redox-active chromophores, *Eur. J. Org. Chem.*, 4316-4324 (DOI: 10.1002/ejoc.200900539).
16. (a) Misra R., Gautam P. (2014), Tuning of the HOMO–LUMO gap of donor-substituted symmetrical and unsymmetrical benzothiadiazoles, *Org. Biomol. Chem.*, 12, 5448–5457, (DOI: 10.1039/C4OB00629A). (b) Dhokale B., Jadhav T., Mobin S. M., Misra R. (2016), Dalton Trans., Tetracyanobutadiene functionalized ferrocenyl BODIPY dyes, 45, 1476, (DOI: 10.1039/C5DT04037J). (c) Rout Y., Gautam P., Misra R. (2017), Unsymmetrical and Symmetrical Push–Pull Phenothiazines, *J. Org. Chem.*, DOI: 10.1021/acs.joc.7b00991. (d) Misra R., Sharma R., Mobin S. M. (2014), Star shaped ferrocenyl truxenes: synthesis, structure and properties, *Dalton Trans.*, 43, 6891-6896, (DOI: 10.1039/C4DT00210E). (e) Sharma R., Maragani R., Misra R. (2016), Ferrocenyl aza-dipyrrromethene and aza-BODIPY: Synthesis and properties, *J. Organomet. Chem.*, 825, 8–14, (DOI:org/10.1016/j.jorganchem.2016.10.019).
17. (a) Gautam P., Sharma R., Misra R., Keshtov M. L., Kuklin S. A., Sharma G. D. (2017), Donor–acceptor–acceptor (D–A–A) type 1, 8-

- naphthalimides as non-fullerene small molecule acceptors for bulk heterojunction solar cells, *Chem. Sci.*, 8, 2017–2024, (DOI: 10.1039/C6SC04461A). (b) Patil Y., Misra R., Singhal R., Sharma G. D. (2017), Ferrocene-diketopyrrolopyrrole based non-fullerene acceptors for bulk heterojunction polymer solar cells, *J. Mater. Chem. A*. DOI: 10.1039/C7TA03322B.
18. Poddar M., Misra R. (2017), NIR-Absorbing Donor–Acceptor Based 1,1,4,4-Tetracyanobuta-1,3-Diene (TCBD)- and Cyclohexa-2,5-Diene-1,4-Ylidene-Expanded TCBD-Substituted Ferrocenyl Phenothiazines, *Chem. Asian, J.* 16, 2908–2915, (DOI: 10.1002/asia.201700879).
19. Kanibolotsky A. L., Berridge R., Skabara P. J., Perepichka I. F., Bradley D. D. C., Koeberg M. (2004), Synthesis and properties of monodisperse oligofluorene-functionalized truxenes: highly fluorescent star-shaped architectures, *J. Am. Chem. Soc.*, 126, 13695, (DOI: 10.1021/ja039228n).
20. Cao X., Zi H., Zhang W., Lu H., Pei J. (2005), Star-Shaped and Linear Nanosized Molecules Functionalized with Hexa-peri-hexabenzocoronene: Synthesis and Optical Properties, *J. Org. Chem.*, 70, 3645–3653, (DOI: 10.1021/jo0480139).
21. Poddar M., Gautam P., Rout Y., Misra R. (2017), Donor–acceptor phenothiazine functionalized BODIPYs, *Dyes and Pigments*, 146, 368–373, (doi.org/10.1016/j.dyepig.2017.07.017).
22. Chen S., Li Y., Liu C., Yang W., Li Y. (2011), Strong Charge-Transfer Chromophores from [2+ 2] Cycloadditions of TCNE and TCNQ to Peripheral Donor-Substituted Alkynes, *Eur. J. Org. Chem.*, 32, 6445–6451, (DOI: 10.1002/ejoc.201101009).
23. (a) Dhokale, B., Gautam, P., & Misra, R. (2012). Donor–acceptor perylenediimide–ferrocene conjugates: synthesis, photophysical, and electrochemical properties, *Tetrahedron Letters*, 53(18), 2352–2354, <http://doi.org/http://dx.doi.org/10.1016/j.tetlet.2012.02.107>. Rochford J., Rooney M. T. P. (2007), Redox Control of meso-Zinc(II) Ferrocenylporphyrin Based Fluorescence Switches, *Inorg. Chem.*, 46,

- 7247, (DOI: 10.1021/ic0703326). (c) Rao M. R., Pavan K. V., Ravikanth M. (2010), Synthesis of boron-dipyrromethene–ferrocene conjugates, *J. Organomet. Chem.*, 695, 863–869, (doi.org/10.1016/j.jorganchem.2010.01.009).
24. Fery-Forgues, S., Delavaux-Nicot, B., (2000), Ferrocene and ferrocenyl derivatives in luminescent systems, *J. Photochem. Photobiol., A*, 132, 137–159, (DOI: [http://dx.doi.org/10.1016/S1010-6030\(00\)00213-6](http://dx.doi.org/10.1016/S1010-6030(00)00213-6)); (b) Barlow, S., Marder, S. R., (2000), Electronic and optical properties of conjugated group 8 metallocene derivatives, *Chem. Commun.*, 1555–1562, (DOI: 10.1039/B004907G).
25. (a) Francl F., Pietro W. J., Hehre W. J., Binkley J. S., Gordon M. S., Defrees D. J., Pople J. A. (1982), Self-consistent molecular orbital methods. XXIII. A polarization-type basis set for second-row elements, *J. Chem. Phys.*, 77, 3654–3665, (doi.org/10.1063/1.444267). (b) Ding F., Chen S., Wang H. (2010), Computational study of ferrocene-based molecular frameworks with 2, 5-diethynylpyridine as a chemical bridge, *Materials*, 3, 2668–2683, (doi:10.3390/ma3042668).
26. (a) Lai R. Y., Fabrizio E. F., Lu L., Jenekhe S. A., Bard A. J. (2001), Synthesis, Cyclic Voltammetric Studies, and Electrogenenerated Chemiluminescence of a New Donor-Acceptor Molecule: 3,7-[Bis[4-phenyl-2-quinolyl]]-10-methylphenothiazine, *J. Am. Chem. Soc.*, 123, 9112, (DOI: 10.1021/ja0102235). (b) Kulkarni A. P., Wu P. T., Kwon T. W., Jenekhe S. A. (2005), Phenothiazine-phenylquinoline donor–acceptor molecules: Effects of structural isomerism on charge transfer photophysics and electroluminescence, *J. Phys. Chem. B.*, 109, 19584, (DOI: 10.1021/jp0529772).
27. Pedone A. (2013), Role of Solvent on Charge Transfer in 7-Aminocoumarin Dyes: New Hints from TD-CAM-B3LYP and State Specific PCM Calculations, *J. Chem. Theory Comput.*, 9, 4087–4096 (DOI: [/abs/10.1021/ct4004349](http://dx.doi.org/10.1021/ct4004349)).

Chapter 7

β -Substituted Truxene Porphyrins: Synthesis and Photophysical Properties

7.1. Introduction

The synthesis of π -conjugated macromolecules has become a vigorous research topic due to their applications in material science, organic light-emitting diodes (OLED), nonlinear optics, covalently linked assemblies involving energy and electron transfers, and optoelectronic devices.¹⁻⁵

Truxene is a planar C_3 -symmetric, fused fluorine trimer and a promising building block for the construction of larger molecular architectures.⁶ The facile functionalization at the para position (2,7,12 positions) of the truxene core results in a variety of π -conjugated macromolecules.⁷ There are handful of reports which reveals that truxene based donor-acceptor systems are potential candidates for application in two-photon absorption, organic light-emitting diodes (OLED), and organic fluorescent probes.⁸⁻¹² Recently, Guijiang Zhou *et al.* have reported spirobifluorene substituted truxene based emitters for blue-emitting OLEDs.¹³ Our group has also explored the ferrocenyl substituted truxene based donor-acceptor systems.¹⁴

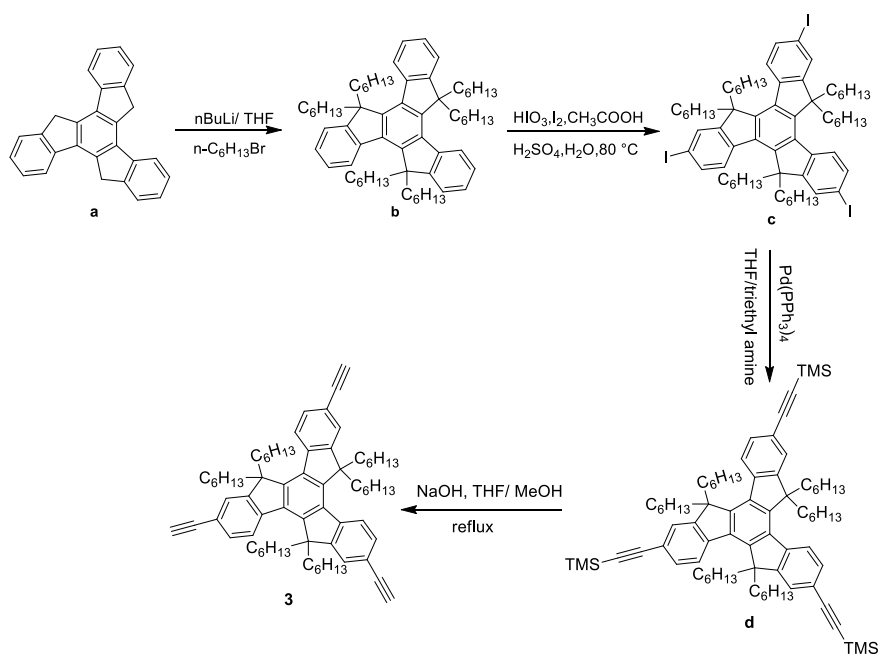
Porphyrin is an important building block which provides extensively conjugated π -system and facile synthetic approach.¹⁵ There are couple of reports on truxene containing porphyrins through *meso* position, which explored photoinduced energy transfer processes.¹⁶ Particularly, Pierre D. Harvey *et al.* and Jian Pei *et al.* have studied the porphyrins containing truxene and tritruene linked at the *meso* positions for singlet and triplet energy transfer process,^{17,18} where huge dihedral angle due to the covalent bond linkage and poor orbital overlap between the truxene and porphyrin hinders the electronic communication. Therefore, to enhance the electronic communication, the β -substitution through ethynyl linkage

is of interest because this substitution is in direct conjugation with the 18π -molecular system, which results in substantial perturbation of the photophysical and electrochemical properties.¹⁹ Our group has explored β -substituted ferrocenyl porphyrins²⁰ and triarylborane appended porphyrins for sensing applications.²¹ To our knowledge, there are no reports on truxene substituted through β -position of porphyrin. In continuation of our work on β -substituted porphyrins we have designed and synthesized the star shaped π -conjugated truxene **4**, where truxene core is flanked by three units of porphyrin through β -position and its Zn-metalated derivative **5** using the Pd-catalyzed Sonogashira cross-coupling reaction and metalation reaction. Their photophysical properties and computational calculations were studied.

7.2. Results and discussion

The synthetic route of porphyrin substituted truxenes **4** and **5** are shown in Scheme 1. The porphyrin substituted truxenes **4** was synthesized by the Pd-catalysed Sonogashira cross-coupling reaction of the β -bromo tetraphenyl porphyrin with the ethynyl truxene **3**.

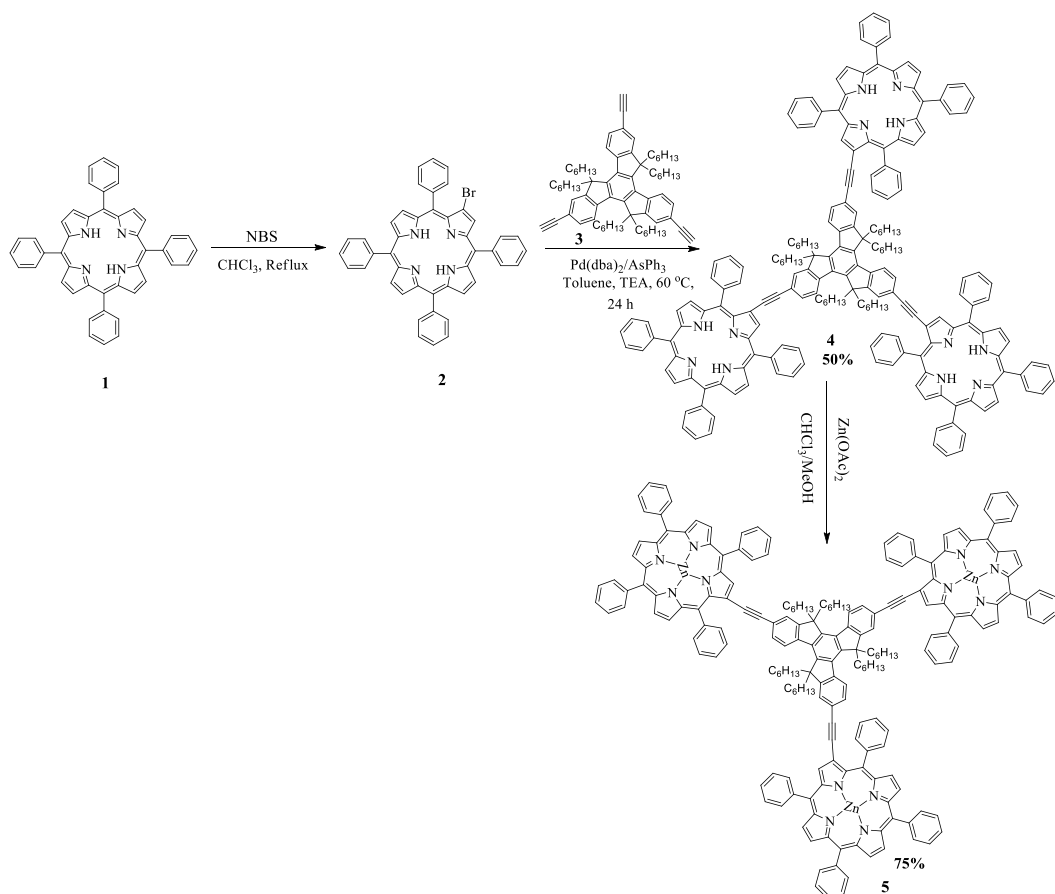
The tetraphenylporphyrin (H_2TPP) **1** was synthesized by the condensation reaction of pyrrole and benzaldehyde following the Lindsey procedure.²² The β -bromination of porphyrin using N-bromosuccinimide in refluxing $CHCl_3$ resulted in β -bromo tetraphenyl porphyrin **2**, which was purified by column chromatography using dichloromethane–hexane (10:90) as the eluent.²³ The truxene core (a) was synthesized by 1-indanone in the presence of acetic acid and hydrochloric acid followed by the alkylation reaction and iodination reaction resulted hexahexylated tri-iodo truxene (c) (Scheme 7.1).^{24,25} The reaction of tri-iodo truxene (c) with TMS-acetylene using Sonogashira cross-coupling reaction condition, followed by deprotection of TMS group by NaOH resulted truxene **3** in 70% yield (Scheme 7.1).²⁶



Scheme 7.1: Synthesis of ethynyl truxene **3**.

The Sonogashira cross-coupling reaction of β -bromo porphyrin **2** with truxene **3** under the catalytic system $\text{Pd}(\text{dba})_2/\text{AsPh}_3$, resulted star shaped porphyrin substituted truxene **4** in 50% yield. The porphyrin substituted truxene **4** was purified by column chromatography on silica gel and repetitive crystallization. The β -substituted truxene porphyrin **4** was further reacted with four equivalents of zinc acetate ($\text{Zn}(\text{OAc})_2 \cdot 2\text{H}_2\text{O}$) at room temperature in chloroform/methanol which resulted Zn-metalated truxene porphyrin **5** in 75% yield (Scheme 7.2). The porphyrin substituted truxene **4** and **5** possess good solubility in common organic solvents. The porphyrin substituted truxene **4** and **5** were well characterized by ^1H NMR and ^{13}C NMR and MALDI techniques. The ^1H NMR spectrum of porphyrin substituted truxene **4** displays one singlet at 9.17 (3H) and multiplet between 8.75-8.93 (18H), corresponding to the β -protons of porphyrin ring. The chemical shifts for the internal NH-pyrrole proton appear as a singlet at -2.62 due to the symmetric nature, which confirms the formation of truxene **4**. The two doublets of nine protons at 8.41 and 8.33 ppm are ascribed to the truxene core protons. The doublets at 8.27, 8.22 and multiplets between 7.68-7.86 and 7.46-7.53 belongs to the phenyl rings of porphyrin. In the aliphatic region, multiplet signals between 3.04-3.17 and 2.20-2.34 ppm belongs to the hexyl chain protons. The Zn metalated

truxene **5** exhibit similar ^1H NMR spectra, the disappearance of internal NH proton signals confirms the Zn metalated product formation. The ^1H NMR data are given in the experimental section and the spectra are placed in the supporting information.



Scheme 7.2: Synthesis of porphyrin substituted truxene **4** and **5**.

7.3. Photophysical properties

The UV-vis absorption and emission spectra of the porphyrin substituted truxene **4** and **5** were recorded in dichloromethane at room temperature (Figure 7.1), and the data are compiled in Table 7.1. The porphyrin substituted truxene **4** and **5** show truxene centered absorption band at 334 nm corresponding to $\pi\text{-}\pi^*$ transition. The porphyrin substituted truxene **4** show intense Soret band at 424 nm and four Q-bands in the region of 524–655 nm. The metalated truxene porphyrin **5** exhibit characteristic Soret band at 430 nm, and two Q-bands in the region of

557–593 nm. The truxene linked with β -position of porphyrins **4** and **5** resulted in bathochromic shift of the Soret band and the Q-bands. The Soret band of porphyrin substituted truxene **4** and **5** are red shifted by 6 nm and 8 nm compared to H₂TPP and ZnTPP respectively (Table 7.1).

The emission properties of the porphyrin substituted truxene **4** and **5** were studied by steady state fluorescence technique. The emission spectra are shown in Figure 7.1b. The porphyrin substituted truxene **4** and **5** show considerable red shift in fluorescence maxima compared to TPP and ZnTPP respectively. The porphyrin substituted truxene **4** and **5** show enhanced fluorescence quantum yields of 0.30 and 0.20 respectively. These results demonstrate that there is considerable electronic communication between β -substituted porphyrins and truxene core.

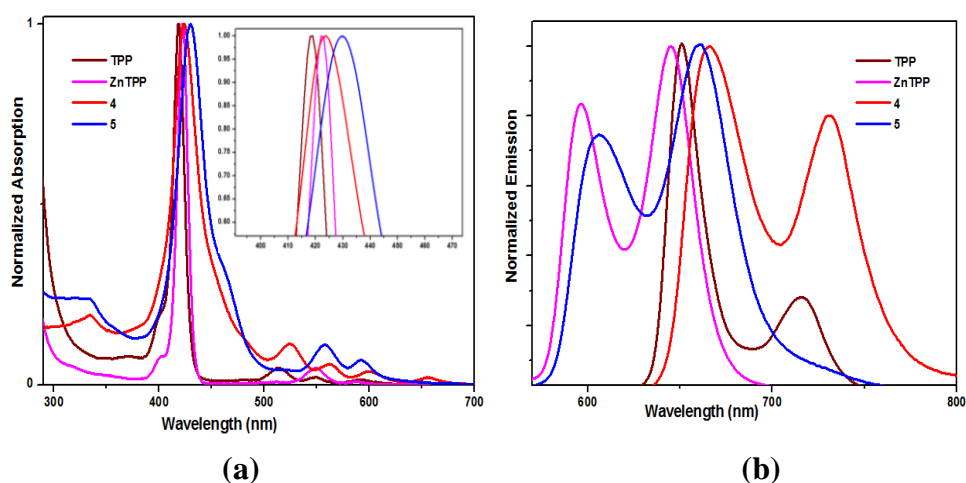


Figure 7.1. (a) Electronic absorption spectra of the **TPP**, **ZnTPP** and porphyrin substituted truxene **4** and **5** at 1.0×10^{-6} M concentration, recorded in dichloromethane. The inset shows enlarged view. (b) Emission spectra of **TPP**, **ZnTPP** and porphyrin substituted truxene **4** and **5**.

Table 7.1. Absorption and emission data of porphyrin substituted truxene **4** and **5**

Compound	$\lambda_{\text{abs}}(\text{nm})^{\text{a}}$			$\lambda_{\text{em}}(\text{nm})$	$^{\text{c}}\Phi_{\text{f}}$	
	truxene abs.band	Soret band	$^{\text{b}}\epsilon(\text{M}^{-1}\text{cm}^{-1})\times 10^3$			
TPP	-	418	-	515, 551, 589, 647	650,716	0.11
ZnTPP	-	422	-	549,587	595,645	
4	334	424	550	524,563,600,655	666,731	0.30
5	334	430	441	557,593	606,660	0.20

^aMeasured in DCM. λ_{abs} (nm): absorption maximum of the Soret band. ^b ϵ , extinction coefficient.

^cDetermined by using H₂TPP as a standard ($\Phi_{\text{st}} = 0.11$)

7.4. Computational Studies:

To understand the photophysical properties of porphyrin substituted truxene **4** and **5** the density functional theory (DFT) and time dependent density functional (TD-DFT) calculation was performed. The geometries of porphyrin substituted truxene **4** and **5** were optimized using Gaussian 09 program at the B3LYP/6-31G** level for C, H, N and LANL2DZ for Zn.²⁷ The TD-DFT calculations were carried out in the dichloromethane using the polarized continuum model (CPCM) of Gaussian 09 software. The 6-31G**/CAM-B3LYP basis set was used for all the calculations.²⁷ In porphyrin substituted truxene **4** and **5**, the truxene core and porphyrin rings are almost in same plane (Figure 7.2), which favours the electronic communication. The Figure 7.3 shows the electron density distribution of the HOMO and LUMO of the porphyrin substituted truxene **4** and **5**. In truxene **4** the HOMO and LUMO orbitals are mainly localized on the porphyrin unit whereas in truxene **5** HOMO is delocalized over truxene core and two units of porphyrin and LUMO is delocalized on the porphyrin unit.

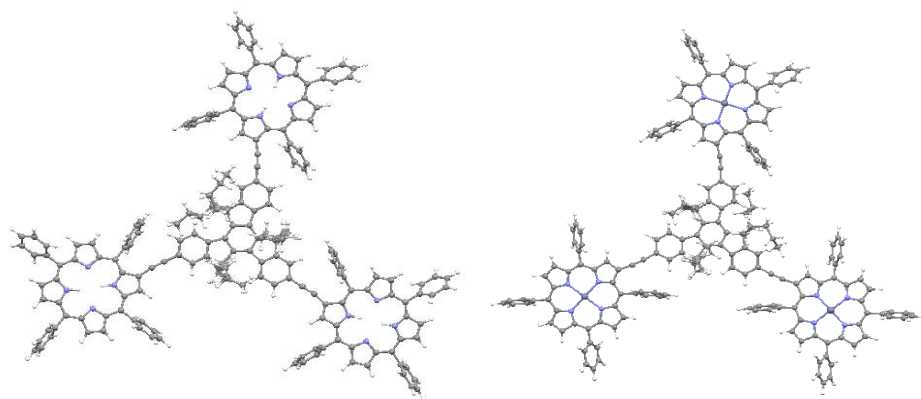


Figure 7.2. The DFT optimized structure of porphyrin substituted truxene **4** and **5** using B3LYP level. The 6-31G** basis set for C, N, H and LANL2DZ for Zn.

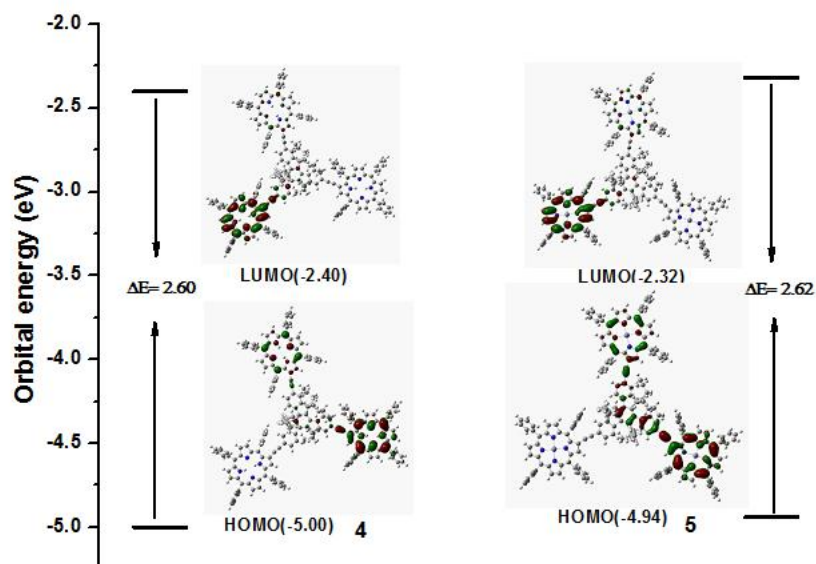


Figure 7.3. The energy level diagram of the frontier molecular orbitals of the porphyrin substituted truxene **4** and **5** using B3LYP/6-31G(d,p) level of DFT theory.

7.5. Experimental section

General experimental.

All reagents were obtained from commercial sources, and used as received unless otherwise stated. ^1H NMR (400 MHz) and ^{13}C NMR (100 MHz) spectra were recorded on a Bruker Avance (III) 400 MHz instrument by using CDCl_3 as solvent. ^1H NMR chemical shifts are reported in parts per million (ppm) relative to the solvent residual peak (CDCl_3 , 7.26 ppm). Multiplicities are given as s (singlet), d (doublet), t (triplet), q (quartet), and m (multiplet), and the coupling constants, J , are given in Hz. ^{13}C NMR chemical shifts are reported relative to the solvent residual peak (CDCl_3 , 77.36 ppm). UV-visible absorption spectra of all compounds in Dichloromethane were recorded on a Carry-100 Bio UV-visible Spectrophotometer. The quantum yields (Φ) were calculated using H_2TPP ($\Phi = 0.11$) as reference.

Fluorescence quantum yield.

The fluorescence quantum yields (Φ_{F}) of truxene **4** and **5** were calculated (eqn(1)) by the steady-state comparative method using H_2TPP as a standard ($\Phi_{\text{st}} = 0.11$).

$$\Phi_{\text{F}} = \Phi_{\text{st}} \times S_{\text{u}}/S_{\text{st}} \times A_{\text{st}} / A_{\text{u}} \times n^2 D_{\text{u}}/n^2 D_{\text{st}} \text{ (Eq.1)}$$

where Φ_{F} is the emission quantum yield of the sample, Φ_{st} is the emission quantum yield of the standard, A_{st} and A_{u} represent the absorbance of the standard and the sample at the excitation wavelength, respectively, while S_{st} and S_{u} are the integrated emission band areas of the standard and the sample, respectively, and nD_{st} and nD_{u} are the solvent refractive index of the standard and the sample, and u and st refer to the unknown and the standard, respectively.

Synthesis and Characterization

Procedure for the preparation of truxene 4 and 5.

Truxene 4: A solution of 2-bromo-5,10,15,20-tetraphenylporphyrin (150 mg, 0.21 mmol) and ethynyl truxene **3** (50 mg, 0.05 mmol) in toluene/triethylamine 2:1 (60 mL), was deaerated for 15 min with argon bubbling and then, Pd(dba)₂ (40 mg, 0.07 mmol) and AsPh₃ (170 mg, 0.55 mmol) were added. The solution was deaerated for further 5 min; after that, reaction was left under argon at 80 °C. After completion, the mixture was cooled at room temperature and the solvent was evaporated. The product was purified by column chromatography on silica gel eluting with CH₂Cl₂/Hexane. The product was further recrystallized from dichloromethane/methanol to give porphyrin **4** in 50% yield.

Red solid (yield: 50%) ¹H NMR (400 MHz, CDCl₃): δ (ppm) 9.17 (s, 3H), 8.75-8.93 (m, 18H), 8.41 (d, 3H, *J* = 9.19 Hz), 8.33 (d, 6H, *J* = 7.22 Hz), 8.27 (d, 6H, *J* = 8.26 Hz), 8.22 (d, 12H, *J* = 7.22 Hz), 7.68-7.86 (m, 36H), 7.46-7.53 (m, 6H), 3.04-3.17 (m, 6H), 2.20-2.34 (m, 6H), 0.95-1.10 (m, 36H), 0.64-0.76 (m, 30H), -2.62 (s, 6H). ¹³C NMR (100 MHz, CDCl₃): 153.2, 145.8, 142.2, 142.1, 141.8, 141.4, 140.0, 138.2, 134.6, 134.6, 134.5, 128.7, 127.9, 127.8, 126.8, 126.8, 126.7, 121.8, 120.7, 120.5, 120.1, 120.1, 120.0, 99.9, 86.5, 55.8, 53.4, 37.2, 31.9, 31.6, 29.7, 29.6, 24.1, 22.7, 22.4, 13.1, 14.1, 14.0.

MALDI calcd for M⁺ (C₂₀₁H₁₇₄N₁₂): 2757.61 found: 2757.59.

Synthesis of truxene 5:

A solution of Zn(OAc)₂·2H₂O (15 mg, 0.06 mmol) in MeOH (2 mL) was added to a solution of compound **4** (20 mg, 0.02 mmol) in 15 mL of chloroform and the reaction mixture was stirred for overnight at room temperature. The reaction mixture was concentrated in vacuo and further purified by column

chromatography using dichloromethane/hexane. The porphyrin **5** was obtained as a red colour solid in 75% yield.

Red solid (yield: 75%) ^1H NMR (400 MHz, CDCl_3): δ (ppm) 9.36 (s, 3H), 8.82-9.02 (m, 18H), 8.45 (d, 3H, $J = 8.69$ Hz), 8.35 (d, 6H, $J = 6.51$ Hz), 8.30 (d, 6H, $J = 7.24$ Hz), 8.25 (d, 12H, $J = 7.24$ Hz), 7.73-7.86 (m, 36H), 7.53-7.68 (m, 6H), 3.09-3.21 (m, 6H), 2.26-2.37 (m, 6H), 1.01-1.12 (m, 36H), 0.71-0.77 (m, 30H). MALDI calcd for M^{+1} ($\text{C}_{201}\text{H}_{168}\text{N}_{12}\text{Zn}_3$): 2948.70 found: 2949.59.

7.6. Conclusions:

In summary, C_3 symmetric, star shaped β -substituted truxene porphyrin **4** and its Zn-metalated derivative **5** have been designed and synthesized by using the Pd-catalyzed Sonogashira cross-coupling and metalation reaction. The substitution of porphyrin results in bathochromic shift of absorbance and fluorescence maxima. The absorption and emission studies exhibit considerable electronic communication. The β -substituted truxene porphyrins reported here are potential candidate for optoelectronic application and their energy transfer studies are currently in progress in our laboratory.

7.7. References

- (a) Moore J. S. (1997), Shape-Persistent Molecular Architectures of Nanoscale Dimension, *Acc. Chem. Res.*, 30, 402, (DOI: 10.1021/ar950232g).
(b) Caminade A. M., Majoral J. P. (2004), Nanomaterials based on phosphorus dendrimers, *Acc. Chem. Res.*, 37, 341, (DOI: 10.1021/ar020077n)
(c) Schlüter A. D., Rabe J. P. (2000), Dendronized polymers: synthesis, characterization, assembly at interfaces, and manipulation, *Angew. Chem., Int. Ed.*, 39, 864, (DOI: 10.1002/(SICI)1521-3773(20000303)).
(d) Harth E. M., Hecht S., Helms B., Malmstrom E. E., Fréchet J. M. J., Hawker C. J. (2002), The effect of macromolecular architecture in nanomaterials: a comparison of site isolation in porphyrin core dendrimers and their isomeric linear analogues, *J. Am. Chem. Soc.*, 124, 3926, (DOI: 10.1021/ja025536u).

- (e) Ma Q., Remsen E. E., Kowalewski T., Wooley K. L. (2001), Two-dimensional, shell-cross-linked nanoparticle arrays, *J. Am. Chem. Soc.*, 123, 4627, (DOI: 10.1021/ja0156542).
2. (a) Halim M., Pillow J. N. G., Samuel I. D. W., Burn P. L. (1999), Conjugated Dendrimers for Light-Emitting Diodes: Effect of Generation, *Adv. Mater.*, 11, 371, (DOI: 10.1002/(SICI)1521-4095(199903)). (b) Lupton J. M., Samuel I. D. W., Beavington R., Burn P. L., Baessler H. (2001), Control of Charge Transport and Intermolecular Interaction in Organic Light-Emitting Diodes by Dendrimer Generation, *Adv. Mater.*, 13, 258, (DOI: 10.1002/1521-4095(200102)).
3. (a) Beavington R., Frampton M. J., Lupton J. M., Burn P. L., Samuel I. D. W. (2003), The Effect of Core Delocalization on Intermolecular Interactions in Conjugated Dendrimers, *Adv. Funct. Mater.*, 13, 211, (DOI: 10.1002/adfm.200390032). (b) Kwon T. W., Alam M. M., Jenekhe S. A. (2003), n-Type Conjugated Dendrimers: Convergent Synthesis, Photophysics, Electroluminescence, and Use as Electron-Transport Materials for Light-Emitting Diodes, *Chem. Mater.*, 16, 4657, (DOI: 10.1021/cm0494711).
4. (a) Ma H., Jen A. K. Y. (2001), Functional Dendrimers for Nonlinear Optics, *Adv. Mater.*, 13, 1201, (DOI: 10.1002/1521-4095(200108)). (b) Goodson T. G. (2005), Optical Excitations in Organic Dendrimers Investigated by Time-Resolved and Nonlinear Optical Spectroscopy, *Acc. Chem. Res.*, 38, 99, (DOI: 10.1021/ar020247w). (c) Porre`s L., Mongin O., Katan C., Charlot M., Pons T., Mertz J., Blanchard-Desce M. (2004), Enhanced two-photon absorption with novel octupolar propeller-shaped fluorophores derived from triphenylamine, *Org. Lett.*, 6, 47, (DOI: 10.1021/ol036041s).
5. Liu D., Zhang H., Grim P. C. M., Feyter S. De, Wiesler U. M., Berresheim A. J., Mu`llen K., Schryver F. C. De (2002), Self-assembly of polyphenylene dendrimers into micrometer long nanofibers: An atomic force microscopy study, *Langmuir*, 18, 2385, (DOI: 10.1021/la011270d).

6. Ventura B., Barbieri A., Barigelletti F., Diring S. E., Ziesel R. (2010), Energy Transfer Dynamics in Multichromophoric Arrays Engineered from Phosphorescent PtII/RuII/OsII Centers Linked to a Central Truxene Platform, *Inorg. Chem.*, 49, 8333–8346, (DOI: 10.1021/ic1008413).
7. (a) Yuan M., Fang Q., Liu Z., Guo J., Chen H., Yu W., Xue G., Liu D. S. (2006), Acceptor or Donor (Diaryl B or N) Substituted Octupolar Truxene: Synthesis, Structure, and Charge-Transfer-Enhanced Fluorescence, *J. Org. Chem.*, 71, 7858-7861, DOI: 10.1021/jo061210i. (b) Duan X. F., Wang J. L., Pei J. (2005), Nanosized π -conjugated molecules based on truxene and porphyrin: synthesis and high fluorescence quantum yields, *Org. Lett.*, 7, 4071, (DOI: 10.1021/ol051221i).
8. (a) Pei J., Wang J., Cao X., Zhou X., Zhang B. (2003), Star-Shaped Polycyclic Aromatics Based on Oligothiophene-Functionalized Truxene: Synthesis, Properties and Facile Emissive Wavelength Tuning, *J. Am. Chem. Soc.*, 125, 9944, (DOI: 10.1021/ja0361650). (b) Cao X. Y., Zhang W. B., Wang J. L., Zhou X. H., Lu H., Pei J. (2003), Extended π -Conjugated Dendrimers Based on Truxene, *J. Am. Chem. Soc.*, 125, 12430, (DOI: 10.1021/ja037723d).
9. Cao X. Y., Liu X. H., Zhou X. H., Zhang Y., Jiang Y., Cao Y., Cui Y. X., Pei J. (2004), Giant Extended π -Conjugated Dendrimers Containing the 10,15-Dihydro-5H-diindeno[1,2-a;1',2'-c]fluorene Chromophore: Synthesis, NMR Behaviors, Optical Properties, and Electroluminescence, *J. Org. Chem.*, 69, 6050, (DOI: 10.1021/jo049268p).
10. (a) Zong X., Liang M., Fan C., Tang K., Li G., Sun Z., Xue S. (2012), Design of truxene-based organic dyes for high-efficiency dye-sensitized solar cells employing cobalt redox shuttle, *J. Phys. Chem. C*, 116, 11241–11250, (DOI: 10.1021/jp301406x). (b) Xie Y., Zhang X., Xiao Y., Zhang Y., Zhou F., Qib J., Qu J. (2012), Fusing three perylenebisimide branches and a truxene core into a star-shaped chromophore with strong two-photon excited fluorescence and high photostability, *Chem. Commun.*, 48, 4338–4340, (DOI: 10.1039/C2CC31261A).

11. (a) Yang Z., Xu B., He J., Xue L., Guo Q., Xia H., Tian W. (2009), Solution-processable and thermal-stable triphenylamine-based dendrimers with truxene cores as hole-transporting materials for organic light-emitting devices, *Org. Elec.*, 10, 954–959, (DOI:org/10.1016/j.orgel.2009.04.024). (b) Xua H. J., Dub B., Gros C. P., Richarda P., Barbea J. M., Pierre D. H. (2013), Shape-persistent poly-porphyrins assembled by a central truxene: synthesis, structure, and singlet energy transfer behaviors, *J. Porphyrins Phthalocyanines*, 17, 44–55, (DOI:org/10.1142/S1088424612501271).
12. (a) Kimura M., Kuwano S., Sawaki Y., Fujikawa H., Noda K., Taga Y., Takagi K. (2005), New 9-fluorene-type trispirocyclic compounds for thermally stable hole transport materials in OLEDs, *J. Mater. Chem.*, 15, 2393–2398, (DOI: 10.1039/B502268A). (b) Yuan M. S., Liu Z. Q., Fang Q. (2007), Donor-and-Acceptor Substituted Truxenes as Multifunctional Fluorescent Probes, *J. Org. Chem.*, 72, 7915–7922, (DOI: 10.1021/jo071064w).
13. Yao C., Yu Y., Yang X., Zhang H., Huang Z., Xu X., Zhou G., Yue L., Wu Z. (2015), Effective blocking of the molecular aggregation of novel truxene-based emitters with spirobifluorene and electron-donating moieties for furnishing highly efficient non-doped blue-emitting OLEDs, *J. Mater. Chem. C*, 3, 5783, (DOI: 10.1039/c5tc01018g).
14. Misra R., Sharma R., Mobin S. M. (2014), Star shaped ferrocenyl truxenes: synthesis, structure and properties, *Dalton Trans.*, 43, 6891-6896, (DOI: 10.1039/C4DT00210E).
15. The Porphyrins; Dolphin, D. (1978), Ed.; *Academic Press*: New York.
16. Xua H., Dub B., Gros C. P., Richarda P., Barbe J., Harvey P. D. (2013), Shape-persistent poly-porphyrins assembled by a central truxene: synthesis, structure, and singlet energy transfer behaviors, *J. Porphyrins Phthalocyanines*, 17, 44–55, (doi.org/10.1142/S1088424612501271).
17. Du B., Fortin D., Harvey P. D. (2011), Singlet and Triplet Energy Transfers in Tetra-(meso-truxene)zinc(II)- and Tetra-(meso-tritruexene)zinc(II)

- Porphyrin and Porphyrin-Free Base Dendrimers, *Inorg. Chem.*, 50, 11493–11505, (DOI: 10.1021/ic2013667).
18. Duan X., Wang J., Pei J. (2005), Nanosized π -Conjugated Molecules Based on Truxene and Porphyrin: Synthesis and High Fluorescence Quantum Yields, *Org. Lett.*, 7, 4071-4074, (DOI: 10.1021/ol051221i).
 19. Lembo A., Tagliatesta P., Guldi M. D. (2006), Synthesis and Photophysical Investigation of New Porphyrin Derivatives with β -Pyrrole Ethynyl Linkage and Corresponding Dyad with [60] Fullerene, *J. Phys. Chem. A*, 110, 11424–11434, (DOI: 10.1021/jp062735h).
 20. Sharma R., Gautam P., Mobin S. M., Misra R. (2013), β -Substituted ferrocenyl porphyrins: synthesis, structure, and properties, *Dalton Trans.*, 42, 5539-5545 (DOI: 10.1039/C3DT00003F).
 21. Sharma R., Gautam P., Misra R. Shukla S. K. (2015), β -Substituted triarylborane appended porphyrins: photophysical properties and anion sensing, *RSC Adv.*, 5, 27069, (DOI: 10.1039/C5RA03931B).
 22. Adler A. D., Longo F. R., Finarelli J. D., Goldmacher J., Assour J., Korsakoff L. (1967), A simplified synthesis for meso-tetraphenylporphine, *J. Org. Chem.*, 32, 476, (DOI: 10.1021/jo01288a053).
 23. (a) Gao G. Y., Ruppel J. V., Allen B. D., Chen Y., Zhang P. X. (2007), Synthesis of β -Functionalized Porphyrins via Palladium-Catalyzed Carbon–Heteroatom Bond Formations: Expedient Entry into β -Chiral Porphyrins, *J. Org. Chem.*, 72, 9060–9066, (DOI: 10.1021/jo701476m). (b) Yeung M., Ng A. C. H., Drew M. G. B., Vorpagel E., Breitung E. M., McMahon R., Ng D. K. P. (1998), Facile Synthesis and Nonlinear Optical Properties of Push–Pull 5,15-Diphenylporphyrins, *J. Org. Chem.*, 63, 7143–7150, (DOI: 10.1021/jo971597c).
 24. Kanibolotsky A. L., Berridge R., Skabara P. J., Perepichka I. F., Bradley D. D. C., Koeberg M. (2004), Synthesis and properties of monodisperse oligofluorene-functionalized truxenes: highly fluorescent star-shaped architectures, *J. Am. Chem. Soc.*, 126, 13695, (DOI: 10.1021/ja039228n).

25. Cao X., Zi H., Zhang W., Lu H., Pei J. (2005), Star-Shaped and Linear Nanosized Molecules Functionalized with Hexa-peri-hexabenzocoronene: Synthesis and Optical Properties, *J. Org. Chem.*, 70, 3645-3653, (DOI: 10.1021/jo0480139).
26. Chen Q., Liu F., Ma Z., Peng B., Wei W., Huang W. (2007), Synthesis and Optical Properties of Ethynylene-Linked Starburst Oligofluorene Based on Hexahexyltruxene, *Synlett*, 20, 3145–3148, (DOI: 10.1055/s-2007-1000815).
27. Pedone A. (2013), Role of Solvent on Charge Transfer in 7-Aminocoumarin Dyes: New Hints from TD-CAM-B3LYP and State Specific PCM Calculations, *J. Chem. Theory Comput.*, 9, 4087–4096 (DOI: /abs/10.1021/ct4004349).

Chapter 8

Conclusions and Future Scope

8.1. Conclusions

Truxene is a donor moiety and its derivatives exhibit red shifted absorption, fluorescence and high thermal stability.^{1,2} The photonic properties of truxene derivatives can be tuned by π -donors and π -acceptors.³ We have functionalized truxene with various donor/acceptor units to tune photophysical and electrochemical properties.⁴

In Chapter 3, the truxene core was functionalized with ferrocenyl donor unit at 2, 7, and 12 positions through various π -spacers and π -linkers. The electronic absorption and electrochemical studies show effective electronic interaction, which can be tuned by the introduction of different spacers. The enhancement of conjugation leads to red shift of the absorption bands in truxenes.⁴

In Chapter 4, the tetraphenylethylene (TPE) substituted truxene and 2,3,3-triphenyl acrylonitrile (TPAN) substituted truxene were designed and synthesized by the Pd-catalyzed Suzuki and Sonogashira cross-coupling reactions. Their photonic and thermal properties were studied. The TPE substituted truxene show aggregation-induced emission behaviour and TPAN substituted truxene shows aggregation-caused quenching effect in THF/water medium.

Chapter 5 describes the synthesis of star shaped donor-acceptor substituted truxenes. Their photophysical, electrochemical properties, thermal stability and HOMO-LUMO gap can be tuned by varying the strength of donor and acceptor groups. The optical properties of the truxenes were explained from the TD-DFT calculations. The computational calculation show significant lowering of the HOMO-LUMO gap by the incorporation of TCNE and TCNQ groups in truxene. The [2+2] cycloaddition retroelectrocyclization reaction pathway was studied by computational calculations. These studies show that, the donor substituted truxenes are favorable for the cycloaddition reaction whereas truxene substituted

by acceptor groups are not favourable for [2+2] cycloaddition-retroelectrocyclization reactions.⁵

In chapter 6 the C_3 symmetric, star shaped phenothiazene based 1,1,4,4-Tetracyanobuta-1,3-diene (TCBD) and cyclohexa-2,5-diene-1,4-ylidene-expanded TCBD substituted donor-acceptor truxenes **4–7** were designed and synthesized by using the Ullmann, Pd-catalyzed Sonogashira cross-coupling and [2+2] Cycloaddition-retroelectrocyclization reactions. Their photophysical, electrochemical, thermal properties were explored. The truxenes **4–7** exhibited good thermal stability. The substitution of phenothiazine through N-position at truxene core enhances the thermal stability compared to the 3-position substitution. The electronic absorption spectra reveals that the incorporation of TCBD and cyclohexa-2,5-diene-1,4-ylidene-expanded TCBD acceptor group results strong ICT at longer wavelength, donor-acceptor interactions and lower HOMO-LUMO gap. The optical and electrochemical properties of the truxenes **4–7** were explained from the TD-DFT calculations. The computational calculation show significant lowering of the HOMO-LUMO gap by the incorporation of TCNE and TCNQ groups.

Chapter 7 describes the design and synthesis of C_3 symmetric, star shaped β -substituted truxene porphyrin **4** and its Zn-metalated derivative **5** by using the Pd-catalyzed Sonogashira cross-coupling and metalation reaction. The substitution of porphyrin results in bathochromic shift of absorbance and fluorescence maxima. The absorption and emission studies exhibit considerable electronic communication.

8.2. Future scope

- The thesis highlights the tuning of HOMO-LUMO gap of a series of donor-acceptor molecules. The HOMO-LUMO gap of the donor-acceptor molecules can be tuned by changing the strength of donor, acceptor unit or by altering the π -linkers. The strength of donor/acceptor unit results in significant tuning of the optical (HOMO-LUMO) gap as well photophysical and electrochemical properties.⁶⁻¹⁵

- The incorporation of strong acceptor units such as TCNE and TCNQ in the donor–acceptor truxenes result the red shifted absorption and strong intramolecular charge-transfer. These truxene molecules are promising candidates for solar cell applications.
- The TPE substituted truxenes show aggregation-induced emission behaviour and TPAN substituted truxene shows aggregation-caused quenching effect in THF/water medium, which makes them useful for optoelectronic applications.

8.3. References

1. Kanibolotsky A. L., Berridge R., Skabara P. J., Perepichka I. F., Bradley D. D. C., Koeberg M. (2004), Synthesis and properties of monodisperse oligofluorene-functionalized truxenes: highly fluorescent star-shaped architectures, *J. Am. Chem. Soc.*, 126, 13695, (DOI: 10.1021/ja039228n).
2. Cao X., Zi H., Zhang W., Lu H., Pei J. (2005), Star-Shaped and Linear Nanosized Molecules Functionalized with Hexa-peri-hexabenzocoronene: Synthesis and Optical Properties, *J. Org. Chem.*, 70, 3645-3653, (DOI: 10.1021/jo0480139).
3. Misra R., Gautam P., Maragani R. (2015), Ferrocenyl thiazoles: synthesis and properties, *Tetrahedron Lett.*, 56, 1664-1666 (DOI: org /10.1016 /j.tetlet.201502031).
4. Misra R., Sharma R., Mobin S. M. (2014), Star shaped ferrocenyl truxenes: synthesis, structure and properties. *Dalton Trans.*, 43, 689, (DOI:10.1039/C4DT00210E).
5. Sharma R., Maragani R., Misra R*. (2018), C_3 -Symmetric star shaped donor–acceptor truxenes: synthesis and photophysical, electrochemical and computational studies, *New J.Chem.*, (DOI: 10.1039/C7NJ03934D).
6. Mathew S., Yella A., Gao P., Humphry-Baker R., Curchod B. F., Ashari-Astani N., Tavernelli I., Rothlisberger U., Nazeeruddin M. K., Grätzel M. (2014), Dye-Sensitized Solar Cells with 13% Efficiency Achieved

- Through the Molecular Engineering of Porphyrin Sensitizers, *Nat. Chem.*, 6, 242–247 (DOI: 10.1038/nchem.1861).
7. Chen C. Y., Wang M., Li J. Y., Pootrakulchote N., Alibabaei, L., Ngoc-le C. H., Decoppet J. D., Tsai J. H., Grätzel C., Wu S. M., Zakeeruddin C. G., Grätzel M. (2009), Highly Efficient Light-Harvesting Ruthenium Sensitizer for Thin-Film Dye-Sensitized Solar Cells, *ACS Nano.*, 3, 3103–3109 (DOI: 10.1021/nn900756s).
 8. Aghazada S. Gao P., Yella A., Marotta G., Moehl T., Teuscher J., Moser J. E., Angelis F. D., Grätzel M., Nazeeruddin M. K. (2016), Ligand Engineering for the Efficient Dye-Sensitized Solar Cells with Ruthenium Sensitizers and Cobalt Electrolytes, *Inorg. Chem.*, 55, 6653–6659 (DOI: 10.1021/acs.inorgchem.6b00204).
 9. Yella A., Lee H. W., Tsao H. N., Yi C., Chandiran A. K., Nazeeruddin M. K., Diau E. W. G., Yeh C. Y., Zakeeruddin S. M., Grätzel M. (2011), Porphyrin-Sensitized Solar Cells with Cobalt(II/III)-Based Redox Electrolyte Exceed 12% Efficiency, *Science*, 334, 629–634 (DOI: 10.1126/science.1209688).
 10. Mathew S., Yella A., Gao P., Baker, R. H., Curchod B. F. E., Astani C. A., Tavernelli L., Rothlisberger U., Nazeeruddin M. K., Grätzel M. (2014), Dye-Sensitized Solar Cells with 13% Efficiency Achieved Through the Molecular Engineering of Porphyrin Sensitizers, *Nat. Chem.*, 6, 242–247 (DOI: 10.1038/nchem.1861).
 11. He J., Guo F., Li X., Wu W., Yang J., Hua J.(2012), New Bithiazole-Based Sensitizers for Efficient and Stable Dye-Sensitized Solar Cells, *Chem. Eur. J.* 2012, 18, 7903 – 7915 (DOI: 10.1002/chem.201103702).
 12. He J., Wu W., Hua, J., Jiang Y., Qu S., Li J., Long, Y., Tian H. (2011), Bithiazole-bridged dyes for dye-sensitized solar cells with high open circuitvoltage performance, *J. Mater. Chem.*, 21, 6054-6062 (DOI: 10.1039/c0jm03811c).
 13. Zhang B., Cao K. S., Xu Z. A., Yang Z. Q., Chen H. W., Huang W., Yin G., You X. Z. (2013), Cell-compatible fluorescent chemosensor for Zn²⁺

- based on a 38-extended,1,10-phenanthroline derivative, *Eur. J. Inorg. Chem.*, 24, 3844–3851 (DOI: /10.1002/ejic.201200423).
14. Tao T., Peng Y. X., Huang W., You X. Z. (2013), Coplanar bithiazole-centered heterocyclic aromatic fluorescent compounds having different donor/acceptor terminal groups, *J. Org. Chem.*, 78, 2472–2481 (DOI: /abs/10.1021/jo302706t).
15. Genga J., Liua Y., Li J., Yina G., Huang W., Wang R., Quana Y. (2016), A ratiometric fluorescent probe for ferric ion based on a 2,2-bithiazole derivative and its biological applications *Sensors and Actuators B.*, 222, 612–617 (DOI: org/10.1016/j.snb.2015.08.076).